HERPES SIMPLEX VIRUS TYPE 1:
SECRETION, CELL SIGNALING, AND GENE EXPRESSION

A Dissertation

Presented to the Faculty of the Graduate School

of Cornell University

In Partial Fulfillment of the Requirements for the Degree of

Doctor of Philosophy

by

Kari L. Roberts

May 2011

HERPES SIMPLEX VIRUS TYPE 1:
SECRETION, CELL SIGNALING, AND GENE EXPRESSION

Kari L. Roberts, Ph. D.

Cornell University 2011

Herpes simplex virus type 1 (HSV-1) replicates in the nucleus and buds through the nuclear membrane to access the cytosol and complete the maturation process. The HSV-1 protein pU_L31, along with its binding partner, pU_L34, has been previously shown to be required for nucleocapsids to successfully bud through the nuclear membrane. pU_L31 is also required for efficient viral DNA synthesis and packaging. After the HSV-1 exits the nucleus, the capsid acquires several accessory proteins (tegument) and finally a mature envelope by budding into vesicles of the *trans*-Golgi network (TGN). These virion-laden vesicles traffic toward the cell periphery and through cortical actin until ultimately the virion is secreted upon fusion of the TGN vesicle with the plasma membrane.

The data presented here reveals new roles for pU_L31, as cells infected with a U_L31-null virus were delayed for viral gene expression as well as activation of NFκB and c-Jun N-terminal kinase (JNK) in multiple cell lines. At least one representative from each kinetic class of viral genes was examined at various times post infection. The protein expression defects were not caused by a failure to enter cells, was not rescued by ICP27 expressed *in trans* and correlated with NFκB activation. The data shows that these defects were not

observed in the absence of the pU_L31 binding partner, pU_L34, and that while most pU_L31 is expressed at late times post infection, low levels are detectable as early as 2 hours post infection.

Data presented in this work also demonstrates a role for the actin motor myosin Va in the secretion of HSV-1 virions. Expression of two isoforms of dominant negative myosin Va (DN-myoVa) decreased virion secretion by 50-75% as well as significantly decreased surface expression of viral glycoproteins B, M and D. DN-myoVa colocalized with TGN markers and the conformation of native myosin Va in infected cells was altered by 4 hours post infection. These data suggest that myosin Va is involved in the egress of virion-laden TGN vesicles as they transit through cortical actin toward the plasma membrane.

BIOGRAPHICAL SKETCH

Kari Roberts grew up along the central and southern California coastline. She graduated with a Bachelor of Science degree from California Polytechnic State University in San Luis Obisbo, Ca. in 2005 and was the first in her family to receive such a degree. She came to Cornell University in 2006 to pursue a PhD in microbiology under the direction of Dr. Joel Baines, completing the degree in 2011.

This work is dedicated to my family.

ACKNOWLEDGMENTS

Most importantly, I would like to thank my mentor Dr. Joel Baines for his invaluable guidance and support. I would also like to thank the members of the Baines' lab, including Luella Scholtes, Carol Duffy, Elizabeth Wills, Kui Yang, Fan Mou, Serena Chang, and Lucy Li for helpful discussions and support. I would also like to thank my committee members, Drs. James Casey and Gary Whittaker for their advice throughout the PhD program. I also thank the members of the Department of Microbiology and Immunology for their assistance and generous sharing of equipment and reagents.

TABLE OF CONTENTS

LIST OF FIGURES

LIST OF FIGURES (CONTINUED)

LIST OF TABLES

CHAPTER I

Introduction

Overview of *Herpesviridae*

The family *Herpesviridae* consists of more than 120 different viruses and can be subdivided into three subfamilies: *alpha*-, *beta*- and *gammaherpesvirinae* (132). The primary difference between the viruses comprising each subfamily is the viral replication kinetics, with the alphaherpesviruses replicating and spreading the fastest (less than 24 hours). The best studied alphaherpesvirus, herpes simplex virus type 1 (HSV-1), is the model virus of this family and is the subject of many review articles (85,96-98,121,146).

The hallmark of herpesvirus infections is the ability to establish latency. For the neurotropic alphaherpesviruses, latency is established in sensory neurons where the linear DNA genome circularizes and exists as a stable episome for the lifetime of the host. Occasionally, environmental stresses such as UV exposure will cause the quiescent genomes to reactivate and produce infectious virions. During active infections, HSV-1 causes cold sores (lesions on or near the mouth), and more rarely, blindness and encephalitis.

Overview of Virion Structure

Herpesviruses are enveloped and contain a double stranded, linear DNA genome of 152kb encoding more than 80 genes. The genome consists of two covalently linked segments, unique long (U_L) and unique short (U_S) and is encased within an icosohedral capsid shell (7). The two genomic segments

are flanked by inverted repeats, designated *ab* and *b'a'* bordering the U_L segment and *a'c'* and *ca* flanking the U_S segment (figure 1.1) (7). Genes encoded within the viral genome are transcribed in three sequentially regulated phases: α, β and γ. These three classes of genes mostly encode transcription regulators, DNA replication machinery and structural (capsid) components, respecitively. The virion is approximately 225 nm in diameter (51). Between the capsid and envelope is a complex matrix of many viral and host proteins (tegument) (83). The capsid is non-centered, with one side of the capsid close to the envelope and the other separated by about 35 nm of tegument (51). Embedded within the envelope are virally-encoded glycoproteins which facilitate both entry into the host cell and egress from the nucleus. These features are described in detail below and pictured in figure 1.1.

HSV-1 Entry

Entry of HSV-1 virions requires the attachment of the virion to the host through the interaction of a viral glycoprotein(s) with host surface receptor(s). Although HSV-1 has at least 12 envelope proteins (83), only four are required for entry: glycoprotein D (gD), gB, and the heterodimer gH and gL (gH/gL) (121). A receptor for gD is required for HSV-1 to attach and enter a cell, and attachment is enhanced by gB and the non-essential gC binding to heparin sulfate (HS) proteoglycans. Other than HS, known gB receptors include paired Ig-like type 2 receptor α (PILRα), and surprisingly, the heavy chain of non-muscle myosin IIA (NMIIA) (4,136). NMIIA is a cytoplasmic actin binding

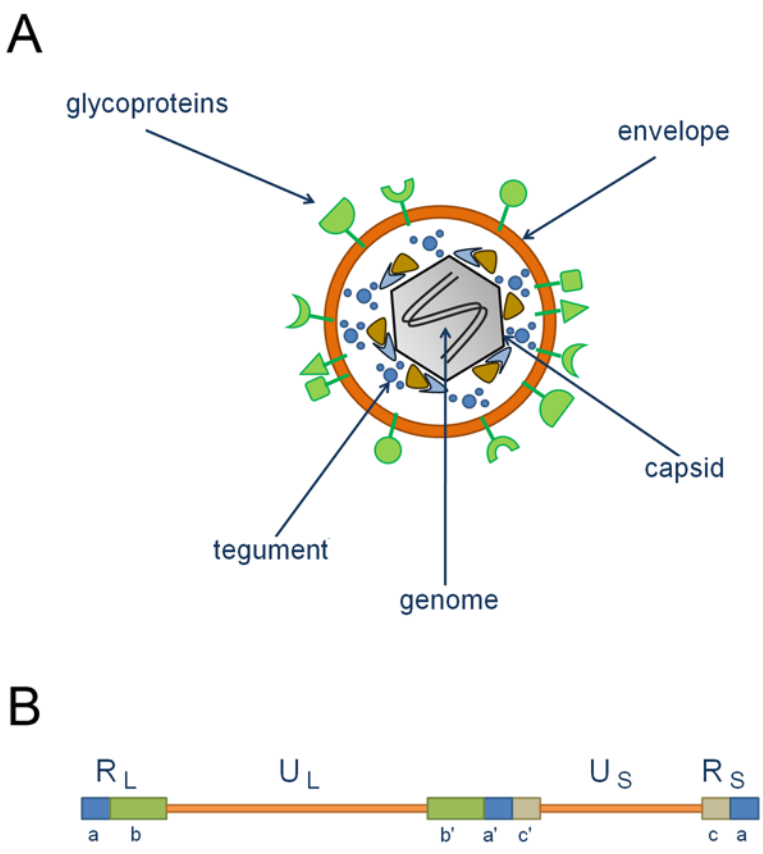

Figure 1.1 Structure of HSV-1 virion and genome. (A) Structure of an HSV-1 virion. Pictured are viral glycoproteins, the host-derived envelope, tegument, capsid and packaged genome. (B) Structure of the linear DNA genome of HSV-1. Pictured is a map of the unique long (U_L) and unique short (U_S) regions as well as the long and short inverted repeats (R_L and R_S, respectively).

protein that can bundle and contract parallel actin filaments (22,162). How this cytoplasmic protein is expressed on the cell surface and acts as a biologically relevant receptor for HSV-1 attachment remains to be determined.

Although gB and/or gC can enhance HSV-1 entry by binding the cell surface, only binding by gD is absolutely required for entry. The three known classes of gD receptors are (i) HVEM (herpesvirus entry mediator), a member of the tumor necrosis factor (TNF) receptor family; (ii) nectin-1 and nectin-2, members of the immunoglobulin (Ig) superfamily; and (iii) 3-O sulfated heparin sulfate (3-O-HS). After attachment by gD, the virion fuses its envelope with the host membrane to access the cytosplasm. Fusion is accomplished by the coordinated actions of the central fusion machinery: gB and gH/gL (121). Although gD is required for entry, is not believed to be part of the fusion machinery because the structure of this glycoprotein does not resemble a fusion protein. Fusion of the virion envelope with the host membrane can occur at the plasma membrane surface or within an endocytosed vesicle and varies between cell lines (19,100,106,107,169). This is described with greater detail in chapter II.

After the HSV-1 capsid has accessed the cytoplasm, many of the outer tegument proteins disperse away from the capsid and prime the cell for infection. The capsid maintains association with some (inner) tegument, such as the gene products for U_L36 and U_L37 (pU_L36 and pU_L37, respectively), and utilizes microtubules and the microtubule motor dynein to traffic to a nuclear pore (32,144). It is unclear which inner tegument protein(s) and/or capsid proteins are interacting with the dynein motor and if any other cellular factors

are involved. pU_L36 and/or pU_L37 are potential candidates for dynein interaction, as both are required for entry and have been shown to remain associated with incoming capsids (7). After trafficking along the microtubules and reaching the nucleus, the capsid docks at an unknown component of the nuclear pore complex (NPC) and releases the genome into the interior of the nucleus (6,154).

As the capsid delivers the genome to the nucleoplasm, outer tegument proteins work to establish an environment conducive to HSV-1 infection. For example, pU_L41 [virion host shut off protein (vhs)], destabilizes the preexisting mRNAs within the host cell (42,137,151). This is beneficial for two reasons: (i) by removing the bulk of preexisting host mRNA the cellular machineries will favor translation of newly transcribed viral mRNA; and (ii) by destabilizing the half-lives of mRNA, vhs increases the efficiency of transitioning from one phase of viral transcription to the next. Other examples of tegument influencing early cellular events include pU_L37, which has been shown to activate NFκB (nuclear factor κB) signaling pathways through an interaction with TNF receptor-associated factor 6 (TRAF6) (82); and pU_L48 [also known as α-transinducing factor (α-TIF), VP16 or vmw65] which associates with host cell factor (HCF-1) and Oct-1 in the nucleus and initiates viral transcription (47,148,175).

Transcription Kinetics of HSV-1

Herpesviruses transcribe their genes in a temporally regulated cascade comprised of three basic classes: immediate early (α), early (β), and late (γ).

The γ genes can be further subdivided into γ_1 and γ_2 (leaky late and true late, respectively). The distinction between γ_1 and γ_2 gene expression is separated by the requirement for viral DNA (vDNA) replication. If vDNA replication is inhibited, γ_1 gene expression is diminished and γ_2 gene expression is precluded. The kinetic class of HSV-1 genes is largely defined by the corresponding promoter (see figure 1.2) and the temporal cascade of gene expression is mediated in part by viral proteins acting as transactivators.

One very important activator of viral genes is α-TIF, which is brought in with the viral tegument. The N-terminal half of α-TIF associates with the host factors HCF-1 and Oct-1 and the complex binds to consensus TAATGARAT (R is a purine residue) DNA sequences within α gene promoters (108,115,116,148,164,175). This protein-DNA interaction occurs at single or multiple sites upstream of individual genes and initiates α gene transcription. As the α genes are made, new regulators act to influence viral gene expression. If translation is blocked at the start of infection, only α gene transcripts are produced from the viral genome.

Promoters for α genes contain TATA and CAAT boxes, similar to other polymerase II promoters in cellular genes. Unique to α promoters are the α-TIF interacting regions. These immediate early promoters have a TAATGARAT DNA binding site for α-TIF complexed with host proteins to initiate α gene expression. Immediate early promoters also have a variable number of repeated SP1 binding sites upstream of the TATA box. Some α promoters also have an ICP4 binding site. The α gene products are mostly

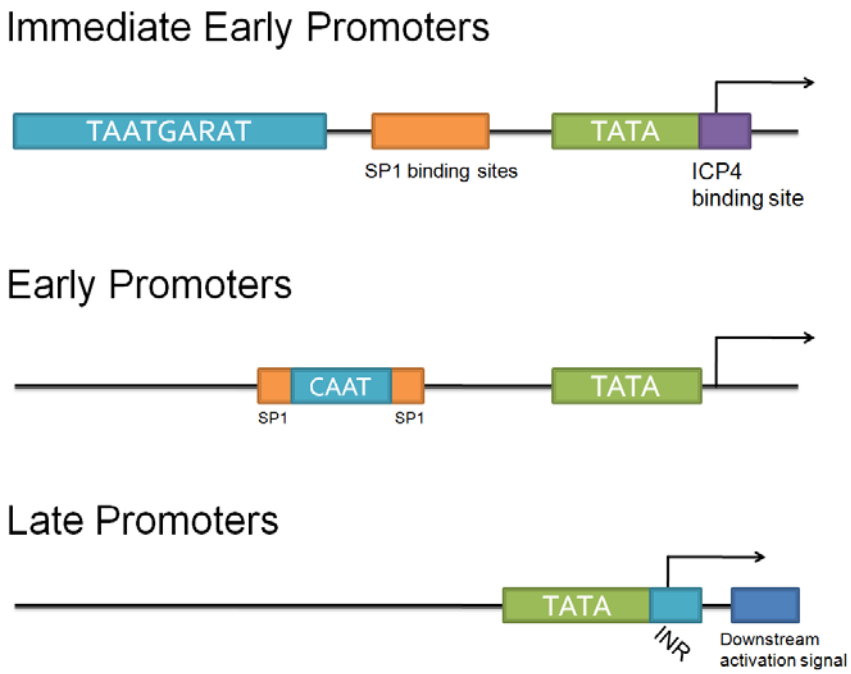

Figure 1.2 Examples of HSV-1 immediate early, early and late promoters. Schematic representation of generic examples of HSV-1 promoters of each kinetic class and the *cis*-acting regulatory segments is shown above. The immediate early promoters have a TAATGARAT DNA binding site for α-TIF complexed with host proteins to initiate α gene expression. These promoters also have a variable number of repeated SP1 binding sites upstream of the TATA box and some have an ICP4 binding site. β promoters contain eukaryotic elements upstream of the TATA box, but no known downstream elements. These promoters resemble typical polymerase II promoters existing in host cells. γ promoters contain *cis*-acting elements downstream of the TATA box, including an initiator element (INR) at the transcription start site and some γ promoters also have downstream activation sites.

transcription regulators, including ICP0, ICP4 and ICP27. Among other roles, ICP0 augments expression of α, β and γ genes. ICP27 augments γ gene expression and interacts with RNA polymerase II to help initiate transcription (176) by recruiting the polymerase to viral replication sites within the nucleus (26). Once these viral transcripts are produced, ICP27 binds viral mRNA (23,135) and helps mediate its export to the cytoplasm (75,135,145). ICP27 has also been shown to be required for the activation of NFκB during HSV-1 infection (57). ICP4 augments β and γ gene expression and also down regulates mRNA expression of some α genes, including itself.

ICP4 is one of the best studied HSV-1 genes. It is encoded by R_S1 and present in two copies within the viral genome. Functional ICP4 protein is required for the progression of both β and γ gene expression (7). The mechanism of ICP4-mediated repression involves an ICP4 binding site near the transcription start site (figure 1.2) but does not act through steric interference of transcription. Instead, ICP4 is believed to associate with other transcriptional regulatory factors such as the TATA-binding protein (TBP) and the transcription factor TFIIB (53,77). The mechanism(s) of ICP4-mediated activation of HSV-1 genes is not fully understood, but the transactivation by ICP4 appears to involve interaction of ICP4 with TFIID (52) through an interaction with the TBP-associated factor (TAF) 250 (13).

β genes encode proteins important for vDNA replication. Some of the essential β gene products include pU_L30 (DNA polymerase), pU_L29 (ICP8) and pU_L42 (DNA binding proteins), and pU_L5 (helicase/primase complex). Without these and other β gene products, vDNA replication cannot proceed

and consequently γ gene transcription is blocked.

Thymidine kinase (TK or U_L23) is another example of a β gene product and was one of the first viral genes to be studied in detail. TK gene expression requires ICP4 for expression, but mutational experiments on the promoter controlling expression of TK revealed the perplexing finding that the *cis*-acting elements were the same as those required for eukaryotic genes. These elements include a TATA box, two SP1 binding sites and a CAAT element (figure 1.2) and no other elements were found to be necessary (21,34,89-92). It is still unclear how β gene expression is regulated and why TK mRNA transcription requires ICP4 when all of the *cis*-acting elements required for expression by host machinery appear to be present.

Upon high levels of vDNA replication, the γ genes are transcribed and the cell is committed to producing virions until eventually the cell is destroyed. The late genes encode mostly structural proteins and are produced in two subclasses: γ_1 (leaky late) and γ_2 (true late). Inhibition of vDNA synthesis will decrease the efficiency of γ_1 gene expression, preclude γ_2 gene expression and prolong the expression of early genes. Thus, the transition from early to late gene expression is linked with vDNA replication and requires ICP4-mediated activation at the TATA box within γ promoters.

Late gene promoters have a TATA box and downstream *cis*-acting elements, but these promoters do not have other *cis*-acting elements upstream of the TATA box (figure 1.2) (54,66,73,87). Examples of γ_1 gene products include ICP34.5 (a neurovirulence gene required for

dephosphorylation of eIF2-α and protein synthesis) and VP5 (U_L19, the major capsid protein). Examples of γ_2 gene products include gC and VP16 (U_L48, a tegument protein) (7).

During the transition from β to γ gene expression, the viral genome forms into specialized domains known as viral replication compartments (RCs). Late gene transcription, vDNA replication and encapsidation take place within these domains. As the RCs develop, host chromatin is marginalized against the inner nuclear membrane, nuclear lamina and RCs. Eventually the host chromatin becomes fragmented as the RCs mature and extend to the nuclear periphery in a process dependent upon pU_L34 and pU_L31 (142). These nuclear alterations and reorganization of vDNA may be a key process in viral gene regulation. Further studies are required to elucidate this possibility.

Alterations in Nuclear Architecture During HSV-1 Infection

During HSV-1 infection, the host nucleus undergoes many changes to accommodate the replication of vDNA and the assembly and egress of nascent nucleocapsids. As the vDNA replicates, replication compartments (RCs) form and marginalize host chromatin to the nuclear rim. As the RCs mature, they push through the marginalized chromatin to the nuclear periphery (102,142). The nucleus has been shown to expand in size two-fold in infected HeLa cells at about 8 hours post infection (102). HSV-1 induced nuclear expansion was shown to require pU_L31 and pU_L34 and was precluded by treatment with the actin depolymerizing drug cytochalasin D (143). The nuclear lamina is also modified by pU_L31, pU_L34 and U_S3, which may be

important for egressing nucleocapsids to access the inner nuclear membrane and bud out of the nucleus (described below) (122-124,128,131,163).

Nucleocapsid Assembly

HSV-1 capsids are icosahedral (T=16) with 162 capsomers and 12 vertices. The capsid is made up of several viral proteins, including pU_L19 (VP5, the major capsid protein), pU_L18 and pU_L38 (triplex proteins), U_L6 (the portal) and pU_L35 (VP26, a non-essential protein that decorates the hexon tips). Assembly of these proteins occurs autocatalytically in the nucleoplasm, and the capsid builds around a scaffold protein ($pU_L26.5$).

Encapsidation occurs by driving unit length genomic material from vDNA concatamers through the portal by the terminase complex (pU_L15, pU_L28 and pU_L33) and is ATP-dependent. Packaging of vDNA is concomitant with proteolytical cleavage of the scaffold by pU_L26 (the protease). Cleavage of the scaffolding is followed by its expulsion from within the nucelocapsid. A fully packaged capsid with the scaffolding completely extruded is referred to as a “C capsid.” DNA-free capsids which have lost the scaffold are referred to as “A capsids” and capsids that contain scaffold but failed to package vDNA are “B capsids.”

Also required for vDNA packaging and retention of the packaged genome within the capsid are pU_L17 (134,152) and pU_L25 (20,93,149), respectively. These proteins are believed to form the C capsid-specific complex (CCSC) located on top of the triplexes of C capsids as a heterodimer (155,156), and presence of the triplex protein U_L18 (VP23) is required for pU_L17 to efficiently

coimmunoprecipitate with pU_L25 (138). The CCSC is proposed to engage the envelopment machinery at the inner nuclear membrane (see figure 1.3) (70,156).

Nuclear Egress of HSV-1

Nucleocapsids engage in ATP-, actin- and possibly myosin-dependent movement within the nucleus (see chapter II). In order for these capsids to exit the nucleus, they must engage the inner nuclear membrane (INM) and bud into the perinuclear space, acquiring a primary envelope. This envelope is lost as the virion fuses with the outer nuclear membrane (ONM), at which point the capsid has accessed the cytoplasm and can continue the maturation process. Two viral proteins are essential for successful nuclear budding: pU_L34 and pU_L31 (figure 1.3). pU_L34 is a type II membrane protein that localizes to the INM and binds the nuclear phosphoprotein pU_L31.

The pU_L34/pU_L31 complex is required for egress of capsids from the nucleus and the presence of both proteins is required for their proper localization (123,124,128). In the absence of pU_L31, pU_L34 is dispersed throughout the INM and endoplasmic reticulum. In the absence of pU_L34, pU_L31 is dispersed within the nucleoplasm and does not associate with the INM. pU_L31 has also been shown to be important for vDNA packaging (15), and efficient activation of NFκB and viral gene expression (chapters IV and V). pU_L34, pU_L31 and the viral kinase encoded by U_S3 are also required for modification of the nuclear lamina.

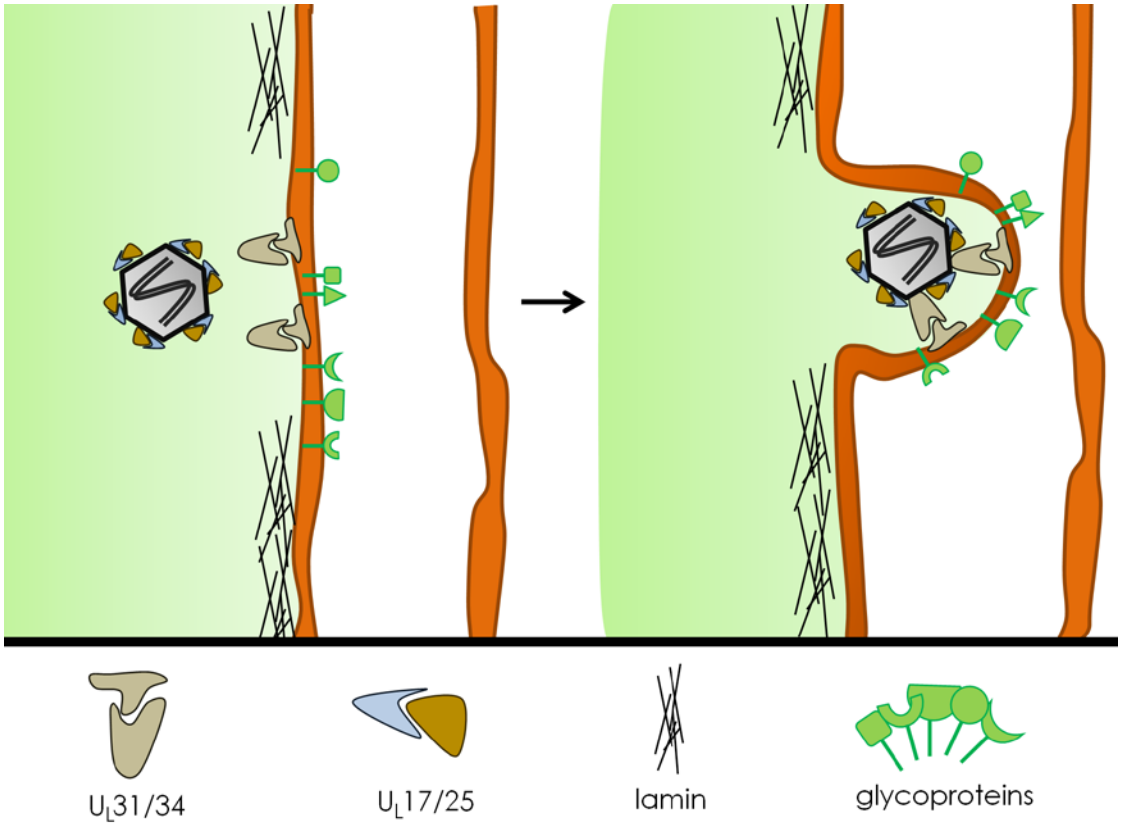

Figure 1.3 HSV-1 budding into the inner nuclear membrane [reprinted from reference (70)]. Association of an HSV-1 nucleocapsid with the U_L31/U_L34 complex at the inner nuclear membrane and subsequent budding into the perinuclear space.

The nuclear lamina is a proteinaceous layer beneath the INM composed of integral membrane proteins (e.g. lamin-associated protein 2 and lamin B receptor) and a meshwork of intermediate filaments (1,49,172). The membrane proteins interact with lamins A, B and C, which are intermediate filaments that polymerize in a head-to-tail fashion forming a network lining the INM. Lamin C is a splice variant of lamin A. This network of lamins is a barrier between egressing nucleocapsids and the INM. HSV-1 induced alterations of the lamina are therefore proposed to be required for capsids to gain access to the INM and the pU_L34/pU_L31 complex.

Both pU_L34 and pU_L31 are able to bind directly to lamins, and transient expression of pU_L34, pU_L31 or pU_S3 leads to alterations in the nuclear lamina (8,103,122). Over expression of pU_L34 leads to a partial redistribution of lamin A/C into the cytoplasm, while over expression of pU_L31 redirects lamin A/C into nucleoplasmic aggregates. Over expression of the U_S3 kinase causes disruption of the nuclear lamina (8). The pU_L34/pU_L31 complex can also recruit other factors to the nuclear lamina, including the cellular protein kinase C (PKC), which is enriched on the nuclear periphery and phosphorylates lamins during infection (111). pU_S3 hyperphosphoryates the lamin-interacting nuclear membrane protein emerin in a pU_L34-dependent manner, which modifies emerin's localization (79). Thus, both viral and cellular factors play a role in lamina modifications and nucleocapsid budding at the INM.

In addition to modifications of nuclear lamina, viral glycoproteins are also required for successful nuclear egress of HSV-1. Deletion of both gB and gH results in an accumulation of virions in the perinuclear space (39,98).

However, only minor defects were observed with single deletions of either gB or gH (39). The apparent redundancy between gB and gH (presumably complexed with gL) for fusion with the ONM is notably distinct from entry requirements, where gB and gH/gL must be present for fusion to occur at the plasma membrane (121).

Cytoplasmic Maturation of HSV-1

Once the capsid has transversed the nuclear membranes it must accumulate the full complement of tegument proteins and traffic to the *trans*-Golgi network (TGN), where it will undergo secondary envelopment (see figure 1.4 for an illustrative summary of HSV-1 egress). TGN-derived vesicles both provide virions with the membrane for their secondary ("mature") envelope and act as the vehicle for delivery to the plasma membrane for secretion.

After fusion of the primary envelope with the ONM, the released capsids appear to lack tegument by electron microscopy, but immunolabeling experiments have indicated that they are associated with pU_S3, pU_L36 and pU_L37 (45). The large, multifunctional tegument protein pU_L36 has been shown to bind the capsid (16,177) and the phosphoprotein pU_L37 (46,74).

Other tegument proteins, including pU_L11 and pU_L49, assemble at TGN vesicles awaiting secondary envelopment with cytosolic capsids. Deletion of gE and gD precludes secondary envelopment in HSV-1 infections, and large numbers of tegumented capsids accumulate in the cytoplasm (38). pU_L49 has been proposed to bind the carboxy-terminal domain of gD (17). The complex protein-protein interactions comprising the entire complement of HSV-1

Figure 1.4 Nuclear and cytoplasmic egress of HSV-1 [reprinted from reference (70)] Nucleocapsid budding at inner nuclear membrane and egressing through the cytoplasm, budding into the TGN and leaving the host cell.

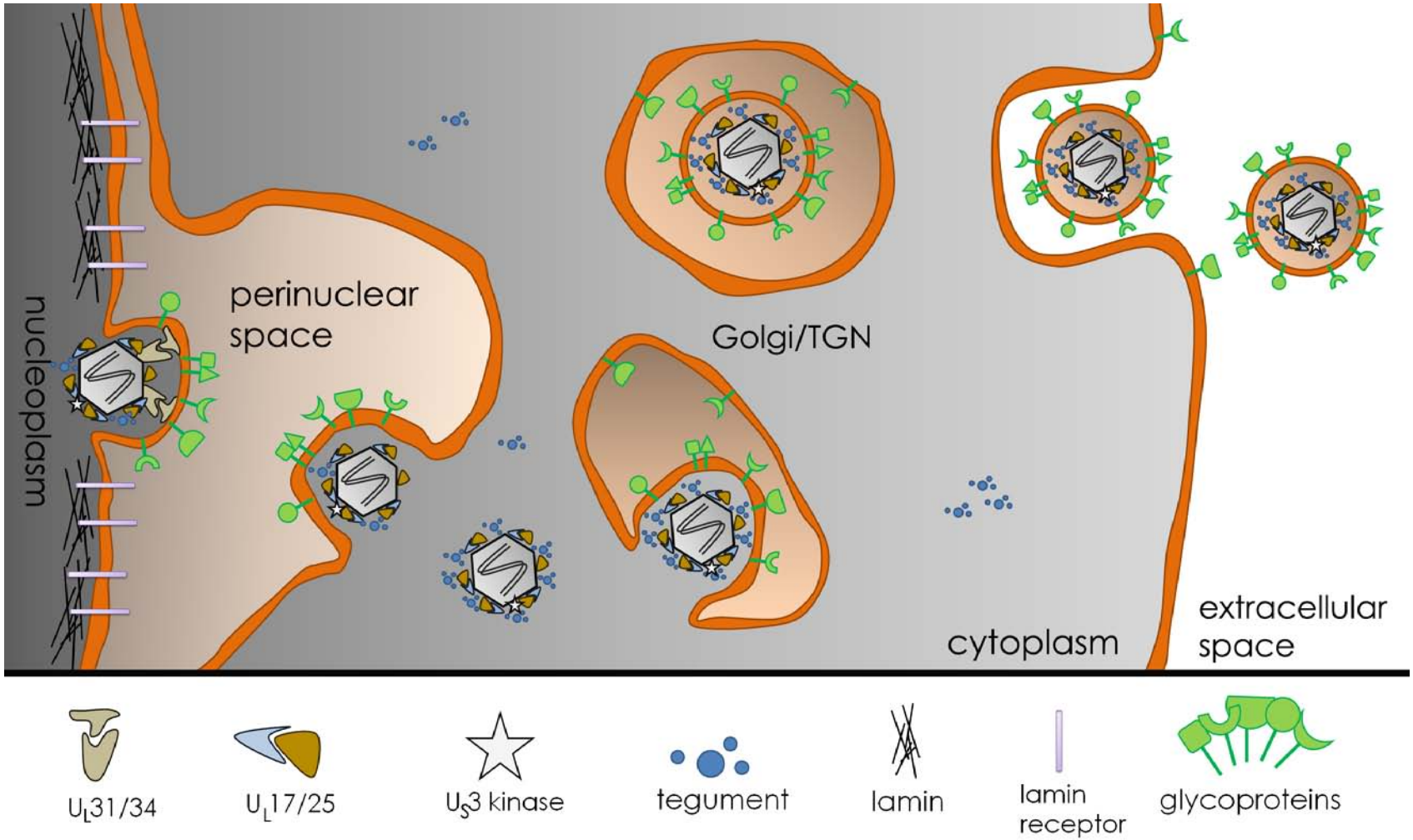
nucleoplasm
perinuclear space
Golgi/TGN
cytoplasm
extracellular space
U_L31/34
U_L17/25
U_S3 kinase
tegument
lamin
lamin receptor
glycoproteins

tegument have yet to be fully elucidated.

In the absence of either inner tegument protein pU_L36 or pU_L37, virion formation is blocked (30,31) and it has been shown that inner tegument proteins promote HSV-1 capsid movement along microtubules (84,170). Similar to entry (above), pU_L36 and pU_L37 may be important for interactions of trafficking capsids with microtubules. Entering and egressing capsids must recruit the appropriate motor: the minus-end directed microtubule motor dynein for entry and the plus-end directed motor kinesin for egress. It is unclear how the appropriate motors are recruited to the capsid, but differences in inner tegument composition may be key to this distinction. No direct evidence of tegument proteins pU_L36 and/or pU_L37 interacting with a cellular motor protein has been presented (85).

Secondary Envelopment and Secretion of HSV-1

Egressing capsids would be expected to acquire their secondary envelope at sites of glycoprotein enrichment in cellular organelles. Although several putative sites have been postulated including the Golgi, the endoplasmic reticulum-Golgi intermediate compartment (ERGIC) and endosomes, the strongest evidence suggests that TGN-derived vesicles are the major site of secondary envelopment (85,96,98). These vesicles have been shown to accumulate viral glycoproteins even in the absence of capsid egress; and GFP-labeled capsids were observed to accumulate at the TGN under conditions that slowed intracellular transport (158).

Although microtubules have been shown to be important for HSV-1 egress,

intracellular transport of cargo often requires multiple motors and microfilaments. Switching between microtubule and actin motors is not unexpected, and very little is known about how the virion-laden TGN vesicles traffic to and fuse with the plasma membrane to release HSV-1 (85,96,98). Another consideration is the cortical actin lining the plasma membrane. Similar to the nuclear lamina (described above), the meshwork of actin filaments lining the plasma membrane is a potential barrier to egressing HSV-1 that must be overcome for successful secretion.

Studies of secretion of other vesicles, such as melanosomes and secretory granules, has lead to the discovery for a role for myosin Va in vesicle transport through the cortical actin (130,173,174). In these systems, microtubule motors (e.g. kinesin) are utilized to traffic to the cortical actin at which point there is a “hand off” of kinesin-microtubule based locomotion to myosin-actin based locomotion. Experiments observing the trafficking events of melanosomes demonstrated a role for myosin Va in the secretion of vesicular cargo (173,174).

Myosin Va is an unconventional actin motor that consists of two heavy chains which dimerize to form duplicate N-terminal head domains and binds cargo at two C-terminal globular tail domains (GTDs). This actin motor moves cargo along filamentous actin (F-actin) through a series of processive “hand-over-hand” steps toward the plus end of F-actin (157,159). A dominant negative myosin Va construct expressed in melanocytes resulted in melanosomes trafficking toward the cell periphery (kinesin-mediated movement) and then back toward the center of the cell (dynein-mediated

movement). In these cells, the melanosomes accumulated at the center of the cell and failed to be secreted (174). Differently, in control cells these vesicles were observed to traffic toward and accumulate at the cell periphery (174). This was described as a “capture model” where myosin Va was necessary for the vesicular cargo to be locally secured within the cortical actin as it continued toward the plasma membrane for secretion.

Another actin motor, non-muscle myosin IIA (NMIIA), appears be involved in HSV-1 egress, as treatment of cells with the putative myosin II inhibitor BDM (2,3-butanedione monoxime) resulted in decreased secretion of HSV-1 infectivity 20- to 50-fold (161). Roles for myosin motors in HSV-1 infections is discussed further in chapter II and data supporting a role for myosin Va in HSV-1 secretion is presented in chapter III. Conclusions and future studies for the work presented in this report are presented in chapter VI.

CHAPTER II

Actin in Herpesvirus Infection*

Kari L. Roberts and Joel D. Baines, Department of Microbiology and Immunology, Cornell University, Ithaca, NY 14853.

*Reprinted from **Roberts, KL, and J.D. Baines.** (2011). Actin in Herpesvirus Infection. Viruses, 3:336-346.

Abstract

Actin is important for a variety of cellular processes, including uptake of extracellular material and intracellular transport. Several emerging lines of evidence indicate that herpesviruses exploit actin and actin-associated myosin motors for viral entry, intranuclear transport of capsids, and virion egress. The goal of this review is to explore these processes and to highlight potential future directions for this area of research.

Overview of Actin-Related Cytoskeletal Components

Actin is a highly dynamic protein critical for a wide variety of important cellular processes including cell division, adherence, migration, uptake of extracellular material, and intracellular transport of vesicles and other cargo. There are two basic forms of actin: monomeric or globular actin (G-actin) and filamentous actin (F-actin). Formation of F-actin begins by a nucleation event from proteinacious complexes such as actin-related protein 2/3 (Arp2/3) (11). G-actin subunits assemble in a polarized fashion, forming an actin filament with distinctive ends. The plus or “barbed” end of a growing actin filament rapidly elongates while the minus or “pointed” end remains relatively static. This process is reversible causing actin filaments to rapidly depolymerize as subunits dissociate from the plus end. F-actin can also associate with other actin filaments to form more complex structures such as actin arrays or networks.

Three fundamental examples of actin networks are stress fibers, filopodia

and lamellipodia (figure 2.1). Actin stress fibers are short, contractile bundles of F-actin with alternating polarity. The filaments are held together through interactions with the dimeric bundling protein α-actinin and the motor protein myosin II, which enables contraction. These fibers are essential for maintaining cell attachment to the substratum and implementing changes in morphology. Filopodia contain stiff, tightly bound parallel actin bundles that polymerize toward the plasma membrane forming a thin, spike-like protrusion. These structures may act as probes or sensors of the extracellular environment and contain receptors for signaling as well as integrins and cadherins (cell adhesion molecules). Lamellipodia are highly branched networks of actin filaments, with the highest branching frequency occurring nearest the plasma membrane. This “dendritic” sheet-like array of F-actin comprises the leading edge of migrating cells and membrane ruffles. Generation of these actin structures requires the activity of Rho GTPases. These proteins are analogous to molecular switches, existing in either an active (GTP-bound) or inactive (GDP-bound) form. The GTPases associate with downstream effector proteins in signal transduction pathways (36,55). The three most extensively characterized mammalian Rho GTPases, and those known to be involved in herpesvirus infections, are RhoA, Rac1 and Cdc42. RhoA is associated with the generation of actin stress fibers, Cdc42 with filopodia, and Rac1 with lamellipodia and ruffling.

Rho GTPases have been shown to be important for phagocytosis (55), a form of endocytosis involving the internalization of large particles at the cell surface, and known to be used by incoming herpesviruses (explained below).

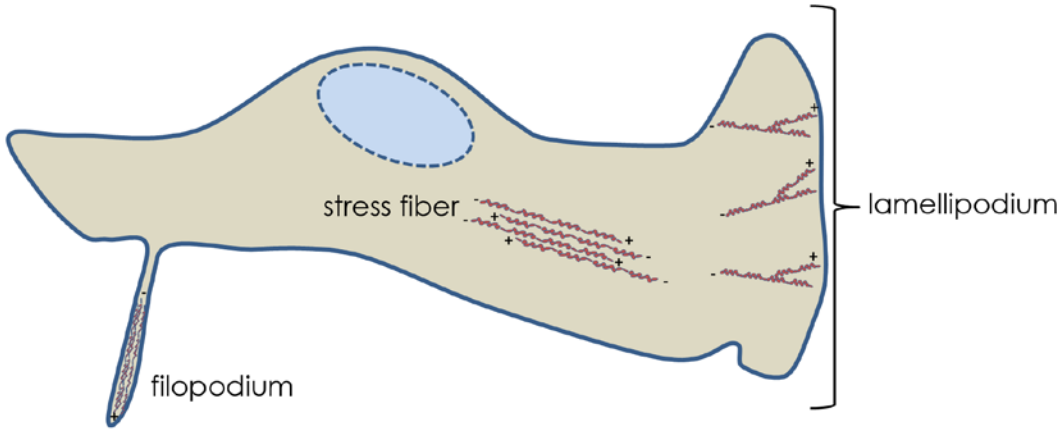

Figure 2.1 Examples of actin networks. Filopodium, stress fiber, and lamellipodium structures are featured showing actin polarities.

Initiation of phagocytosis involves receptor-mediated rearrangement of cortical actin localized near the position of the stimulating particle. During Fc receptor (FcR)-mediated phagocytosis F-actin accumulates beneath a pedestal-like formation and the particle is engulfed by extending pseudopodia that wrap around the particle and subsequently fuse (18). In FcR-mediated phagocytosis in rat basophil leukemia mast cells, expression of dominant-negative Cdc42 results in the formation of pedestal-like structures beneath the particles but pseudopodia do not form, as observed by scanning electron microscopy (SEM) (86). Expression of dominant-negative Rac1 results in particles enclosed within pseudopodia that do not fuse (86). While FcR-mediated phagocytosis is known to require Cdc42 and Rac1, receptors for complement (CR)-mediated phagocytosis induce RhoA-dependent recruitment of Arp 2/3 to F-actin rich foci at the site of particle attachment. Although Arp 2/3 is involved in both types of phagocytosis, there are no pseudopod extensions in CR-mediated phagocytosis. Instead, the particle seems to sink into the cell and Cdc42 and Rac1 are dispensable for particle uptake, unlike the case of FcR-mediated phagocytosis.

Since actin is crucial to many cellular processes, including uptake and short-range intracellular transport (such as the movement of melanosomes towards the plasma membrane), it is perhaps not surprising that herpesviruses utilize host actin during infection.

Overview of Herpesvirus Replication

The family Herpesviridae can be further categorized into three subfamilies:

alpha-, beta- and gamma-herpesvirinae, all of which establish life-long infections in their hosts. Herpes simplex virus type 1 (HSV-1), varicella-zoster virus (VZV) of humans, and pseudorabies virus (PrV) of swine are examples of alphaherpesviruses. Human and mouse cytomegalovirus (HCMV and MCMV, respectively) are commonly studied betaherpesviruses, and Epstein-Barr virus (EBV) and Kaposi's sarcoma-associated herpesvirus (KSHV) are both gammaherpesviruses that infect humans. The virions of herpesviruses comprise a double stranded linear DNA genome contained within a proteinaceous capsid. A number of proteins surround the capsid and are collectively called the tegument. Surrounding the tegument is an envelope containing a number of viral glycoproteins.

Herpesviruses enter cells either by fusion at the plasma membrane or are endocytosed by the cell to eventually fuse within an intracellular vesicle (19,100,106,107,169). Regardless of how the virus enters, once the capsid accesses the cytosol, viral tegument proteins dissociate from the capsid to prime the cell for infection while the capsid traffics toward the nucleus along microtubules using the molecular motor dynein (32,144). Capsids migrate to and dock at nuclear pores where they subsequently release the viral genome through a unique capsid vertex (the portal) and the genome enters the nucleus through the nuclear pore (6,109,154). Nuclear genomes are used as templates for viral transcription, which occurs in three temporal stages (67,68). Nascent replicated genomes are then packaged into newly assembled capsids. The packaged capsids associate with the inner nuclear membrane and subsequently bud into the perinuclear space to acquire a primary envelope.

This envelope is lost as the virion envelope fuses with the outer nuclear membrane and the nucleocapsid is released in the cytosol. Next, the capsid associates with tegument proteins as it traffics towards the trans-Golgi network (TGN). TGN-derived vesicles are believed to be the major site of secondary envelopment where the virus acquires its final mature envelope, which is embedded with viral glycoproteins (158). Fusion of these transport vesicles with the plasma membrane releases virions into the extracellular environment.

Actin and Herpesvirus Entry

Incoming herpesvirions first encounter host actin during entry into cells [for another review on herpesvirus interactions with the cytoskeleton see reference (85)]. The cortical actin lining the cytosolic side of the plasma membrane is a meshwork of F-actin connected to the cell surface through surface receptors. Various signaling pathways can alter the cortical actin. In the case of viral infection, virion glycoproteins bind to specific host cell receptors, ultimately causing the envelope and plasma membrane to fuse, delivering the capsid and tegument into the cytosol. Whereas glycoprotein D (gD) is an important receptor binding protein in most alphaherpesviruses except VZV, gB, gH and gL are all required for virion fusion (62,81,146).

Depending on the cell type, the fusion event required for HSV-1 entry occurs at a neutral pH at the plasma membrane (e.g. Hep2 and Vero cells) (169), through a pH-dependent endocytic pathway [e.g. HeLa cells and modified Chinese hamster ovary (CHO) cells expressing HSV-1 receptors] (107) or through a pH-independent endocytic pathway (C10 murine melanoma

cells) (86). Polymerized actin was shown to be dispensable for pH-independent entry of HSV-1 into Vero cells based on insensitivity to the actin depolymerizing drug cytochalasin D (169). However, actin dynamics are required for the pH-dependent pathway utilized by HSV-1 in corneal fibroblasts (CF) and CHO cells, because HSV-1 entry was inhibited by cytochalasin D (19). Thus, the dependence of actin during entry appears to be dictated by the pathway of entry and type of cell infected.

In actin-dependent entry, initial binding to the cell surface can influence cortical actin. For example, binding of HSV-1 gD to the surface receptor nectin-1 (a member of the immunoglobulin superfamily and also known as HveC and CD111) stimulates Rho GTPase signaling, which in turn can alter the morphology of cortical actin. In cell lines such as CF, Madin-Darby canine kidney II (MDCKII) and CHO cells, HSV-1 entry has been shown to induce Cdc42 signaling (69). During entry into CHO cells expressing HSV-1 receptors, HSV-1 virions induce and attach to protrusions from the plasma membrane (19). The presence of these protrusions correlates with RhoA activation. A model was proposed in which virions move along these protrusions (a process also known as “surfing”) to portions of the cell body for eventual entry in an actin-dependent phagocytosis-like uptake (19). Phagocytosis and another form of endocytosis, known as macropinocytosis, have many similarities. These similarities include the requirement for actin, Rac1 and Cdc42. In contrast, phagocytic cells (e.g. macrophages) require RhoA in addition to Rac1 and Cdc42 (95). Differently from the CHO cells, inhibition of RhoA activation did not block HSV-1 entry into MDCKII cells (69).

In these cells entry correlates with Cdc42 and Rac1 activation rather than RhoA (69). As another example of cell specific roles of actin in entry, evidence indicates that HSV-1 utilizes a pH-dependent endocytotic pathway to infect keratinocytes (106). Despite the fact that such pathways normally require activation of Rho GTPases, another study demonstrated HSV-1 entry into keratinocytes was insensitive to knock-down of Rac1, Cdc42 or RhoA. Therefore, entry in these cells may utilize a novel and, as of yet, unidentified entry pathway (114). In contrast, the gamma herpesvirus KSHV gB mediates entry through association with the α3β1 integrin receptor and activates Rac1, Cdc42 and RhoA. As might be expected from activation of these Rho GTPases, KSHV induces the formation of actin stress fibers, filopodia and ruffling within 30 minutes post infection of human foreskin fibroblast cells (104).

PrV entry into sensory neurons of the trigeminal ganglion, which is an important step for the establishment of latent infections, induces the formation of varicosities (bulges or swellings along neuronal axons) or synaptic boutons (27). Glycoprotein D was found to be both necessary and sufficient for formation of these virally-induced varicosities, and this formation was dependent upon Cdc42 but not Rac1 or RhoA (27). Synaptic boutons have also been shown to be important egress sites for both PrV (14,27) and HSV-1 (133).

Herpesviruses and Nuclear Actin

Once internalized into the cell, the capsid must deliver the viral genome

into the nucleus. Trafficking the sometimes considerable distance from the cell periphery to nucleus (axons of some sensory neurons are many centimeters in length) is mediated by microtubules and the molecular motor dynein (32,144). As the cell begins transcribing viral genes and replicating the viral DNA, viral replication compartments form and the host chromatin is marginalized to the nuclear periphery. The HSV-1 infected nucleus also expands at about 8 hours post infection (143). This nuclear expansion as well as marginalization of host chromosomes has been shown to require G-actin (143).

In HSV-1 infected Hep2 cells, nucleocapsid movement was shown to be sensitive to ATP depletion by sodium azide, decreased temperature, the actin depolymerizing agent latrunculin A and butanedione monoxime (BDM), a chemical inhibitor of myosin motors (43). These results suggest that herpesvirus nucleocapsids move toward the inner nuclear membrane in directed and ATP-dependent manner as opposed to free diffusion. Additionally, intranuclear movement was insensitive to cytochalasin D, implying that nucleocapsids may be utilizing non-classical actin that lacks the binding site for this drug. Future work is needed to determine definitively if a myosin motor is trafficking capsids to the nuclear periphery along F-actin, and if so, the specific myosin involved.

As a possible explanation of the mechanism of nucleocapsid intranuclear movement, actin filaments have been shown to form within the nucleoplasm of infected cells. Specifically, serial-section block-face scanning electron microscopy (SBFSEM) and immunofluorescence demonstrated that nuclear F-actin closely associates with capsids in PrV infected neurons (41). Myosin Va

was also found to co-localize with F-actin and GFP-labeled capsids (41). The direct stimulus for the generation of nuclear actin filaments during herpesvirus infections is unclear. It is possible that these filaments in conjunction with an actin motor (e.g. myosin Va or other processive myosins) provide the ATP-dependent force for nucleocapsid movement.

An electron tomography study of HSV-1 nucleocapsids budding into the perinuclear space revealed 8-19 nm fibers resembling F-actin, which appeared to be connecting the capsid to the primary envelope (5). It is also possible that these fibers represent tegument proteins, including the nuclear envelopment complex containing pUL31/pUL34 or proteins associated with them. The nuclear envelopment complex is essential for HSV-1 budding into the perinuclear space (123).

Based on this body of evidence, it seems plausible that herpesvirus nucleocapsids induce nuclear F-actin polymerization and utilize or recruit a myosin motor to traffic capsids to the inner nuclear membrane for primary envelopment.

Virion Egress and Actin

Late in infection the alphaherpesvirus kinase U_S3 plays a major role in nuclear egress, but also is responsible for depolymerizaion of actin stress fibers (124,139,163). In PrV infections, the U_S3 kinase causes both actin stress fiber disassembly and the generation of actin-containing cellular extensions in sparsely seeded swine testicle cells (40). These cellular extensions did not form with a U_S3-null virus or in cells treated with the actin-

stabilizing drug jasplakinolide (40). These protrusions are important for cell to cell spread, particularly in sparsely seeded cells (40). The U_S3 kinase has been shown to bind and phosphorylate (activate) group A p21-activated kinases (PAKs), which are downstream effectors of Cdc42/Rac1 Rho GTPase signaling pathways (160). In mouse embryo fibroblasts (MEFs), U_S3-mediated disassembly of actin stress fibers required PAK2 and the formation of cellular projections required PAK1 (160). Sparsely seeded MEFs derived from PAK1 knock-out mice resulted in reduced PrV spread, but PAK1 was dispensable for viral spread in monolayers, while MEFs derived from PAK2 knock-out mice were impaired for PrV spread in both sparsely seeded and MEF monolayers (160). It is tempting to speculate that the U_S3-induced cell extensions may be important primarily when infected cells are not in direct contact with neighboring target cells. The contribution of these extensions for virus spread in vivo requires further study.

Actin has been shown to be present in purified herpesviruses. How this incorporation takes place as well as its potential role in infection is unknown. It is possible that the presence of F-actin in virions plays a structural role, since incorporation was enriched in PrV virions lacking tegument components (28,99,171).

Myosin motors have also been shown to be involved in viral egress. In HSV-1, the tegument protein VP22 has been shown to interact with non-muscle myosin IIA (NMIIA) (161). Additionally, treatment of Vero cells with the myosin inhibitor BDM at 12 hpi reduced HSV-1 secretion 20-fold and had little effect on the amount of cell-associated virus produced (161). NMIIA is a non-

processive motor that regulates F-actin by cross-linking and contracting actin filaments (22,162). It has also been shown to be important for fusion pore expansion during exocytosis, which could have implications for virions as they escape from the TGN-derived vesicles and enter the extracellular environment (105). Recently NMIIA and F-actin, along with Rab6, were shown to be required for the fission of vesicles emerging from the Golgi complex (101). In cells where NMIIA or Rab6 were inhibited or knocked down, tubules were observed to emanate from the Golgi apparatus representing unfissioned budding vesicles. Protein kinase D (PKD) has been similarly described as required for membrane fission at the TGN (9) and for HSV-1 egress (120). This presents the possibility that NMIIA, along with Rab6 and PKD, is important for generating vesicles distinct from the Golgi that are free to traffic to the plasma membrane for virion release. Inhibition of NMIIA would prevent these vesicles from severing, but would likely not decrease intracellular infectivity (assuming the unfissioned, emerging tubules are competent for viral budding), consistent with previous observations (161).

Myosin Va (myoVa) is known to be important for secretion of melanosomes (174) and secretory granules (130) by providing transport through cortical F-actin. The transition between microtubule filaments and cortical actin has been described as a “capture” process where the microtubule motor kinesin traffics cargo to the cell periphery where myoVa is required for association of the cargo within the cortical actin and eventually secretion. MyoVa has also been linked to HSV-1 secretion as well as cell surface expression of at least gD, gB and gM (126). In this study, two red fluorescent protein (RFP)-tagged

dominant-negative isoforms (brain and skin) of myoVa were expressed during HSV-1 infection. Secretion of infectivity was down 50-75% compared to control cells expressing RFP alone. Under the same conditions, surface expression of gD, gB and gM were significantly decreased compared to RFP expressing control cells. It is possible that egressing virions within TGN-derived vesicles could behave similarly to other myosin dependent cargo. In this model, kinesin delivers virion-laden vesicles to cortical actin and myoVa transports the vesicles the remaining short distance to the plasma membrane for fusion. Thus, both NMIIA and myoVa may be involved in functionally distinct and important steps during egress of HSV-1 and likely other herpesviruses. Further work is needed to test the models proposed above and to fully understand the roles of actin and myosin motors during herpesvirus infections.

Conclusion

Like all viruses, herpesviruses are obligate, intracellular pathogens relying on host machinery to replicate and spread. Actin plays a critical and diverse role in the cell and in the lifecycle of herpesviruses. In this way, virology research is useful not only for expanding our understanding of how viruses function, but help reveal the intricate biology of our own cells. Many details about the interaction of herpesviruses with actin remain to be investigated. For example, it would be of interest to know what specific viral proteins interact with host myosin motors and how myosin-driven activities are regulated during infection. Nuclear actin is an emerging area of study in virology, as well as cell biology. A better understanding of how nuclear F-actin formation is triggered

and how it contributes to viral infection would be of great interest to both fields. Elucidating the mechanism behind the ATP-, F-actin and possibly myosin-dependent movement of nucleocapsids would be an important discovery for nuclear trafficking events. Undoubtedly, much remains to be learned from the interplay of virus and host.

Figure 2.2 Model of herpesvirus entry, maturation and egress. (A) Herpes virion “surfing” towards the plasma membrane along membrane protrusions for entry. (B) Capsid trafficking toward the nuclear periphery for budding via a myosin motor on F-actin. (C) U_S3-mediated depolymerization of actin stess fibers. (D) U_S3-mediated generation of membrane projection and cell-to-cell spread of herpesvirus. (E) Myosin IIA- and Rab6-dependent fission of nascent vesicles from the Golgi body. (F) Enveloped virion within a TGN-derived vesicle trafficking through cortical actin via myosin Va toward the plasma membrane for secretion.

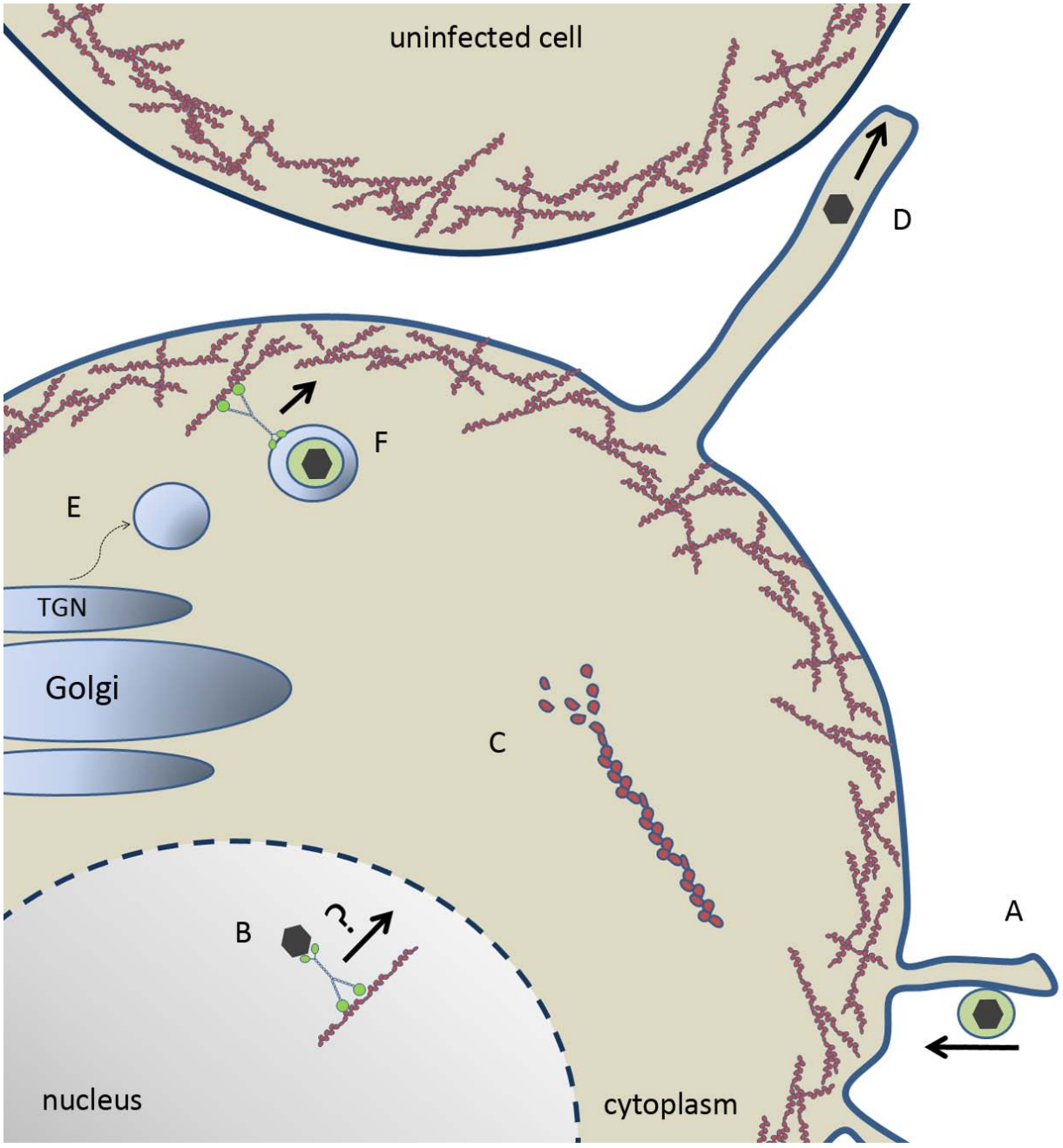
uninfected cell
D
F
E
TGN
Golgi
C
B
?
A
nucleus
cytoplasm

CHAPTER III

Myosin Va enhances secretion of herpes simplex virus 1 virions and cell surface expression of viral glycoproteins*

Kari L. Roberts and Joel D. Baines, Department of Microbiology and Immunology, Cornell University, Ithaca, NY 14853.

*Reprinted from **Roberts, KL, J.D. Baines.** (2010). Myosin Va enhances secretion of herpes simplex virus 1 virions and cell surface expression of viral glycoproteins. J Virol 84:9889-9896.

Abstract

The final step in the egress of herpes simplex virions requires virion-laden vesicles to bypass cortical actin and fuse with the plasma membrane, releasing virions into the extracellular space. Little is known about the host or viral proteins involved. In the current study, we noted that the conformation of myosin Va (myoVa), a protein known to be involved in melanosome and secretory granule trafficking to the plasma membrane in melanocytes and neuroendocrine cells, respectively, was altered by four hours after infection with HSV-1 such that an N-terminal epitope expected to be masked in its inactive state was rendered immunoreactive. Wild type myoVa localized throughout the cytoplasm and to a limited extent in the nucleus of HSV-infected cells. Two different dominant negative myoVa molecules containing cargo-binding domains but lacking the lever arms and actin-binding domains co-localized with markers of the trans-Golgi network. Expression of dominant negative myoVa isoforms reduced secretion of HSV-1 infectivity into the medium by 50-75%, reduced surface expression of glycoprotein B, M and D and increased intracellular virus infectivity to levels consistent with increased retention of virions in the cytoplasm. These data suggest that myoVa is activated during HSV-1 infection to help transport virion- and glycoprotein-laden vesicles from the TGN, through cortical actin, to the plasma membrane. We also cannot exclude a role for myoVa in promoting fusion of these vesicles with the inner surface of the plasma membrane. These data also indicate that myoVa is involved in exocytosis in human epithelial cells as well as other cell types.

Introduction

Herpes simplex virus virions, like those of all herpesviruses, comprise a lipid envelope surrounding a layer of proteins called the tegument that covers the surface of the proteinaceous DNA-containing capsid. After assembly in the nucleus, herpes simplex virus nucleocapsids bud through the inner nuclear membrane to obtain an initial virion envelope. In the most widely accepted model of virion egress, the envelopes of nascent virions residing in the perinuclear space then fuse with the outer nuclear membrane, releasing the de-enveloped capsid into the cytoplasm (147). The now cytosolic capsid then buds into a membranous organelle in the cytoplasm to obtain its final envelope. The site of secondary envelopment where the final budding event occurs is believed to contain markers of the trans-Golgi network (158) and would be expected to contain the full complement of virion envelope and tegument proteins. Cellular budding machinery would also be expected to be involved, such as that required for multivesicular body formation (10,25). Other models of virion egress propose that nucleocapsids can exit the nucleus through an expanded nuclear pore (167,168), or that the original virion envelope derived from the inner nuclear membrane is retained throughout egress (71). In the latter scenario, enveloped virions are incorporated into a vesicle derived from the outer nuclear membrane. This model is not consistent with the observations that a membrane protein encoded by U_L34 along with its tegument binding partner encoded by U_L31 are present in perinuclear virions, but absent from extracellular virions (44,124).

Regardless of the prior steps involved, all models of virion egress propose a similar final step, namely that vesicles bearing one or more complete enveloped virions are transported to and fuse with the plasma membrane, releasing the virions into the extracellular space. The extent to which this final exit step contributes to the life cycle is virus and cell type dependent. For example, approximately 10% of total infectivity is secreted into the extracellular space of cultured Vero cells infected with herpes simplex virus 1 (HSV-1), whereas Varicella Zoster Virus remains almost completely cell associated in cultured MeWo cells (12). Despite general agreement that it occurs, the mechanism by which the virion-laden vesicles are transported to the plasma membrane has not been studied extensively. Myosin Va (myoVa) is a good candidate to mediate such transport because this motor has been shown to be important for the egress of melanosomes (174) and secretory granules (130) by facilitating their transport through the cortical filamentous actin (F-actin) located beneath the plasma membrane. The mechanism underlying this vesicle transport has been described as a “dual transport“ process whereby cargoes brought to the cortex via microtubule-associated motors (such as kinesin) are subsequently transferred to cortical F-actin. Egress is then facilitated by myoVa (174) which moves along F-actin by processive (consecutive) “hand over hand” steps through a series of ATP hydrolysis reactions [for review see (56,159)]. The motor consists of two heavy chains that dimerize to form duplicate N terminal head domains (the actin- and nucleotide-binding region) extending into lever arms, a single coiled-coil dimerization tail domain, and two C-terminal globular tail domains (GTDs),

which are believed to bind cargo.

The RNA encoding the tail domain of myoVa is alternatively spliced (141,150), causing variations in different isomers encoded by exons B, D and F (encoding 3, 27 and 25 amino acids, respectively). Cargo recognition can be regulated by interactions between various effector proteins, including Rab family GTPases and different myoVa exons. Specifically, exon F is required for interaction with Rab27a (173), exon B is necessary to interact with dynein light chain 2 (DLC2) (64,165), and exon D is essential to bind Rab10 (127). Additionally, Rab11 is known to interact with class V myosins (24). Mutations in the human myoVa gene is the cause of Griscelli syndrome, which can manifest with severe neurological impairment and/or hypopigmentation depending on the locus of the mutation (94,112).

Given its known role in vesicle secretion, the current study investigates a potential role for myoVa in the secretion of HSV-1 virions. In the course of these studies, dominant negative myosin Va (DN-myoVa) constructs were used. These contained the exon-encoded portion of the myoVa tail domain as well as the entire (~400 amino acids) GTD. To address the effects of alternative splicing, and by extension, involvement of different effectors in secretion, we used two DN-myoVa constructs. The MCLT (from melanocyte long tail) construct contained exons D and F but lacked exon B, whereas the brain long tail (BRLT) construct contained exon B, but not D or F.

Materials and Methods

Viruses and Cells

Wild type HSV-1 strain F (HSV-1[F]) and HSV-1 U_L13 deletion virus (R7355) were kindly provided by Bernard Roizman and have been described previously (35,124). vRR1204 (a kind gift from Richard Roller) contains a lysine to alanine mutation at codon 220 in the U_S3 open reading frame that precludes its kinase activity (131). The K26 virus, kindly provided by Prashant Desai, encodes a VP26 capsid protein fused to GFP. Virus stocks were propagated and titered on Vero cell monolayers, which were maintained in growth medium, consisting of Dulbecco's modified Eagle's medium (DMEM) supplemented with 125 units/mL penicillin, 0.125 mg/mL streptomycin and 10% newborn calf serum. After infection, cells were overlayed with 199V medium (DMEM supplemented with 1% newborn calf serum) and monitored for cytopathic effects. To release intracellular virus, the cells were lysed by freezing and thawing.

Plasmids and Transfections

Dominant negative myosin Va (DN-myoVa) constructs contained the exon-encoded portion of the myoVa tail domain as well as the GTD. MCLT stands for Melanocyte Long Tail. BRLT stands for Brain Long Tail. Both isoforms were kindly provided by Dr. John Hammer III.

The dominant negative myoVa isoforms were excised from their supplied vectors by digestion at flanking Not-I restriction sites and ligated into Not-I digested pcDNA3 (Invitrogen). Monomeric red (mRED) was amplified by

polymerase chain reaction (PCR) such that the amplicon ends contained HindIII/EcoRI sites and a mutation changing the stop codon to alanine. Primers used for this purpose were:

5'-AAAAAGCTTATGGCCTCCTCCGAGGACG-3'

Rev primer:

5'-AAAGAATTCCCTGCGGCGCCGGTGGAGTGGCGG-3'.

The amplicon was ligated into the respective pcDNA3 constructs in frame with the 5' ends of the MCLT and BRLT open reading frames. The genotypes of plasmid DNAs were verified by DNA sequencing.

For transfections, cells were transfected when they were approximately 90% confluent with approximately 1.6 µg of plasmid DNA per well in 12-well dishes or 4.0 µg of plasmid DNA per well in 6-well dishes using Lipofectamine 2000 (Invitrogen) according to the directions of the manufacturer.

Immunofluorescence

At 28.5 hours post transfection, the cells were either mock infected or infected with 5.0 PFU/cell of HSV-1(F) or 10 PFU/cell with HSV-1 K26 as indicated. The cells were washed once with phosphate buffered saline (PBS), fixed in 3% paraformaldehyde (PFA) for 15 minutes, and autofluorescence was quenched by immersion in 50 mM NH_4Cl for 15 minutes. In some experiments, the cells were permeabilized with 0.1% Triton-X 100 for 2 minutes followed by a 10 minute block in 10% human serum in PBS. When probing for surface gD, all the steps remained the same, except treatment with Triton-X 100 was omitted. Goat anti-Myosin Va (1:50, Santa Cruz

Biotechnology), rabbit anti-Myosin Va (1:50, Santa Cruz Biotechnology), mouse anti-ICP4 (1:100, Rumbaugh-Goodwin Institute for Cancer Research, Plantation, FL), rabbit anti-ICP8 (1:500, a kind gift from Bill Ruyechan), mouse anti-TGN38 (1:100, BD Transduction Labs cat. no. 610898), and mouse anti-Golgi 58K (1:100, Abcam cat. no. ab6284) primary antibodies were prepared in a 1% bovine serum albumin (BSA)/PBS solution. The mouse anti-gD (DL-6) monoclonal antibody (kindly provided by Roselyn Eisenberg and Gary Cohen) and rabbit anti-gB (kindly provided by David Johnson) was diluted in 1% BSA/PBS 1:100 (or 1:200 in permeabilized cells for gD). The rabbit anti-gM antibody was diluted 1:500 in 1% BSA/PBS. All primary antibodies were incubated with the fixed cells for 30-60 minutes in a humidity chamber held at room temperature. After washing 3 times in PBS, the cells were reacted for 30-60 minutes in a humidity chamber with secondary antibodies FITC-conjugated anti-goat or FITC-conjugated anti-mouse and/or Texas Red or Cy5 conjugated anti-rabbit IgG (Jackson Laboratories) diluted 1:100 in 1% BSA/PBS. The coverslips were then rinsed 3 times in PBS and dipped in ddH20 before mounting on glass slides with mowiol plus 2.5% DABCO to prevent photobleaching. All digital images except for those used for surface gD quantification were taken using an IX70 Olympus confocal microscope and were processed with Adobe Photoshop software. Digital images for gD quantification were taken using a Zeiss Axio Imager.M1 fluorescent microscope and analyzed with IP Lab v3.65a software from Scanalytics.

Immunoblot Analyses

Mock infected and HSV-1(F) infected HEp-2 cells were washed once in PBS then lysed in 100 µL of 2X sodium dodecyl sulfate-polyacrylamide gel electrophoresis (SDS-PAGE) sample buffer (100 mM TrisCl [pH 6.8], 200 mM dithiothreitol, 4% SDS, 20% glycerol, 0.2% bromophenol blue). Lysates were sonicated and boiled for 5 minutes prior to loading. Samples were separated on a 10% polyacrylamide gel and transferred to a nitrocellulose membrane (30 volts for 3.5 hours at 4°C). The membrane was blocked in 5% milk/TBST (1X tris-buffered saline plus 0.1% Tween) for 1 hour at room temperature. Primary antibodies: goat anti-myoVa (1:200, Santa Cruz Biotechnology), rabbit anti-ICP8 (1:10000) and mouse anti-lamin A/C (1:1000, Santa Cruz Biotechnology). Bound primary antibody was detected by addition of anti-goat or anti-rabbit (1:2000, Santa Cruz Biotechnology) horseradish peroxidase-conjugated secondary antibody diluted in 5% milk/TBST and visualized by enhanced chemiluminescence (Pierce) followed by exposure to X-ray film (Pierce).

Analyses of Virion Egress

HeLa cells were transfected as described above. At 15-28 hours post transfection, approximately 0.1 PFU HSV-1(F) per cell in 1 mL 199V was added to each well. The cells were incubated for 1 hour at 37°C with gentile agitation and subsequently washed 3 times with versene (1X PBS and 0.5 mM ethylenediaminetetraacetic acid [EDTA]) and once with a low pH buffer (40 mM citric acid [pH 3.0], 10mM KCl, 135 mM NaCl) to inactivate any residual

infectitivity. This overlay was then removed and 1.5 mL of 199V was added to each well. The 0 hpi time point samples were collected immediately and the remaining samples were incubated at 37°C/5% CO2 for another 20 hours. To assess infectivity, parallel cultures of cells and/or overlaying medium was freeze-thawed to release virus, diluted serially, and subjected to plaque assay on Vero cell monolayers. To check expression of the myoVa constructs, total cell lysates of infected HeLa cells beneath collected supernatants were collected and analyzed by immunoblot as described above. Rabbit anti-RFP antibody (1 µg/mL, GenScript) was used to detect expression of mRED-DN-myoVa MCLT, mRED-DN-myoVa BRLT, and mRED.

Glycoprotein surface expression analysis

HEp-2 cells expressing either mRED, mRED-DN-myoVa BRLT or mRED-DN-myoVa MCLT were infected with HSV-1 K26-GFP (MOI=10 PFU/cell) or mock infected and fixed in 3% PFA at 17 hpi. Fixed cells were immunostained without permeabilization as described above. At least 50 infected cells expressing each construct type were digitally recorded using a Zeiss Imager.M1 Axio fluorescent microscope and the images were analyzed to quantify surface gD expression using IP Lab v6.35a software from Scanalytics, Inc.

Results

Immunoreactivity of Myosin Va is increased during HSV-1 Infection.

The intracellular environment of host cells is highly viscous and not

conducive to free diffusion of HSV-1 particles [for review see (85)]. Myosin Va (myoVa) is an unconventional actin motor which, through ATP hydrolysis, moves cargo along polar actin fibers towards the plus (or barbed) end. In an effort to determine if HSV-1 utilizes this actin motor, we performed immunofluorescence assays to reveal the localization of myoVa in HSV-1(F) infected and mock infected HEp-2 cells. Cells were seeded onto coverslips in a 12-well dish and infected with wild type HSV-1(F) or were mock infected. At 0, 4, 10, 16 and 22 hours post infection (hpi), cells were washed with PBS and fixed in 3% paraformaldehyde (PFA). Fixed cells were permeabilized in 0.1% Triton-X 100, blocked in 10% human serum and were immunostained with goat anti-myoVa and rabbit anti-ICP8 antibodies.

As shown in figure 3.1, the amount of myoVa immunoreactivity increased extensively during the course of infection. This increase was first detectable at 4 hpi, and increased significantly by 16 hpi. MyoVa immunoreactivity localized primarily to the cytoplasm at these time points, although some cells demonstrated substantial intranuclear immunostaininig. By 22 hpi, myoVa immunostaining localized primarily to infected nuclei. Similar results were obtained using Vero and HeLa cells (figure 3.2).

Steady state levels of Myosin Va Protein are Unchanged in HSV-Infected Cells.

To determine whether or not the increased immunoreactivity reflected an increase in steady state levels of myoVa, we analyzed the amount of myoVa

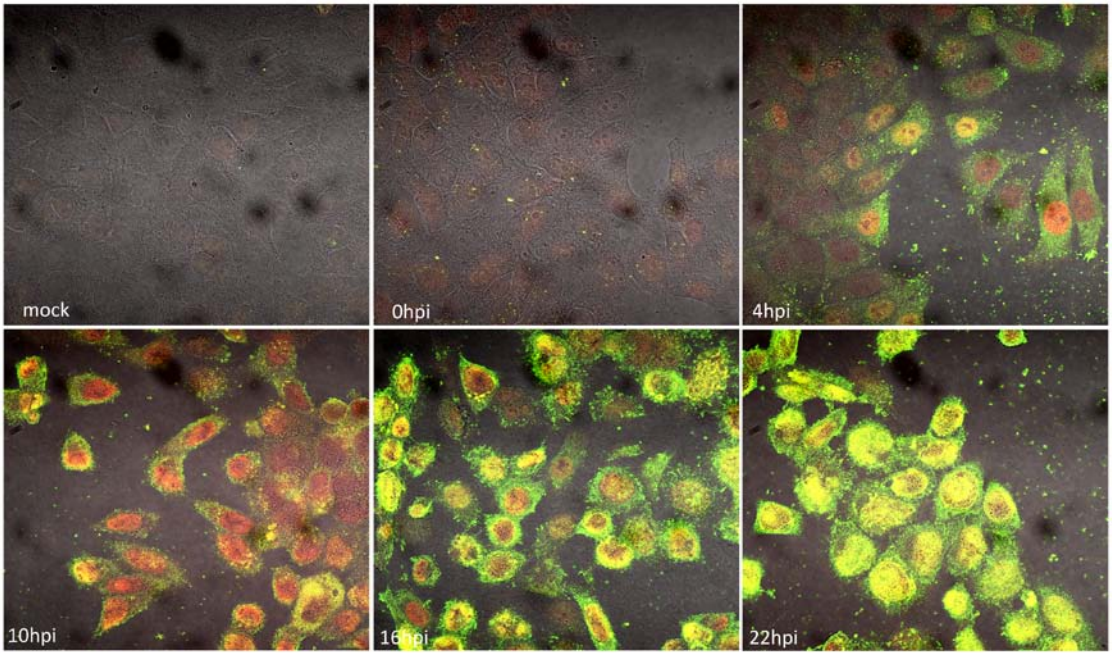

Figure 3.1 Immunoreactivity of myosin Va is increased during HSV-1 infection. HEp-2 cells were mock infected or infected with 5 PFU HSV-1(F) per cell and fixed at 4, 10, 16 and 22 hpi. Cells were washed with PBS and fixed in 3% paraformaldehyde (PFA) for 15 minutes and permeabilized with 0.1% Triton-X 100. The fixed permeabilized cells were immunostained with goat anti-myoVa and rabbit anti-ICP8 antibodies. Single sections of immunostained cells were digitally collected with an Olympus confocal microscope. Green: anti-myosin Va; red: anti-ICP8.

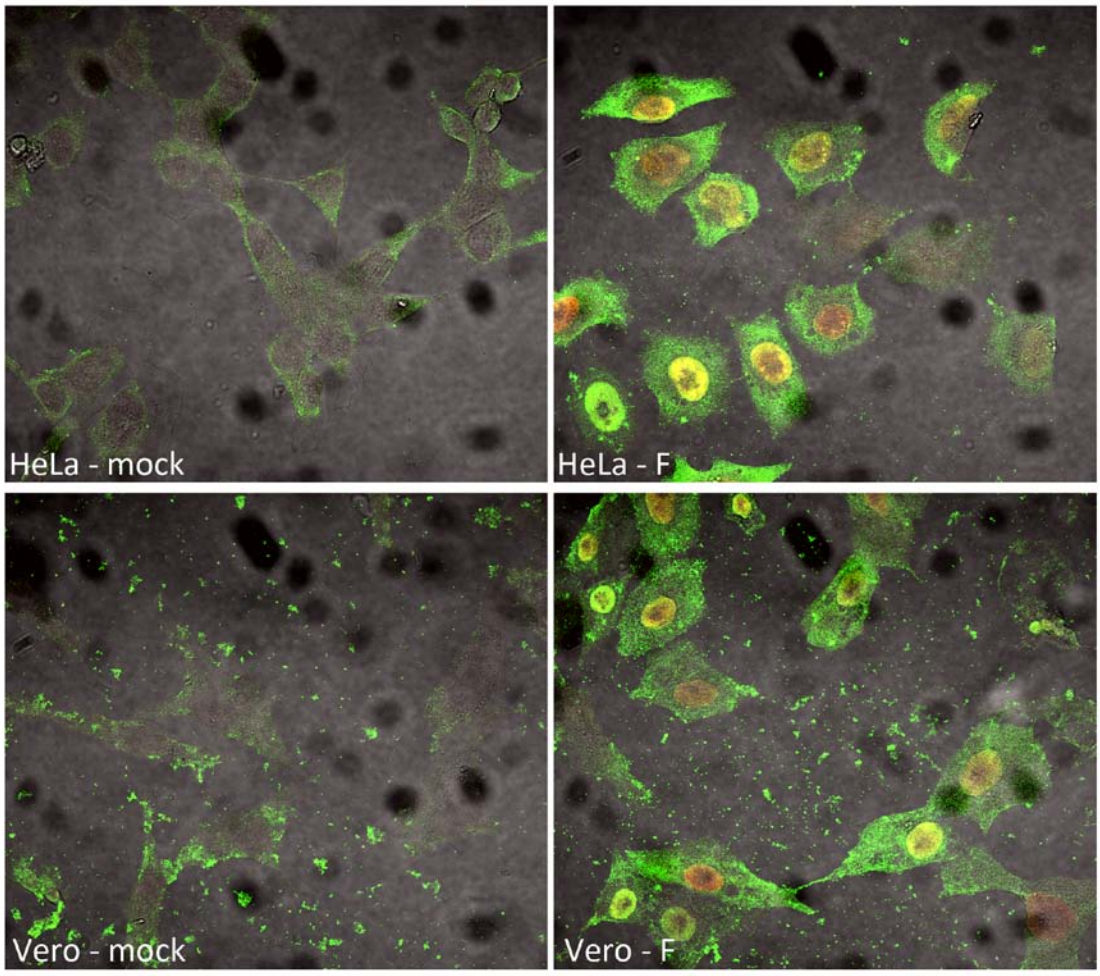

Figure 3.2 Immunoreactivity of myosin Va is increased during HSV-1 infection in multiple cell types. HeLa and Vero cells were mock infected or infected with 5 PFU HSV-1(F) per cell and fixed at 6 hpi. Cells were washed with PBS and fixed in 3% PFA for 15 minutes and permeabilized with 0.1% Triton-X 100. The fixed permeabilized cells were immunostained with goat anti-myoVa and rabbit anti-ICP8 antibodies. Single sections of immunostained cells were digitally collected with an Olympus confocal microscope. Green: anti-myosin Va; red: anti-ICP8.

protein in total cell lysates of mock infected or HSV-1(F) infected HeLa cells (collected over several time points) by immunoblot assay. We also probed the immunoblot with antibodies to ICP8 and lamin A/C as an infection control and loading control, respectively.

As shown in figure 3.3, similar levels of myoVa were detected in mock and all HSV-1(F) infected cell lysates collected at five different time points. Since phosphorylation can also play a role in epitope recognition and activation of myosins, we examined cells infected with a U_S3 kinase-dead mutant HSV-1 (131) as well as an HSV-1 mutant lacking the U_L13 kinase (118) by immunofluorescence. Fluorescent signals from the myoVa antibody were similar to that of HSV-1(F) in both mutant backgrounds (figure 3.4), indicating that these viral kinases were not responsible for the conformational change in myoVa.

A Myosin Va Epitope is Exposed Preferentially in HSV-Infected Cells.

The goat polyclonal antibody used above is directed against (Santa Cruz Biotechnology, sc-17707) an epitope within the N-terminal motor domain of myoVa (amino acids 117-137). This epitope is located near an N terminal region that interacts with a C-terminal domain to hold the myosin molecule in the folded (inactive) conformation. We therefore asked whether a second myoVa antibody binding to an epitope that would be exposed in both the folded (inactive) and extended (active) conformations would produce similar levels of fluorescent intensity upon immunostaining mock- and HSV-infected

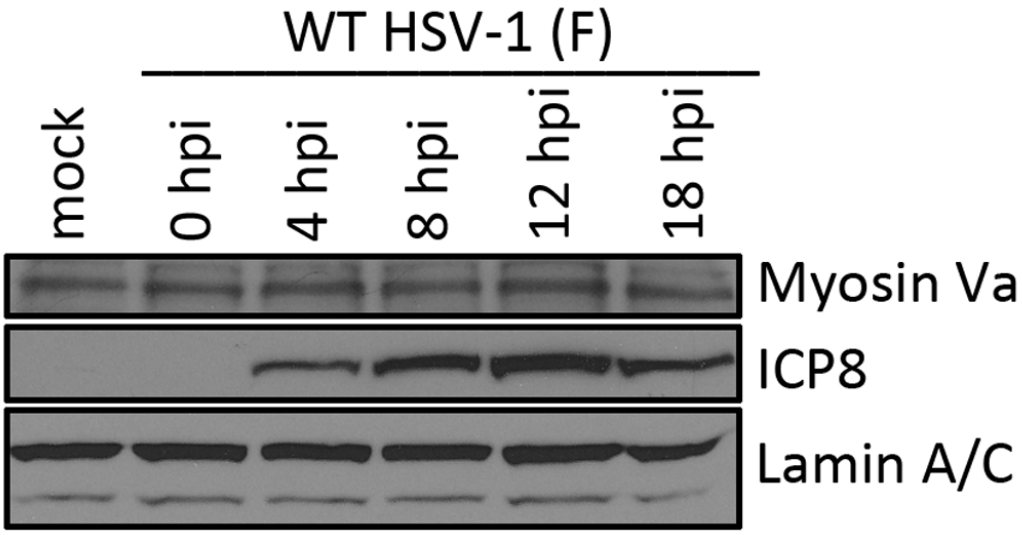

Figure 3.3 Steady state levels of myosin Va protein are unchanged in HSV-infected cells. Immunoblot showing levels of myosin Va in mock and HSV-1(F) infected HEp-2 total cell lysates. Cells were mock infected or infected with 5 PFU per cell HSV-1(F), lysed in 2X denaturing buffer at 18 hpi, and proteins were separated on a polyacrylamide gel and transferred to nitrocellulose. The blots were probed with a goat anti-myoVa antibody and rabbit anti-ICP8 antibody. Immunoreactivity of goat anti-lamin B antibody served as a loading control.

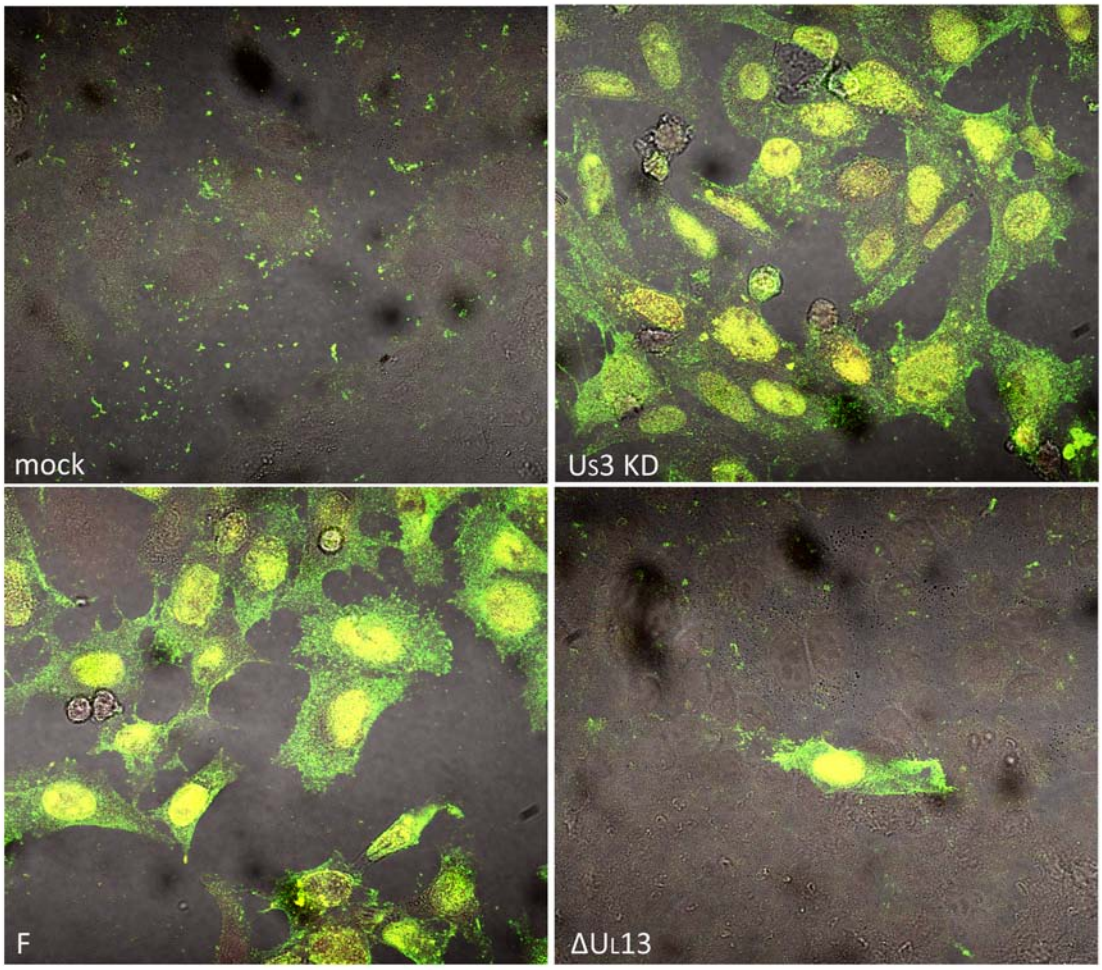

Figure 3.4 Viral kinases pU$_S$3 and pU$_L$13 are not required for increased immunoreactivity of myosin Va during HSV-1 infection. HEp-2 cells were mock infected or infected with HSV-1(F), U$_S$3 kinase dead or ΔU$_L$13 and fixed at 18 hpi. Cells were immunostained and photographed as described in figure 3.1. Green: anti-myosin Va; red: anti-ICP8.

cells. To address this possibility, HeLa cells were either mock infected or HSV-1 infected and co-immunostained with the original goat polyclonal antibody to myoVa, and a second polyclonal antibody made in rabbits that binds to amino acids 981-1070 (Santa Cruz Biotechnology, sc-25726) in the myoVa tail dimerization domain. The cells were also Immunostained with a mouse anti-ICP4 antibody to mark infected cell nuclei. The results are shown in figure 3.5.

Examination of the immunostained cells by confocal microscopy revealed that the tail-specific myoVa antibody stained mock and HSV-infected cells similarly (red), whereas the previous myoVa antibody recognizing the N-terminal epitope (green) preferentially stained HSV-infected cells. These data, taken together with that shown in figure 3.3, suggest that the increase in myoVa immunoreactivity results from unmasking of the myoVa epitope rather than an increase in protein level. We speculate that this unfolding reflects activation of myoVa in HSV-infected cells.

DN-MyoVa Co-localizes primarily with the TGN in HSV-1(F) Infected Cells.

Because HSV-1 virions are thought to transit into or near the trans-Golgi network (TGN) on their way to the extracellular space (158), we hypothesized that expression of a dominant negative myoVa motor would block HSV-1 virion secretion by inhibiting virion-laden TGN vesicles from passing through cortical F-actin. One prediction of this hypothesis is that dominant negative myoVa would localize at the TGN because the globular domain would bind to these vesicles and the absence of the actin-binding domain would preclude

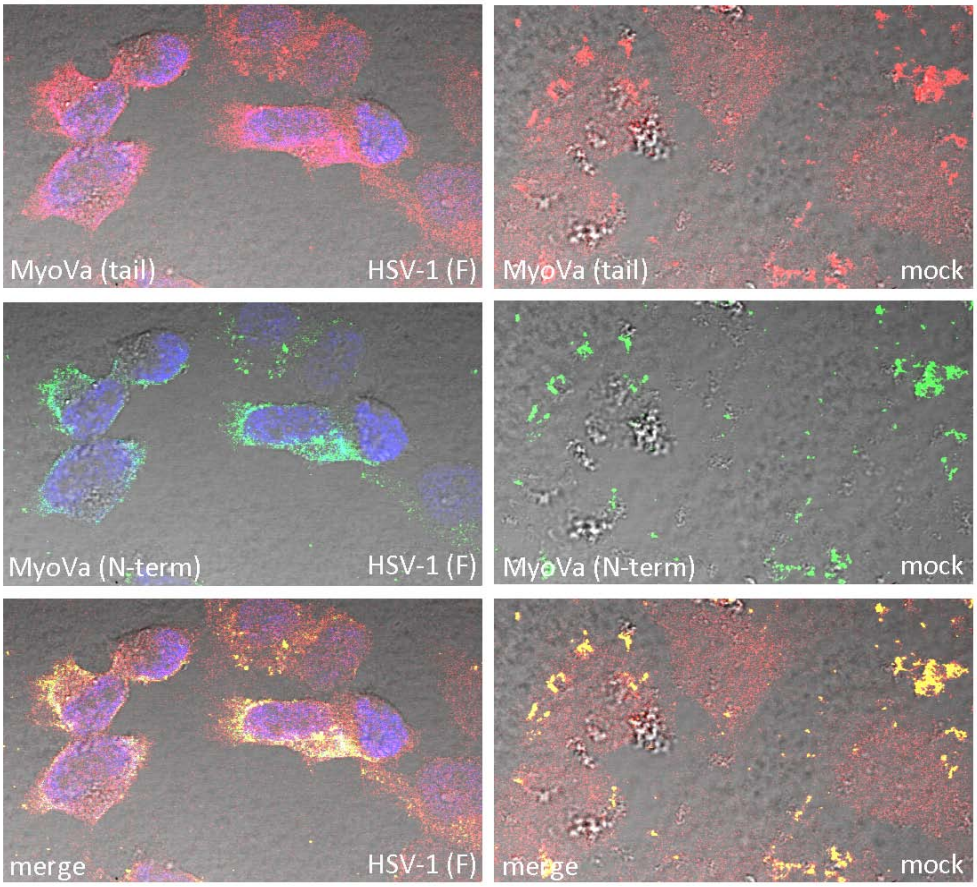

Figure 3.5 A myosin Va epitope is exposed preferentially in HSV-infected cells. HeLa cells were mock infected or infected with HSV-1(F) (MOI = 5 PFU per cell). At 16 hpi the cells were washed in PBS, fixed in 3% PFA for 15 minutes and permeabilized with 0.1% Triton-X 100. Fixed cells were immunostained with rabbit anti-myosin Va (top row) or goat anti-myosin Va (center row). Mouse antibody to ICP4 was used to mark infected cell nuclei. Red: myoVa (epitope in tail region); green: myoVa (epitope in N terminal region); blue: ICP4.

movement to the plasma membrane. To test this prediction, we transfected HeLa cells with the mRED-DN-myoVa constructs and compared localization of mRED-DN-myoVa to TGN and Golgi markers. The results are presented in figure 3.6.

At high PMT levels or in stacked images, the mRED and DNmyoVa constructs localized throughout the cytoplasm, making it difficult to discern the predominant localization of the proteins. At lower PMT settings, image slices taken with a confocal microscope showed that the mRED-DN-myoVa isoforms concentrated within cytoplasmic puncta that were not present in the mRED-expressing control cells. Some of these puncta co-localized with sites containing substantial immunostaining with the TGN38 marker. We did not see substantial co-localization between cytoplasmic foci bearing high concentrations of mRED-DN-myoVa isoforms and markers of the Golgi apparatus, although some overlap of the immunostaining was apparent even at low PMT settings. We found similar results in HEp-2 cells (figure 3.7). The data indicate that the DN-myoVa isoforms localize primarily at the TGN, and to a much lesser extent at the Golgi apparatus.

Myosin Va is Required for Efficient Secretion of HSV-1 infectivity, but not for production of intracellular infectivity.

To test our hypothesis that DN-myoVa impacts virion secretion, we transfected HeLa cells with the mRED-DN-myoVa isoforms and mRED control constructs and infected the cells the next day with HSV-1(F) at an MOI of 0.1

Figure 3.6 DN-myoVa co-localizes with TGN but not Golgi markers in HSV-infected HeLa cells. HeLa cells were transfected with mRED-DN-myoVa BRLT (left column), MCLT (center and right column). At 23 hours post transfection the cells were infected with HSV-1(F) at an MOI of 5 PFU per cell. At 16 hpi the cells were washed with PBS, fixed in 3% PFA for 15 minutes, and permeabilized with 0.1% Triton-X 100. Fixed cells were immunostained with mouse anti-TGN (top row, first and second columns) or mouse anti-Golgi markers (top row, right column). Rabbit anti-ICP8 was used to mark the infected cell nuclei. Red: DN-myoVa; green: TGN and Golgi; blue: ICP8. Arrows indicate sites of co-localization of the respective markers.

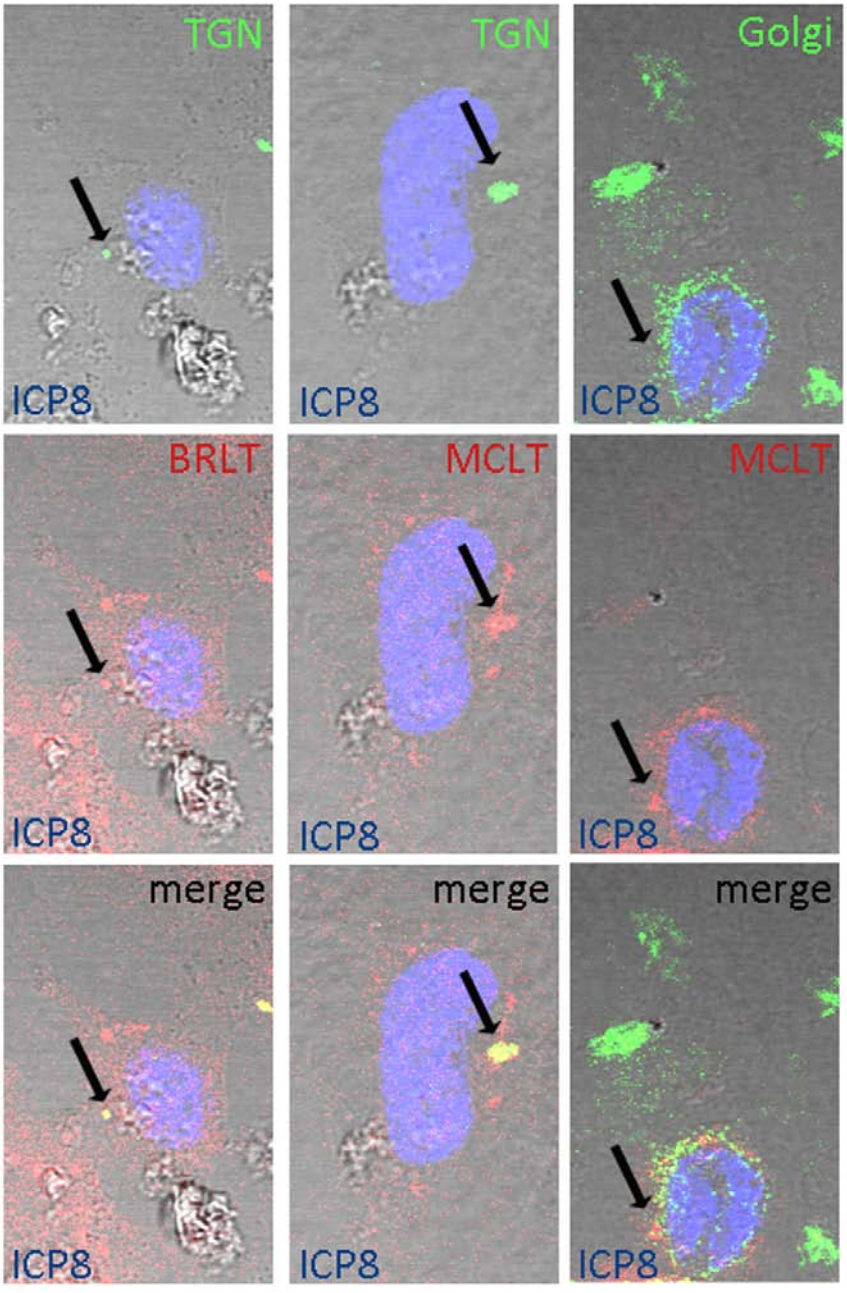
TGN
ICP8
TGN
ICP8
Golgi
ICP8
BRLT
ICP8
MCLT
ICP8
MCLT
ICP8
merge
ICP8
merge
ICP8
merge
ICP8

Figure 3.7 DN-myoVa co-localizes with TGN but not Golgi markers in virus infected HEp-2 cells. HEp-2 cells were transfected with mRED-DN-myoVa BRLT (upper row), MCLT (second row from top and bottom row), or an mRED control construct (third row from top), and at 28.5 hours post transfection were infected with HSV-1(F) at an MOI of 5. At 15.5 hpi cells were washed with PBS, fixed in 3% PFA for 15 minutes, and permeabilized with 0.1% Triton-X 100. Fixed cells were immunostained with mouse anti-TGN (top 3 rows) or mouse anti-Golgi markers (bottom row). Rabbit anti-ICP8 was used to mark the infected cell nuclei. Red: DN-myoVa or mRED control; green: TGN and Golgi; blue: ICP8. Arrows indicate sites of co-localization of the respective markers.

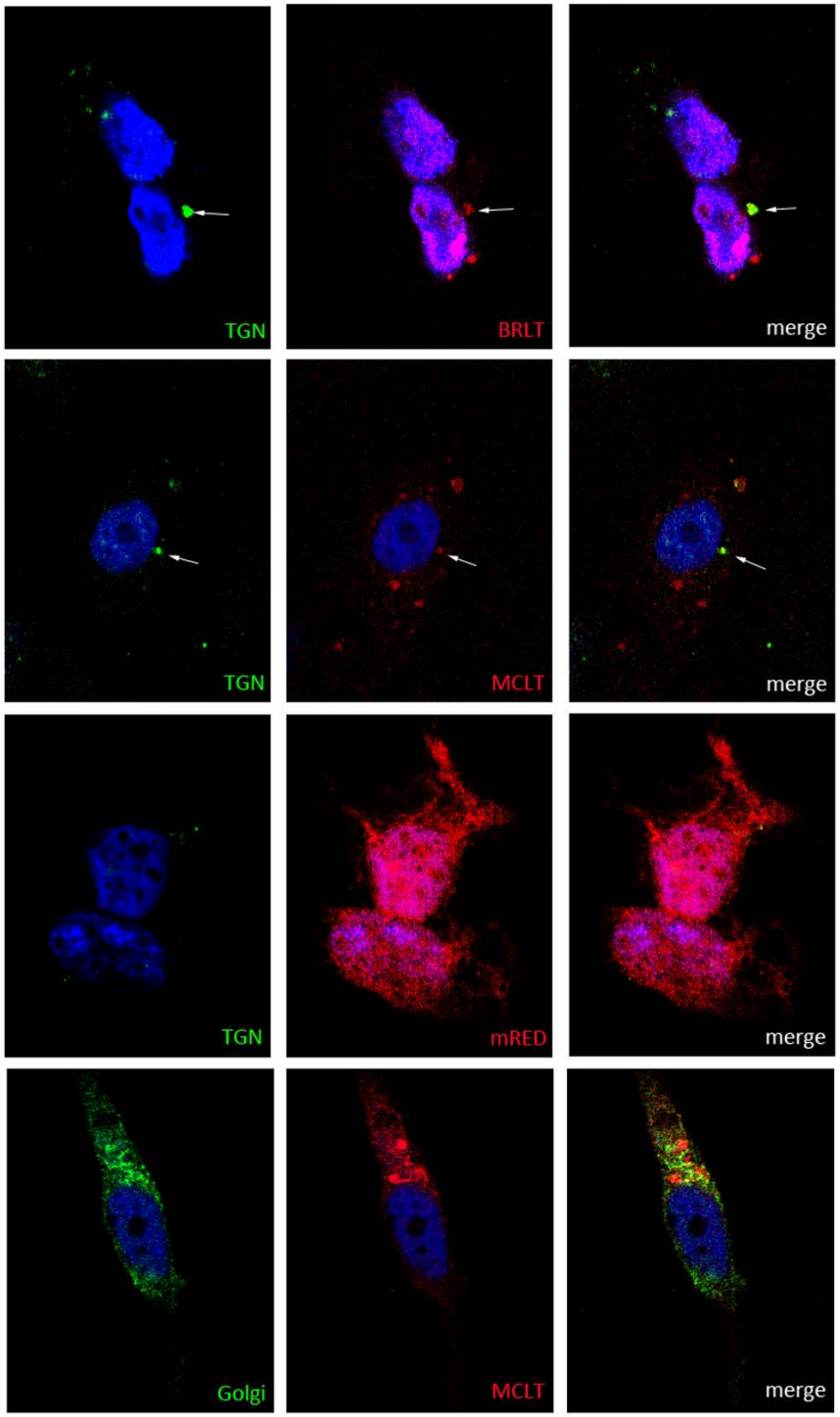
TGN
BRLT
merge
TGN
MCLT
merge
TGN
mRED
merge
Golgi
MCLT
merge

PFU per cell. After virus adsorption for 1 hour, the cells were washed 3 times with PBS and once with a low pH buffer to neutralize any remaining extracellular infectivity. At this time and again 20 hours later, we collected the 199V overlay medium containing secreted virions as well as total cell lysates of the infected cell monolayers beneath the 199V. At the same time points, the remaining cultures containing intracellular virus and medium overlay were subjected to freeze-thawing to release intracellular infectivity. The infectivity was then measured by plaque assay. The expression of the dominant negative and control constructs were monitored in parallel by immunoblot analysis.

As shown in figure 3.8A, the levels of the MCLT and BRLT isoforms were detected as high molecular weight bands (approximately Mr 130,000) that reacted with rabbit anti-RFP antibody, indicating fusion of the fluorescent tag to the construct. MCLT ran slightly slower than BRLT, which was due to the additional exons contained in the MCLT transcript. A band indicative of mRED was detected in lanes containing lysates of the control cells.

As shown in figure 3.8B, at 0 hpi almost no residual HSV-1 infectivity was detected inasmuch as the highest titer was 1 PFU per cell. At 20 hpi, secreted infectivity from the mRED-DN-myoVa BRLT and MCLT transfected cells was lower than the level of infectivity released from cells transfected with the mRED control vector (approximately 51% and 25% of the control, respectively). In contrast, the intracellular infectivity in the BRLT and MCLT expressing cells were higher than the infectivity from mRED expressing control cells (approximately 183% and 172% of the control, respectively). Table 3.1

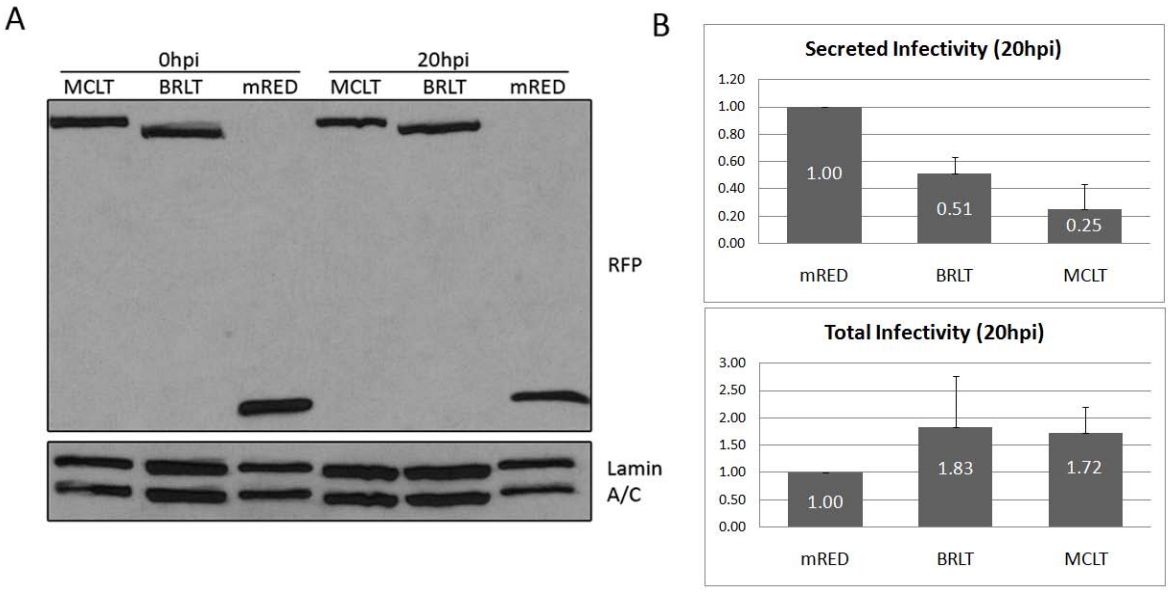

Figure 3.8 Myosin Va is required for efficient secretion of HSV-1 virions, but not for intracellular production of infectivity. (A) HeLa cells were transfected with expression vectors for mRED-DN-myoVa-BRLT, mRED-DN-myoVa-MCLT or mRED alone. Total cell lysates were collected at 26 hours post transfection, separated on a polyacrylamide gel and transferred to nitrocellulose. The blots were probed with a rabbit anti-RFP antibody. Signals from goat anti-lamin B antibody served as loading controls. (B) HeLa cells were transfected with expression vectors for mRED-DN-myoVa-BRLT, mRED-DN-myoVa-MCLT or mRED alone. At 26 hours post transfection, cells were infected with HSV-1(F) at an MOI of 0.1. The resulting infectivity was determined by titration on Vero cells. The graph represents averages of data collected from three separate experiments.

lists the amount of infectivity determined in three separate trials. We interpret these data to indicate that the DN-myoVa blocks release of HSV-1 virions, but not the accumulation of infectious virus within cells.

Expression of DN-myoVa Results in Decreased Glycoprotein Presentation on the Surface of HSV-Infected Cells.

To determine if secretion of cargo other than virions required myoVa, we asked whether or not the mRED-DN-myoVa constructs could preclude viral glycoprotein transport to the cell surface. We therefore transfected HEp-2 cells with the dominant negative BRLT and MCLT isoforms or the mRED control vector. At 24 hours post transfection the cells were mock infected or infected with 10 PFU per cell of HSV-1 K26-GFP, a virus that encodes a VP26 capsid protein fused to GFP. The cells were subjected to analysis by indirect immunofluorescence as indicated above except that they were fixed with PFA in the absence of detergent. To monitor glycoprotein expression at the cell surface, we reacted these unpermeabilized cells with DL6 monoclonal antibody that recognizes a luminal epitope of HSV-1 envelope protein gD, gB antibody or gM antibody and examined the cells by fluorescent microscopy. The results are presented in figure 3.9.

Cells infected with HSV-1 K26-GFP were indicated by the presence of intrinsic bright GFP-mediated fluorescence in their nuclei as described previously (29). Uninfected cells did not display notable gD-specific fluorescence, as expected. In contrast, high amounts of glycoprotein-specific

Table 3.1 Total and secreted HSV-1 infectivity. The table lists titrations of infectivity from all three experiments shown in Figure 5B. These data were normalized to wild type values and used in the bar graph of Figure 5B. Titrations were performed by plaque assay on Vero cell monolayers.

20hpi	*Total Infectivity*			**20hpi**	*Secreted Infectivity*		
PFU/mL	**mRED**	**BRLT**	**MCLT**	**PFU/mL**	**mRED**	**BRLT**	**MCLT**
trial 1	1.0E+03	2.0E+03	2.0E+03	**trial 1**	2.0E+01	8.0E+00	4.0E+00
trial 2	3.0E+02	8.0E+02	6.0E+02	**trial 2**	1.1E+01	7.0E+00	5.0E+00
trial 3	2.3E+02	1.9E+02	2.7E+02	**trial 3**	1.0E+01	5.0E+00	1.0E+00

Figure 3.9 Expression of DN-myoVa decreases glycoprotein immunoreactivity on the surface of HSV-infected HEp-2 cells. (A)HEp-2 cells were transfected with either mRED-DN-myoVa-BRLT, mRED-DN-myoVa-MCLT or mRED control vector. Transfected cells were infected with HSV-1 K26-GFP (MOI = 10 PFU per cell) or mock infected at 26 hours post transfection. At 15.5 hpi the cells were washed with PBS, fixed in 3% PFA for 15 minutes and blocked in 10% human serum. The fixed, unpermeabilized cells were immunostained with a gD monoclonal antibody.K26 infected cells expressing either the mRED control, mRED-DN-myoVa BRLT or mRED-DN-myoVa MCLT were identified at random by intrinsic red and GFP fluorescence, and the amount of gD-spcecific fluorescence was quantified using a Zeiss Imager.M1 Axio fluorescent microscope and IP Lab v3.65a software. At least 50 infected cells expressing each construct were analyzed. Mean fluorescence is the sum of measured fluorescence divided by the area. The mRED-DN-myoVa BRLT- and MCLT-expressing cells were found to have less surface expression of gB, gM and gD as compared to mRED control cells by Student's T test ($p < 0.05$). (B) Example of K26 infected cells transfected with DN-myoVa or the mRED control demonstrating decreased immunoreactivity with gD antibody in DN-myoVa expressing cells. White arrows indicate cells of interest. Green: HSV-1, blue: gD, red: DN-myoVa or mRED control.

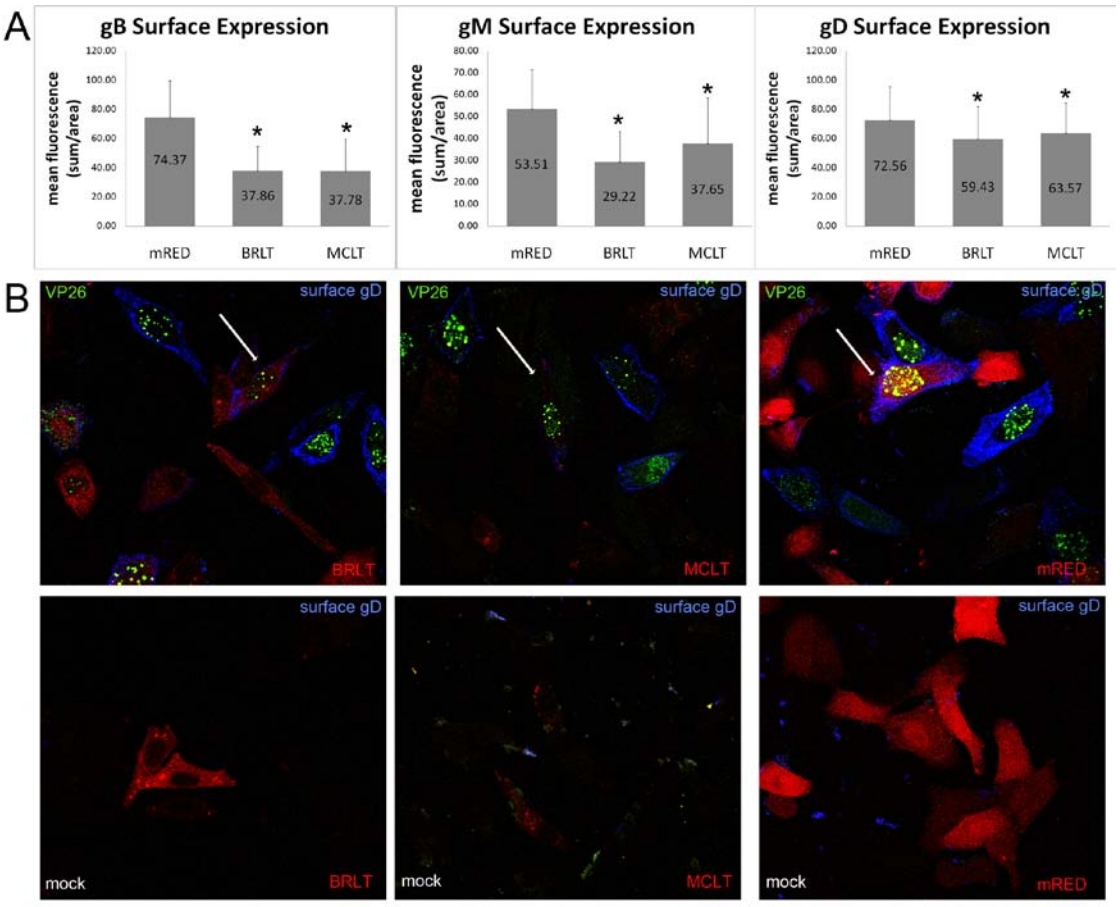
A
gB Surface Expression
mean fluorescence (sum/area)
120.00
100.00
80.00
60.00
40.00
20.00
0.00
74.37
37.86
37.78
*
*
mRED
BRLT
MCLT
gM Surface Expression
mean fluorescence (sum/area)
80.00
70.00
60.00
50.00
40.00
30.00
20.00
10.00
0.00
53.51
29.22
37.65
*
*
mRED
BRLT
MCLT
gD Surface Expression
mean fluorescence (sum/area)
120.00
100.00
80.00
60.00
40.00
20.00
0.00
72.56
59.43
63.57
*
*
mRED
BRLT
MCLT
B
VP26
surface gD
BRLT
VP26
surface gD
MCLT
VP26
surface gD
mRED
surface gD
mock
BRLT
surface gD
mock
MCLT
surface gD
mock
mRED

immunofluorescence were noted in unpermeabilized cells infected with the K26-GFP virus and expressing the mRED control. In infected cells expressing the mRED-DN-myoVa constructs, considerably less glycoprotein-specific immunoreactivity was detected on the cell surface.

Glycoprotein surface expression was quantified in infected cells expressing mRED or the mRED-DN-myoVa constructs by analysis of digital images of at least 50 infected cells (i.e. exhibiting GFP fluorescence) expressing each mRED or mRED-DN-myoVa construct using IP Lab v3.65a software. The quantification data is presented in figure 3.9A and indicates significantly less surface expression of gB, gM and gD on cells expressing both mRED-DN-myoVa constructs compared to those expressing mRED alone ($p < 0.05$ by student's T test). To demonstrate that DN-myoVa expression did not preclude expression we repeated this experiment under similar conditions, but permeabilized the cells with detergent and probed with the gD antibody. We found readily detectable levels of gD within the permeabilized infected mRED-DN-myoVa expressing cells (figure 3.10). Taken together, the data suggest that myoVa plays a role in surface expression of viral glycoproteins.

Discussion

MyoVa has been implicated in transport of secretory granules and melanosomes to the cell surface of neuroendocrine cells (33,130) and melanocytes, respectively (174). Through the use of two different dominant negative myosin Va (DN-myoVa) constructs lacking the actin-binding domain

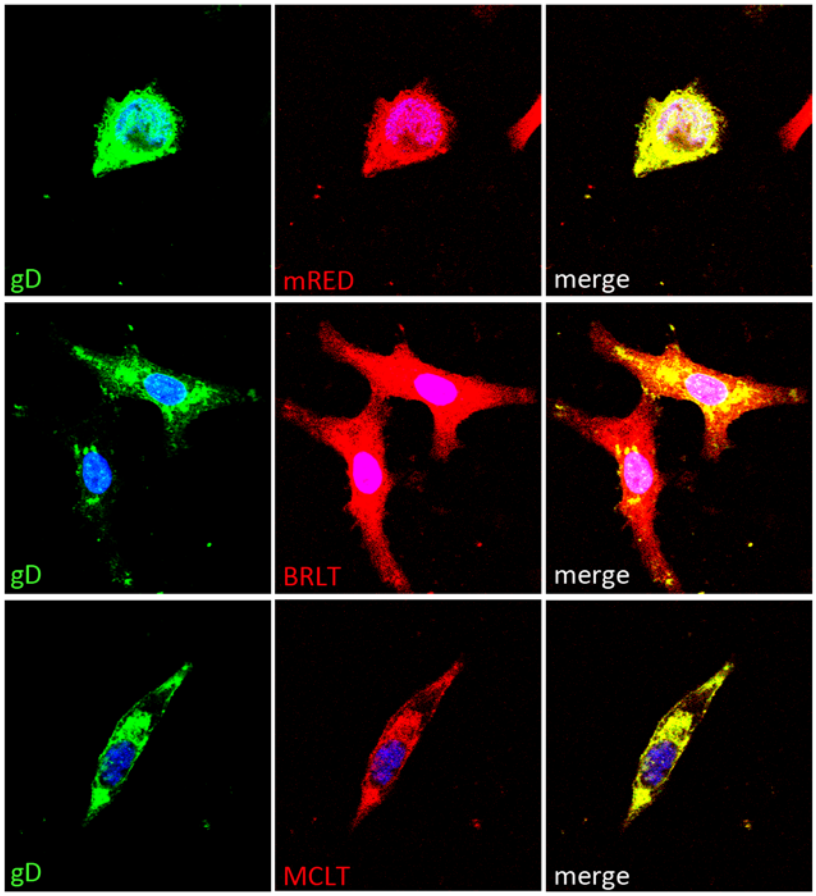

Figure 3.10 mRED-DN-myoVa expression does not preclude gD expression. HEp-2 cells were transfected with either mRED-DN-myoVa-BRLT, mRED-DN-myoVa-MCLT or mRED control vector. At 30 hours post transfection, the cells were infected with 5.0 PFU per cell of HSV-1(F). At 15.5 hpi the cells were fixed in 3% PFA, autofluorescence was quenched by immersion in 50 mM NH_4Cl for 15 minutes and the cells were permeabilized with 0.1% Triton-X 100 for 2 minutes followed by a 10 minute block in 10% human serum in PBS. Cells were immunostained with a gD monoclonal antibody and ICP8 antibody. Green: gD, blue: ICP8, red: DN-myoVa or mRED control.

but containing the exon-encoded portion of the myoVa tail domain and the C terminal cargo-binding domain, we have now shown that myoVa plays a role in exocytosis of HSV virions and glycoproteins in two different epithelial cell lines (specifically HEp-2 and HeLa cells).

HSV alters the conformation of myoVa as indicated by a substantial increase in immunostaining with a myoVa-specific polyclonal antibody starting at about 4 hpi with HSV-1 (figure 1). According to the manufacturer, this antibody recognizes an epitope located between amino acids 260-310. Previous work has shown that myoVa exists in two conformations, folded or extended (166), and that the folded (inactive) conformation is facilitated by an interaction between the C-terminal globular tail domain (GTD) and amino acids 117-137 of the N-terminal motor domain (153). Based on this information, we postulate that the epitope between amino acids 260-310 is masked in the non-active conformation as in uninfected cells, whereas the myoVa antibody preferentially binds to the active (extended) myoVa in infected cells. Thus, the increased fluorescence observed in infected cells stained with this antibody suggests that myoVa activity is augmented during HSV-1 infection. This activation might play to the advantage of the virus inasmuch as substantial transport activity is likely required to support virion secretion.

In a previous study, treatment of HSV infected cells with BDM (2,3-butanedione monoxime) decreased secretion of infectivity into the medium by 20-50-fold and decreased production of intracellular virus by 2-fold. BDM is a potent inhibitor of myosin II, but also affects calcium flux and many other proteins (110,161). The current study specifically implicates myoVa in virus

secretion inasmuch as expression of dominant negative myoVa reduced secretion of infectivity up to 4-fold while titration of extracellular plus intracellular infectivity revealed slightly elevated levels. This observation indicates that myoVa is involved in transporting infectious virions to the extracellular space, whereas earlier steps in the virion assembly pathway in which infectious virus is generated do not require myoVa. A role in the final egress step of the virion egress pathway is consistent with myoVa's role in the final exocytic step allowing transport of melanosomes (174) and secretory granules (130) into the extracellular space.

To address the effects of alternative splicing, we used two DN-myoVa constructs. The MCLT (melanocyte long tail) construct contained exons D and F but lacked exon B, whereas the brain long tail (BRLT) construct contained exon B, but not D or F. Because both constructs affected virion secretion similarly, we conclude that regions of myoVa required for interaction with Rab27a (encoded by exon F) (174), dynein light chain 2 (encoded by exon B) (64,165), and Rab10 (encoded by exon D) (127) were dispensable for the dominant negative effects. Thus, these effectors were either not involved in myoVa-dependent virion secretion or their involvement was redundant.

It was of interest to us that glycoprotein surface expression at the cell surface was significantly ($p < 0.05$) reduced by the expression of DN myoVa isoforms, suggesting that vesicles bearing viral glycoproteins also utilize myoVa to facilitate their transport to the plasma membrane. This suggests that the final step of virion transport is functionally similar to that of glycoprotein transport to the cell surface, at least in the cell types tested. The observation that the

dominant negative proteins colocalized with TGN markers suggest that myoVa primarily mediates transport from the TGN to the plasma membrane. This makes sense in light of the fact that HSV virions are known to transit near or through the TGN on their way to the extracellular space (158).

We also noted substantial amounts of myoVa in the nuclei of infected cells, especially at late times after infection (figure 3.1). MyoVa in the nucleus has also been observed in cells infected with pseudorabies virus, a herpesvirus of swine (41). While it is possible that myoVa plays a role in active intranuclear movement of capsids (43), the production of substantial intracellular infectivity in cells expressing the DN-myoVa suggests very minor or no effects on transport before the final secretion step when virions are released from the plasma membrane.

The current work supports a model in which myoVa is activated during HSV-1 infection to enhance the transport of secretory vesicles bearing virions and viral glycoproteins past cortical actin to eventually fuse with the plasma membrane. The study does not rule out roles for other nonmuscle myosins and does not exclude other roles for myoVa in the final secretion step. For example, the observation that myosin IIa plays a role in stabilizing the fusion pore that links the interior of the secretory vesicle to the extracellular space (105) would conceivably also enhance virion secretion. From a heuristic standpoint, defining the roles of nonmuscle myosins in virion secretion is expected to be a useful approach to study how these proteins perform their functions in uninfected as well as infected cells.

Acknowledgements:

We thank Roselyn Eisenberg and Gary Cohen for the antibody to gD, David Johnson for the antibody to gB, Bill Ruyechan for the ICP8 antibody, Prashant Desai for the K26 virus, and John Hammer for the dominant negative myoVa constructs. These studies were supported by grants R01 AI52341 and T32 AI007618 from the National Institutes of Health.

CHAPTER IV

U_L31 of herpes simplex virus 1 is necessary for optimal NFκB activation and expression of viral gene products*

Kari L. Roberts and Joel D. Baines, Department of Microbiology and Immunology, Cornell University, Ithaca, NY 14853.

*Reprinted from **Roberts, KL, J.D. Baines.** (2011). U_L31 of herpes simplex virus 1 is necessary for optimal NFκB activation and expression of viral gene products. J Virol 85:4947-4953.

Abstract

Previous results suggested that the U_L31 gene of herpes simplex virus 1 (HSV-1) is required for envelopment of nucleocapsids at the inner nuclear membrane, and optimal viral DNA synthesis and DNA packaging. In the current study, viral gene expression and NFκB and c-Jun N-terminal kinase (JNK) activation of a herpes simplex virus mutant lacking the U_L31 gene, designated ΔU_L31, and its genetic repair, designated ΔU_L31-R, were studied in various cell lines. In Hep2 and Vero cells infected with ΔU_L31, expression of the immediate early protein ICP4, early protein ICP8, and late protein glycoprotein C (gC) were delayed significantly. In Hep2 cells, expression of these proteins failed to reach levels seen in cells infected with ΔU_L31-R or wild type HSV-1(F) even after 18 hours. The defect in protein accumulation correlated with poor or no activation of NFκB and JNK upon infection with ΔU_L31 compared to wild type virus infection. The protein expression defects of the U_L31 deletion mutant were not explainable by a failure to enter non-permissive cells, and were not complemented in an ICP27 expressing cell line. These data suggest that pU_L31 facilitates initiation of infection and/or accelerates the onset of viral gene expression in a manner correlated with NFκB activation and independent of the transactivator ICP27. The effects on very early events in expression are surprising in light of the fact that U_L31 is designated as a late gene and pU_L31 is not a virion component. We show herein that while most pU_L31 is expressed late in infection, low levels of pU_L31 are detectable as early as 2 hours post infection consistent with an early role in HSV-1 infection.

Introduction

The herpes simplex virus type 1 (HSV-1) virion, like that of all herpesviruses, consists of an envelope surrounding an icosahedral capsid shell which contains a double-stranded linear DNA genome. Between the proteinaceous capsid and lipid envelope lies an assemblage of more than 20 viral proteins termed the tegument. Upon entry, some tegument proteins are released into the cytosol to help prime the cell for infection. For example, the virion host shut off (vhs) protein degrades mRNA to favor viral gene expression (78,119) and VP16 (viral protein 16, also designated as α-TIF) redirects host transactivators to viral promoters (76,117). Once the virus has entered the cell, the cytoplasmic DNA-containing capsid traffics towards the host nucleus using the microtubule motor dynein (144). Upon engaging a nuclear pore the HSV-1 genome exits the capsid and enters the nucleoplasm (6,154). Expression of viral genes is temporally regulated, starting with immediate early (α) genes and followed sequentially by early (β), and late genes (γ) (67,68). Most α genes encode regulatory proteins. These include, ICP4 (infected cell protein 4), that transcriptionally activates other genes, and ICP27 which augments viral gene expression at both pre- and post-transcriptional levels. Gene products from the β class (e.g. ICP8, an essential DNA binding protein) are involved in DNA replication, whereas the γ genes encode structural proteins like the major capsid protein VP5. Viral DNA (vDNA) replication occurs during the transition from β to γ gene expression; the γ genes can be further subdivided into γ_1 (leaky late) and γ_2 (true late). This subdivision stems from a dependence on vDNA synthesis. If vDNA

replication is blocked, such as with the use of the DNA polymerase inhibitor phosphonoacetic acid (PAA), γ_1 gene expression is diminished and γ_2 gene expression is precluded.

As the virus enters the cell, cellular signaling events mediate a transition in host cell functionality that favors viral propagation. For example, interaction of viral glycoprotein D (gD) with a TNF receptor known as herpesvirus entry mediator (HVEM, also known as HveA, and TNFRSF14) induces a transient activation of NFκB (nuclear factor κB) (140). This induction, lasting approximately 2 hours post infection (hpi), is likely stimulated through the TRAF (TNF receptor associated factor) signal transduction pathway and is dependent on cell type (e.g. the cell must express the appropriate receptor). It has also been reported that the tegument protein U_L37 has been shown to activate NFκB through an interaction with TRAF6 (82). In addition to this transient activation of NFκB, there is a second wave of NFκB activation that requires de novo HSV-1 gene expression (3). This wave of NFκB activation initiates at approximately 6 hpi and has been shown to require the α gene product ICP27 (57). NFκB is a transcriptional regulator found in almost every cell type and is normally activated in response to cell stress, such as inflammation and viral infection [reviewed by (59,60,72)]. While some viruses block NFκB activation [for review see (63)] HSV-1 actually requires activation of NFκB for efficient infection (113). This requirement has been demonstrated by use of dominant negative repressors (2,50,113), knock-out cell lines (50), and inhibitory drugs (37).

This study focuses on U_L31 of HSV-1. Deletion of U_L31 decreases viral

titers to varying degrees in different cell lines: up to 1000-fold in Vero cells, and at least 10-fold in rabbit skin cells (80). pU_L31 (the gene product of U_L31) plays an important role in nuclear egress because viral capsids largely fail to bud through the inner nuclear membrane in cells infected with U_L31 deletion mutants (15,123). A similar phenotype is observed upon deletion of pU_L31's interaction partner pU_L34 (128), an integral membrane protein localizing to the inner nuclear membrane in wild type virus infections. Nuclear rim targeting of pU_L31 is dependent on expression of pU_L34. Without this binding partner, the bulk of pU_L31 localizes in the nucleoplasm (123). Both U_L31 and U_L34 are also required for alteration of the nuclear lamina (122), composed largely of a meshwork of intermediate filaments lining the inner surface of the inner nuclear membrane. The nuclear lamina is required for maintaining the structure of the nucleus and its pU_L31/pU_L34-dependent perforation during HSV infection is believed to promote access of nucleocapsids to the inner nuclear membrane for envelopment. Both pU_L34 and pU_L31 are incorporated into the virion during budding through the inner nuclear membrane into the perinuclear space. The envelope of this perinuclear virion is lost upon fusion with the outer nuclear membrane as the capsid enters the cytosol; thus, pU_L31 is not a component of the final extracellular virion (44,83,124). Deletion of U_L31 also diminishes vDNA replication and packaging (15).

In the current study, U_L31 expression was found to be required for efficient NFκB activation and optimal viral protein expression. The latter observation may be related to pU_L31's effects on DNA packaging that require late viral gene products. The effects on gene expression were shown to be independent

of pU_L31's interaction partner pU_L34. Although U_L31 has been designated as a true late gene based on sensitivity of its mRNA to 1-β-D-arabinofuranosylthymine (65), we have found that pU_L31 is detectable at low levels as early as 2 hours post infection. This observation suggests that pU_L31 made de novo accounts for its effects on viral protein expression.

Materials and Methods

Viruses and Cells

Wild type HSV-1 strain F [HSV-1(F)], ΔU_L31 and ΔU_L31-R were provided by Bernard Roizman and have been described previously (15,35). ΔU_L34 was provided by Richard Roller and has been described previously (128). d27-1, the ICP27-null virus and the ICP27 complimenting cell line V27, were provided by Stephen Rice and have been described previously (125). Wild type virus stocks [HSV-1(F) and ΔU_L31-R] were propagated and titered on Vero cell monolayers whereas rabbit skin cells engineered to express pU_L31 (80) were used to propagate and titer the U_L31 deletion virus, ΔU_L31. The cell lines were maintained in growth medium, consisting of Dulbecco's modified Eagle's medium (DMEM) supplemented with 125 units/mL penicillin, 0.125 mg/mL streptomycin and 10% newborn calf serum. Two different viral stocks of the U_L31 deletion virus were used in the reported studies. These stocks produced at least 1000-fold more viral plaques per ml on monolayers of the complementing cell line than on Vero cells. For all experiments, cells were overlayed with 199V medium (DMEM supplemented with 1% newborn calf

serum) after infection, and monitored for cytopathic effects until harvesting or fixation.

Immunoblot Analyses

Mock infected and HSV-1(F) infected cells were washed once in PBS then lysed in 100 µL of 2X sodium dodecyl sulfate-polyacrylamide gel electrophoresis (SDS-PAGE) sample buffer consisting of 100 mM TrisCl [pH 6.8], 200 mM dithiothreitol, 4% SDS, 20% glycerol, and 0.2% bromophenol blue. Lysates were sonicated and boiled for 5 minutes prior to loading. Samples were separated on a 10% polyacrylamide gel and transferred to a nitrocellulose membrane (31 volts for 3.5 hours at 4°C). The membrane was blocked in 5% milk/TBST (1X tris-buffered saline plus 0.1% Tween) for 1 hour at room temperature. The following primary antibodies were diluted in 5% BSA in TBST as follows: mouse anti-ICP4 (1:1000, Rumbaugh-Goodwin Institute for Cancer Research, Plantation, FL), mouse anti-ICP27 (1:5000, Virusys Corporation, Sykesville, MD) rabbit anti-ICP8 (1:10000, a gift from Bill Ruyechan), mouse anti-gC (1:1000, Rumbaugh-Goodwin Institute for Cancer Research, Plantation, FL), rabbit anti-phospho Jun N-terminal kinase (p-JNK) (1:1000, Cell Signaling #4668), rabbit anti-total JNK (1:1000, Cell Signaling #9252), rabbit anti-IκBα (1:1000, Cell Signaling #9242), mouse anti-Lamin A/C (1:1000, Santa Cruz Biotechnology sc7292). Diluted primary antibodies were reacted with blocked membrane for either 1 hour at room temperature or overnight at 4°C with gentle agitation. After extensive washing in PBS, bound primary antibody was detected by addition of anti-mouse (1:2000, Santa Cruz

Biotechnology) or anti-rabbit (1:2000, Santa Cruz Biotechnology) horseradish peroxidase-conjugated secondary antibody diluted in 5% milk/TBST and visualized by enhanced chemiluminescence (Pierce) followed by exposure to X-ray film (Pierce). Image J was used for densitometry.

Immunofluorescence

Hep2 cells seeded on coverslips in a 12-well dish were either mock infected or infected with 10.0 PFU per cell of HSV-1(F), Δ31 or Δ31-R and fixed every hour between 1 and 10 hours post infection by washing cells once with phosphate buffered saline (PBS) and treating with 3% paraformaldehyde (PFA) for 15 minutes at room temperature. The fixed cells were stained with Hoechst dye (2 μg/mL in PBS, Invitrogen) for 15 minutes followed by immersion in 50 mM NH_4Cl for 15 minutes to quench autofluorescence. The cells were permeabilized with 0.1% Triton-X 100 for 2 minutes followed by a 10 minute block in 10% human serum in PBS. Mouse anti-ICP4 (Rumbaugh-Goodwin Institute for Cancer Research, Plantation, FL) primary antibodies were diluted 1:100 in 1% bovine serum albumin (BSA) in PBS, and incubated with the fixed cells for 30 minutes in a humidity chamber held at room temperature. After washing 3 times in excess PBS, the cells were reacted for 30 minutes in a humidity chamber with secondary antibodies FITC-conjugated anti-mouse IgG (Jackson Laboratories) diluted 1:100 in 1% BSA/PBS. The coverslips were then washed 3 times in PBS and dipped in ddH20 before mounting on glass slides with mowiol plus 2.5% DABCO to prevent photobleaching. All digital images were taken using a Zeiss Axio Imager.M1

fluorescence microscope and were processed with Adobe Photoshop software.

Drug Treatments

In some experiments, Hep2 cells in a 6-well dish were pre-treated with 10 μM cycloheximide (CHX) for 1 hour at 37°C/5% CO2 or left untreated. After 1 hour, cells were washed with versene (PBS plus 0.5 μM EDTA [(ethylenedinitrilo)tetraacedic acid]) and infected with wild type HSV-1(F) at an MOI of 10 PFU/cell or mock infected. 10 μM CHX was included with the added virus for the appropriate wells and the cells were rocked slowly for 1 hour at 37°C to allow for viral attachment and entry. After the 1 hour incubation, the virus or mock overlay was removed, the cells were washed with versene, and fresh 199V was added back to the cells (containing 10 μM CHX where appropriate). At time zero the cells were returned to the 37°C/5% CO2 incubator until collected.

For experiments using phosphonoacetic acid (PAA), Hep2 cells in a 6-well dish were infected with HSV-1(F) at an MOI of 10 PFU/cell or mock infected. At the start of infection, 200 μg/mL PAA was added to the appropriate well. Cells were washed 12 hours later and total cell lysates were collected. For all drug treatment experiments, total cell lysates were collected as described above under “immunoblot analyses”.

Results

Infections with ΔU_L31 but not ΔU_L34 are delayed for α, β and γ gene expression.

It has been previously reported that ΔU_L31 infections result in decreased viral DNA accumulation, cleavage and packaging (15). The current studies were initiated to determine how pU_L31 might contribute to these activities, with the hypothesis that U_L31 might augment viral gene expression. Because pU_L31 interacts with pU_L34, we included a ΔU_L34 virus in the experiment to determine if any detected phenotype was dependent upon the pU_L31-pU_L34 interaction. Hep2 cells were mock infected or infected with wild type HSV-1(F), ΔU_L31 or ΔU_L34 viruses at an MOI of 10 PFU per cell. At 4 and 18 hours post infection (hpi), total cell lysates were collected and proteins separated by SDS-PAGE as described in the materials and methods section. The results are shown in figure 4.1. For this and subsequent immunoblots, quantification was done using Image J. Similar results were noted in Hep2 cells infected with the U_L31 deletion virus at up to 50 PFU per cell (data not shown).

Surprisingly, immunoblotting (figure 4.1) showed that essentially no ICP4 (an α gene product) or ICP8 (a β gene product) accumulated to detectable levels by 4 hpi in cells infected with the ΔU_L31 virus, whereas both proteins were detected at this time point in cells infected with either the wild type HSV-1(F) or ΔU_L34 viruses. At 4 hpi, ICP4 and ICP8 protein levels in the ΔU_L31 infection were only 3% and 5%, respectively, of those seen from the infection

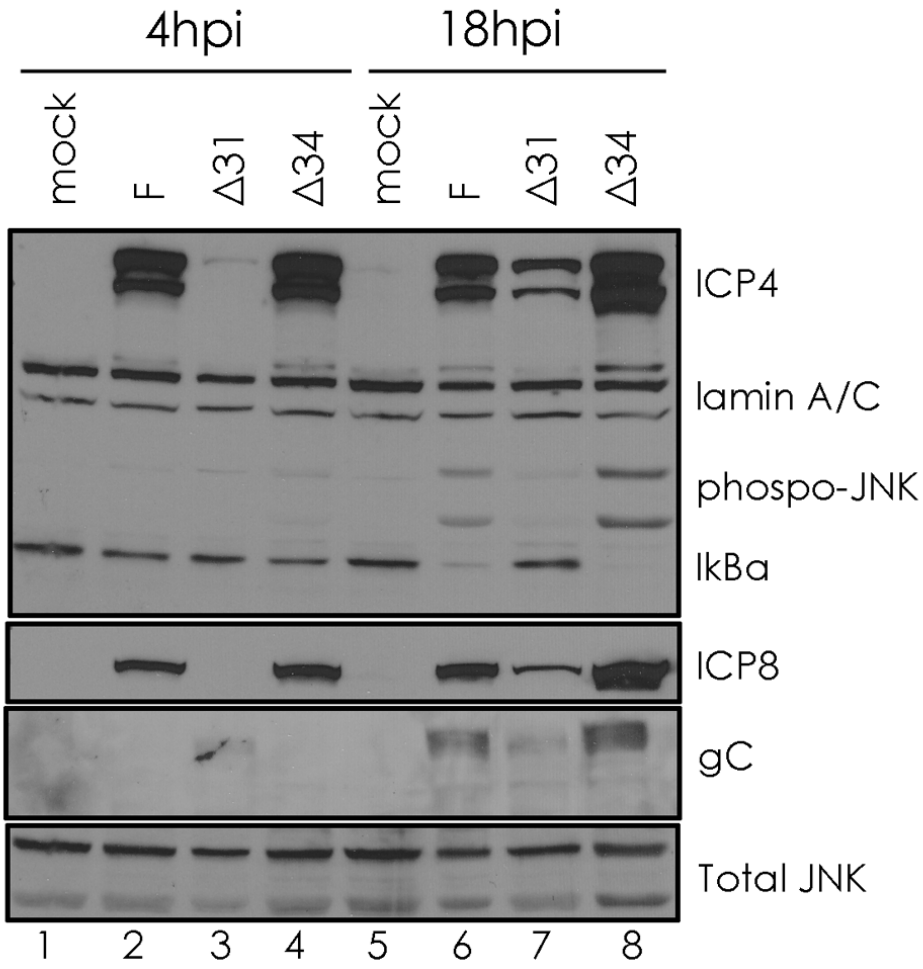

Figure 4.1 Delayed protein expression in Hep2 cells infected with ΔU_L31 but not ΔU_L34 viruses. Hep2 cells were infected with 10 PFU per cell of HSV-1(F), ΔU_L31, ΔU_L34 or were mock infected. Total cell lysates were collected at 4 and 18 hpi. Proteins were denatured and separated by SDS-PAGE, transferred to a nitrocellulose membrane and reacted with antibodies against ICP4, ICP8, gC, p-JNK, total JNK, IκBα or Lamin A/C, which was used as a loading control. Bound antibodies were revealed by reaction with appropriately conjugated antibodies followed by chemiluminescence and exposure to X-ray film as described in materials and methods.

with wild type virus. Although both ICP4 and ICP8 protein levels increased in the lysate of the ΔU_L31 infection by 18 hpi, the levels were only 55% and 41% of levels in HSV-1(F) infection. Protein levels of the γ_2 gene product glycoprotein C (gC) in the ΔU_L31 infection accumulated to only 34% of gC from infection with the wild type HSV-1(F). For all cases, infections with the ΔU_L34 virus resulted in protein levels similar to or higher than wild type infection. We conclude that U_L31 is necessary for optimal expression of at least one member of each kinetic class of viral protein.

Because it has been shown previously that inhibition of NFκB activity by the drug resveratrol resulted in reduced levels of several α gene mRNAs and undetectable levels of gC mRNA (37) we hypothesized that pU_L31 might augment viral protein expression by ensuring activation of the transcriptional regulator NFκB. To test this possibility, we probed immunoblots of total infected cell proteins with antibody to IκBα, the NFκB inhibitor. IκBα binds NFκB in the cytosol inhibiting its translocation into the nucleus, thus maintaining a pool of inactive (transcriptionally incompetent) NFκB (61,72). Upon NFκB activation, IκBα is phosphorylated, polyubiquitinated and finally degraded. Normally in HSV-1 infections, NFκB activation is observed as early as 6 hpi, and this activation can be measured by the concomitant absence of the NFκB repressor, IκBα (57). As shown in figure 4.1, IκBα accumulated to similar levels at 4 hpi in all samples. At 18 hpi, IκBα protein levels from HSV-1(F) and ΔU_L34 infected cells were 8% and 2% of mock infected cells whereas ΔU_L31 infected cell lysates contained protein levels of IκBα at 85% of mock. These data indicate that U_L31 plays a role in ensuring elimination of IκBα in

infected cells, and thus activation of NFκB.

We also examined relative levels of activated (phosphorylated) c-Jun N-terminal kinase (p-JNK) and found that at 18 hpi the ΔUL31 virus induced levels of p-JNK amounted to only 28% of the level detected from the wild type HSV-1(F) infection. In contrast, levels of total JNK were similar in all lanes. Taken together, the results indicate that in addition to a viral protein expression deficiency, the ΔU_L31 virus exhibits deficiencies in NFκB and JNK activation that are normally seen during HSV-1 infection.

NFκB and JNK activation are down-regulated in ΔU_L31 infections of different cell types.

To determine if NFκB and JNK activation seen in the U_L31 deletion virus (ΔU_L31) infected Hep2 cells (figure 4.1) occurred in other cell types, rabbit skin cells (RSC), Vero, HeLa and Hep2 cells, as well as the ΔU_L31 complementing cell line, clone 7 (an RSC derivative) were mock infected or infected with the ΔU_L31, HSV-1(F) or ΔU_L31-R (repair) viruses. All cell types were infected at an MOI of 10 PFU per cell and total cell lysates were collected at 4, 8, 12 and 18 hpi as described in materials and methods. Equal amounts of proteins from each sample at each time point were separated by SDS-PAGE, transferred to nitrocellulose membranes, and were reacted with antibody for IκBα (the NFκB repressor), total JNK and phosphorylated (activated) JNK (p-JNK) as described in materials and methods. Sample loading was assessed by probing with an antibody directed against lamin A/C. Although the amounts loaded in each lane were consistent within samples from a given cell line, they varied

somewhat between cell lines. Nevertheless, the consistency of loading between samples from each cell type enabled comparisons of protein expression by the different viruses in each cell type examined.

Overall, the results indicated a positive correlation between defects in protein synthesis in ΔU_L31 infections (as shown in figure 4.1), and both decreased JNK and NFκB activation in the various cell lines (as shown in figure 4.2) as follows.

In the non-permissive Hep2 and HeLa cell lines, IκBα levels were similar upon infection with all viruses at 4 hpi, whereas at later time points IκBα was down regulated to 36% and 34% of mock infected cells in HSV-1(F) and ΔU_L31-R, respectively. However, in cells infected with ΔU_L31 IκBα was down regulated to only 78% of mock levels. The differences were accentuated at 18 hpi when IκBα was down regulated to 15% and 7% of mock in HSV-1(F) and ΔU_L31-R, respectively, but down regulated to only 76% of mock in the ΔU_L31 infection.

In HeLa cells, activated JNK was first detected at 8 hpi in cells infected with HSV-1(F) and ΔU_L31-R, but in cells infected with ΔU_L31 the p-JNK level was only 8% of that in cells infected with ΔU_L31-R. Even at 18 hpi, the p-JNK level in ΔU_L31 infected cells was only 15% of that in the ΔU_L31-R infection. Although activated JNK was never abundant in Hep2 cells, it was first detected at 8 hpi with the wild type virus. p-JNK levels were significantly lower at later time points (8%, 3% and 0.4% of p-JNK levels in cells infected with ΔU_L31-R

Figure 4.2 NFκB and JNK activation are down-regulated in ΔU_L31 infections of different cell types. Rabbit skin cells (RSC), clone 7 (#7), Vero, Hep2, or HeLa cells were infected with 10.0 PFU per cell of HSV-1(F), ΔU_L31, ΔU_L31-R, or were mock infected. Clone 7 is derived from RSC's and partially complements replication of the UL31 deletion virus. Total cell lysates were collected at 4, 8, 12 and 18 hpi. Proteins were separated by SDS-PAGE, transferred to a nitrocellulose membrane and reacted with antibodies against p-JNK, total JNK, and IκBα. Antibody to Lamin A/C was used as a loading control. Bound antibodies were revealed by reaction with appropriately conjugated antibodies followed by chemiluminescence and exposure to X-ray film as described in materials and methods.

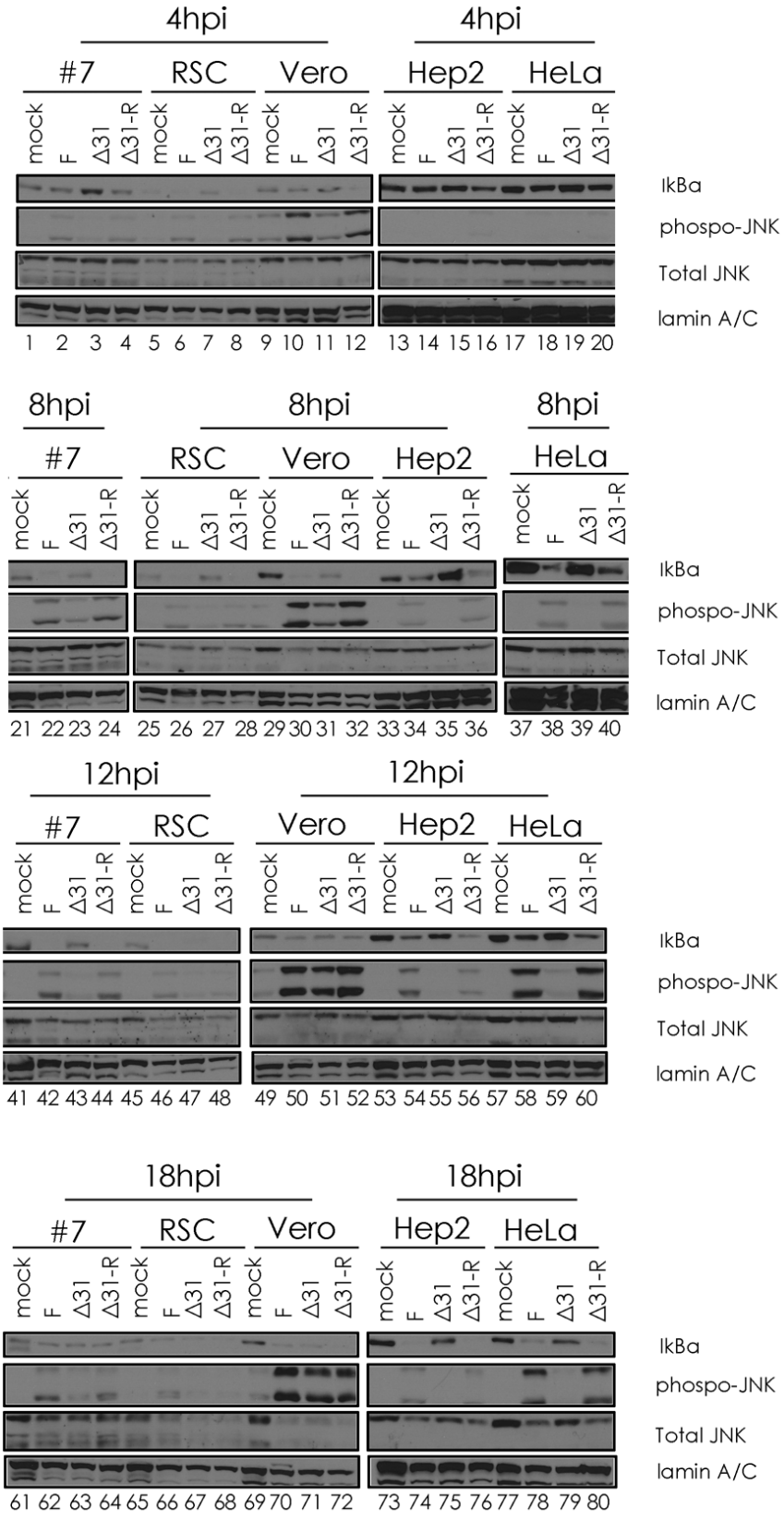
4hpi
4hpi
#7
RSC
Vero
Hep2
HeLa
mock
F
Δ31
Δ31-R
IkBa
phospo-JNK
Total JNK
lamin A/C
1 2 3 4 5 6 7 8 9 10 11 12 13 14 15 16 17 18 19 20
8hpi
8hpi
8hpi
#7
RSC
Vero
Hep2
HeLa
21 22 23 24 25 26 27 28 29 30 31 32 33 34 35 36 37 38 39 40
12hpi
12hpi
#7
RSC
Vero
Hep2
HeLa
41 42 43 44 45 46 47 48 49 50 51 52 53 54 55 56 57 58 59 60
18hpi
18hpi
#7
RSC
Vero
Hep2
HeLa
61 62 63 64 65 66 67 68 69 70 71 72 73 74 75 76 77 78 79 80

at 8, 12 and 18 hpi, respectively).

Vero cells, unlike Hep2 and HeLa cells, exhibited easily detectable phosphorylated JNK as early as 4 hpi, although levels in cells infected with ΔU_L31 were 46% of the level observed upon infection with ΔU_L31-R. The differences in activated JNK levels decreased over time such that by 18 hpi, the level of JNK activation in Vero cells infected with ΔU_L31 was 92% of that in Vero cells infected with ΔU_L31-R. In general, IκBα levels in Vero cells were inversely correlated with those of activated JNK. Although the IκBα level was higher by 8 hpi with ΔU_L31 (22% of mock) than upon infection with the repair virus (0.9% of mock), differences among the different viral infections were negligible by 12 hpi (58% for F, 61% for ΔU_L31 and 47% for ΔU_L31-R relative to mock). We conclude that Vero cells infected with ΔU_L31 are more permissive with respect to NFκB and JNK activation than either Hep2 or HeLa cells infected with this virus.

Immunoblot signals of IκBα were not as strong in RSC's as in the other cell lines examined. Nevertheless, this cell line contained more IκBα when mock infected or infected with ΔU_L31 compared to levels in cells infected with the wild type HSV-1(F) and ΔU_L31-R. Compared to mock IκBα levels in HSV-1(F), ΔU_L31, and ΔU_L31-R were 19%, 167%, and 21%, respectively. The differences in IκBα levels in the different virus infections were largely eliminated by 12 hpi, as percentage of detectable IκBα relative to mock were 3%, 16% and 2% for HSV-1(F), ΔU_L31, and ΔU_L31-R, respectively. Very little activated JNK (p-JNK) was detected in RSC's at any time point. Thus, rabbit skin cells were more permissive with respect to NFκB and JNK activation in

the context of ΔU_L31 than either Hep2 or HeLa cells.

In clone 7 cells, which partially rescue the U_L31 deletion virus (80), less activated JNK and more IκBα were observed after infection with ΔU_L31 than with the other viruses. Specifically, the IκBα levels were only 11% relative to mock in infections with the ΔU_L31-R virus, but 63% with ΔU_L31 at 8 hpi. At 4 and 8 hpi, p-JNK levels in cells infected by ΔU_L31 were 16% and 45%, respectively, compared to levels in infections with the repair virus. Relevant to this observation, we have noted a delay in viral protein expression in clone 7 cells infected with ΔU_L31 (data not shown) and an inability of these cells to restore its replication to the level seen upon infection with ΔU_L31-R (80). Thus, the incomplete rescue of ΔU_L31 replication and protein expression in this cell line correlates with poor JNK and NFκB activation.

ICP27 provided *in trans* does not rescue the observed defects of ΔUL31 infected Vero cells.

Previous reports suggested that loss of ICP27 could produce similar defects to those we have observed in characterization of the U_L31 deletion mutant (57,58). We therefore examined NFκB and JNK activation, and gC expression in an ICP27 expressing cell line (V27) infected with ΔU_L31, HSV-1(F), ΔU_L31-R and d27-1 (ICP27 null) viruses. Vero cells were used as a control because V27 is derived from this cell type (125). The results are presented in figure 4.3.

In both Vero and V27 cells, JNK activation was decreased in the ΔU_L31 infection relative to wild type HSV-1(F) levels. The presence of ICP27 provided

in trans (V27 cells) partially rescued JNK activation in both the ΔU_L31 and ICP27-null virus (d27-1). Specifically, p-JNK protein levels in the ΔU_L31 and d27-1 infections increased from 15% and 31% (respectively) of wild type levels at 4 hpi to 50% and 67% (respectively) of wild type levels at 8 hpi. In contrast, p-JNK protein levels in Vero cells remained at similar levels in cells infected with ΔU_L31 compared to wild type infection at 4 and 8 hpi (66% and 59% of wild type levels, respectively).

ICP4 expression in ΔU_L31 infected Vero and V27 cells was dramatically reduced compared to wild type infections in these cell types. At 4 and 8 hpi, ICP4 protein levels in the ΔU_L31 Vero infections were 0.6% and 54% of wild type, respectively. The presence of ICP27 provided in trans failed to rescue ICP4 expression for both ΔU_L31 and ICP27-null (d27-1) infections by 8 hpi. In ΔU_L31 and d27-1 infections in V27 cells, ICP4 protein levels were only 17% and 8% of wild type infection (respectively) at 4 hpi and increased to only 23% and 11% of wild type infection (respectively) at 8 hpi.

Lysates from ΔU_L31 infected Vero and V27 cells contained readily detectable protein levels of IκBα at 8 hpi (70% and 119% of mock, respectively), whereas wild type infections resulted in IκBα levels that were only 32% and 16% observed in mock infection. This is an indication that NFκB was not activated normally in the ΔUL31 infections. ICP27 provided *in trans* was sufficient to rescue NFκB activation in the ICP27-null virus by 8 hpi since IκBα protein level from the d27-1 infection was only 10% of mock.

Figure 4.3 ICP27 in the V27 cell line does not rescue the protein expression deficits of ΔU_L31 at early times after infection. Vero or the Vero-derived ICP27 expressing cell line V27 were infected with HSV-1(F), ΔU_L31, ΔU_L34, d27-1 or mock infected at an MOI of 10 PFU per cell. Total cell lysates were collected at 4 and 8 hpi and the denatured proteins were separated by SDS-PAGE, transferred to a nitrocellulose membrane and reacted with antibodies against ICP4, ICP27, p-JNK, and IκBα. Lamin A/C was used as a loading control. The order in lanes 1-4 were modified from the original blot to match the order of loaded samples run previously. Bound antibodies were revealed by reaction with appropriately conjugated antibodies followed by chemiluminescence and exposure to X-ray film as described in materials and methods.

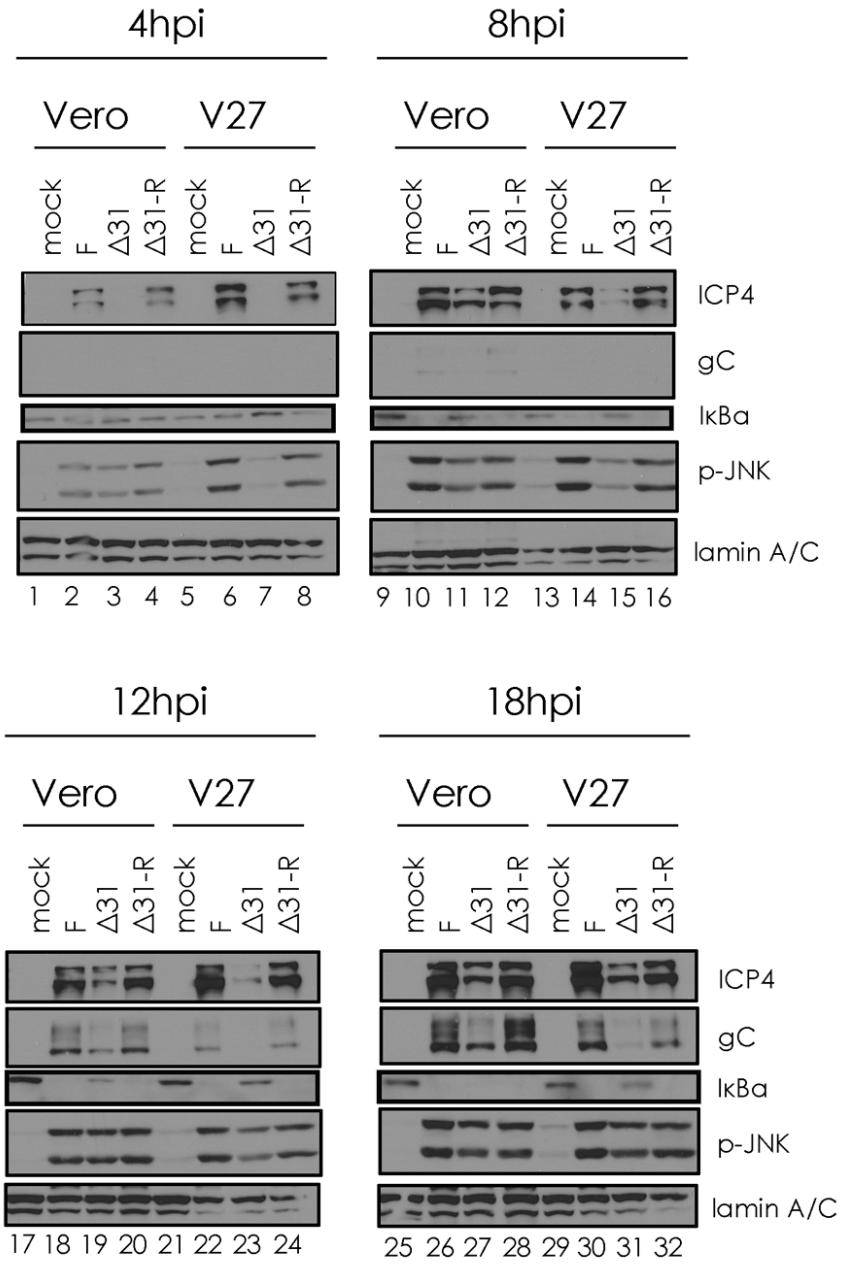
4hpi
8hpi
Vero
V27
mock
F
Δ31
Δ31-R
ICP4
gC
IκBa
p-JNK
lamin A/C
1 2 3 4 5 6 7 8
9 10 11 12 13 14 15 16
12hpi
18hpi
17 18 19 20 21 22 23 24
25 26 27 28 29 30 31 32

We conclude that ΔU_L31's defects in protein expression and NFκB and activation cannot be complemented in an ICP27 expressing cell line, and JNK activation is only partially rescued. This suggests that U_L31's contribution to activation of NFκB and JNK is mostly independent of ICP27.

Infection with ΔU_L31 leads to delayed expression of ICP4 but not failure to initiate infection.

One possible explanation of the current results is that the ΔU_L31 virus is unable to efficiently enter or otherwise infect cells. In this scenario, the observed phenotypes might simply reflect a large number of uninfected cells in the population. To address this possibility, we infected the restrictive Hep2 cell line with the ΔU_L31 or ΔU_L31-R viruses at a multiplicity of infection (MOI) of 10 PFU per cell. Cells were fixed at 1, 6 and 10 hpi and stained with antibody to ICP4 to visualize infected cells, and Hoechst dye to visualize cellular nuclei. The results are presented in figure 4.4A.

At all time points examined, nuclei were present throughout the visual field. At 1 hpi, no ICP4-specific immunofluorescence was visible in ΔU_L31 or ΔU_L31-R infected cells. At 6 hpi many ΔU_L31-R infected cells exhibited ICP4-specific immunofluorescence, whereas only a few cells infected with ΔU_L31 displayed such immunostaining. At 10 hpi, many ICP4-positive cells were found throughout the ΔU_L31-R and ΔU_L31 infected cell monolayers. These observations are consistent with the data presented above indicating that cells infected with wild type viruses express high levels of ICP4 at early time points whereas ICP4 expression in ΔU_L31 infected cells starts at very low

levels that increase with time post infection. The gradual increase in ICP4 expressing cells upon infection with the U_L31 deletion virus cannot be a consequence of cell to cell spread within the culture because (i) this would not be expected at 6 hpi and (ii) the U_L31 deletion virus cannot exit non-complementing cells. A quantification of infection efficiency at 6 hpi and 10 hpi is shown in figure 4.4B. Student's T-test demonstrated that the difference in the number of ICP4-expressing cells out of total cells was statistically significant ($p < 0.001$) whereas this difference was no longer statistically different at 10hpi ($p > 0.05$). The difference in the 6 and 10 hpi time points in ΔU_L31 infected cells was also statistically different ($p < 0.01$), indicating that a significant number of cells transitioned from not expressing ICP4 at detectable levels to detectable expression over the course of 4 hours. We conclude that the defects in ICP4 expression observed in cells infected with the U_L31 deletion were due to a delay in the onset of expression, rather than a failure of the virus to enter and infect a subset of cells.

UL31 expression is detectable early in infection.

The effects of pU_L31 in early protein expression were seemingly incongruous with its sole expression late in infection. To test whether or not U_L31 is only expressed late in infection, Hep2 cells were treated with 10 μM cycloheximide (CHX) or left untreated for 1 hour. The cells were then infected with wild type HSV-1 (MOI = 10) or mock infected. For CHX treated cells, the CHX was maintained at all steps of infection. Total cell lysates were collected at 1, 2, 3 and 5 hours post infection (hpi) and proteins were separated by

Figure 4.4 Infection with ΔU_L31 leads to delayed expression of ICP4 but not failure to initiate infection. (A) Hep2 Cells were infected at an MOI of 10 PFU per cell of either ΔU_L31 or its genetic repair ΔU_L31-R and were fixed at 1, 6 or 10 hpi in PFA, permebilized, and stained with antibody to ICP4 (green) to visualize infected cells, and the cells were counterstained with Hoechst dye (blue) to visualize cellular nuclei. (B) Quantification of ratio of ICP4-expressing cells to total cells infected with ΔU_L31-R or ΔU_L31 (MOI = 10 PFU per cell) at 6 and 10 hpi. The Student's T-test showed a statistically significant difference in ICP4 expression in the ΔU_L31-R and ΔU_L31 infected cells at 6 hpi ($p < 0.001$, noted by *) but not 10 hpi ($p > 0.05$). The same statistical test showed a statistically significant difference in ICP4 expression in ΔU_L31 infected cells fixed at the 6 and 10 hpi time points ($p < 0.01$, noted by *).

A

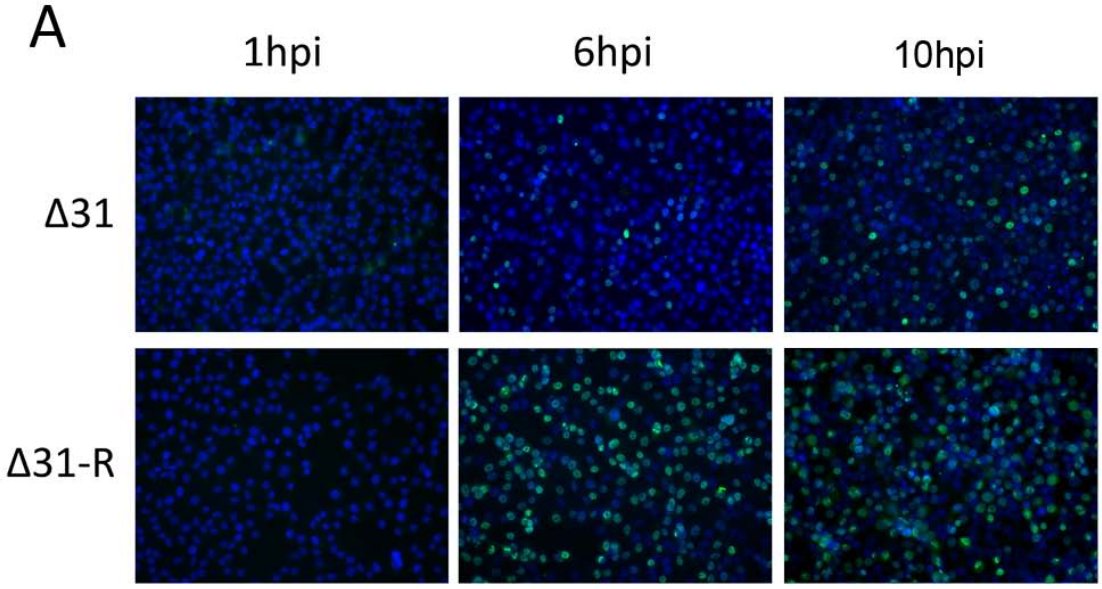
1hpi
6hpi
10hpi
Δ31
Δ31-R

B

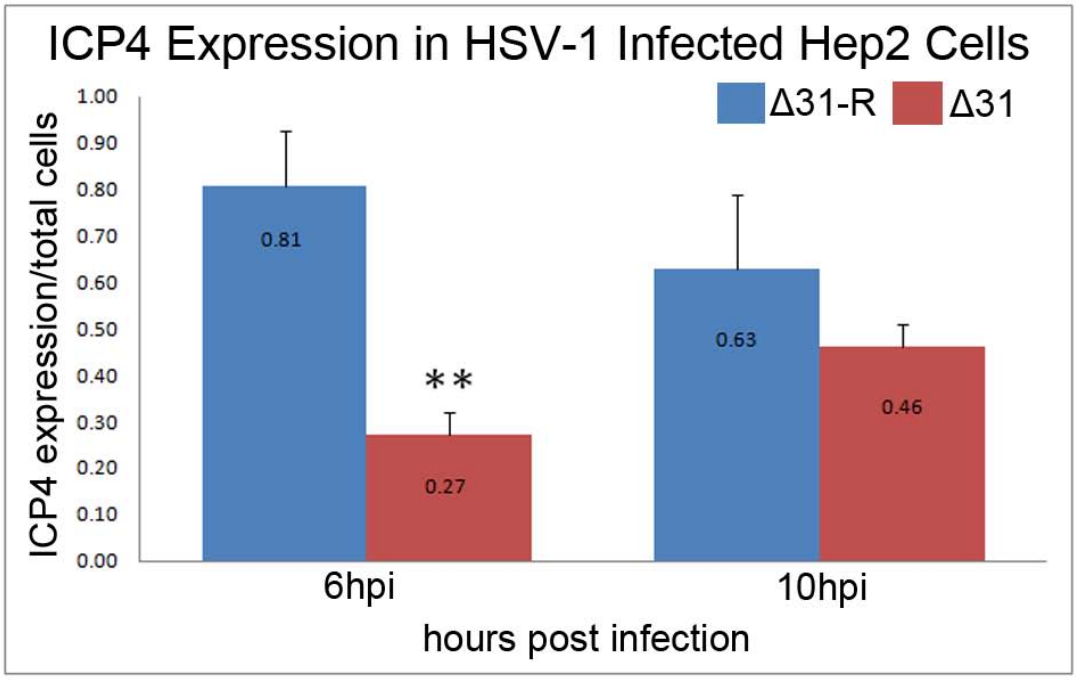
ICP4 Expression in HSV-1 Infected Hep2 Cells
Δ31-R
Δ31
ICP4 expression/total cells
1.00
0.90
0.80
0.70
0.60
0.50
0.40
0.30
0.20
0.10
0.00
0.81
0.27
**
0.63
0.46
6hpi
10hpi
hours post infection

SDS-PAGE. Immunoblots were probed with antibody to pU_L31, ICP4 and lamin A/C (loading control). The results are presented in figure 4.5.

The data indicate that U_L31 is expressed at detectable levels as early as 2 hpi. The kinetics of pU_L31 expression early in infection correlated with those of ICP4 expression whereas at 5 hpi, the amount of pU_L31 increased more dramatically than those of ICP4. Importantly, little or no protein was visible in the CHX-treated lysates, indicating that, as expected, the early detection of pU_L31 is due to active transcription/translation and was not a consequence of its presence within the innoculum. These data indicate that U_L31, previously thought to be expressed only at late times after infection, has low level expression at early times after infection.

U_L31 expression late in infection is PAA-sensitive.

Since true late genes are sensitive to DNA polymerase inhibitors, we asked whether pUL31 expression late in infection was dependent on vDNA synthesis [i.e sensitive to the DNA polymerase inhibitor phosphonoacetic acid (PAA)]. To test this possibility, Hep2 cells were infected with wild type HSV-1(F) (MOI=10) or were mock infected in the presence or absence of 200 µg/mL PAA. At 12 hours post infection total cell lysates were collected and proteins separated by SDS-PAGE. The immunoblot was reacted with antibody to pU_L31 or lamin A/C as a loading control. The results are presented in figure 4.6.

The presence of PAA significantly diminished pU_L31 expression in HSV-1 infected cells. These data are consistent with U_L31 expression as a late gene, but are not inconsistent with an important role(s) of pU_L31 early in infection.

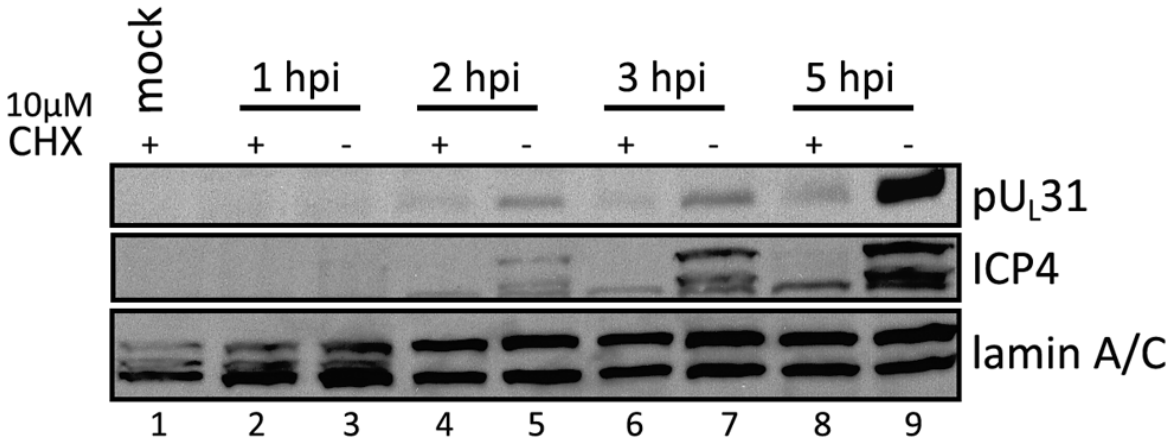

Figure 4.5 U$_L$31 expression is detectable early in infection. Hep2 cells were pre-treated with 10 µM cycloheximide (CHX) for 1 hour at 37°C/5%CO2 or left untreated. After the 1 hour treatment, cells were infected with 10 PFU per cell of wild type HSV-1(F) or were mock infected. Cells were incubated an additional hour at 37°C with gentle agitation to allow for viral attachment and entry, then the overlay was replaced with fresh media containing 10 µM CHX where appropriate. Total cell lysates were collected at 1, 2, 3 and 5 hours post infection and proteins were separated by SDS-PAGE. The immunoblot was reacted with antibody to pU$_L$31, ICP4 or lamin A/C. Bound antibodies were revealed by reaction with appropriately conjugated antibodies followed by chemiluminescence and exposure to X-ray film as described in materials and methods.

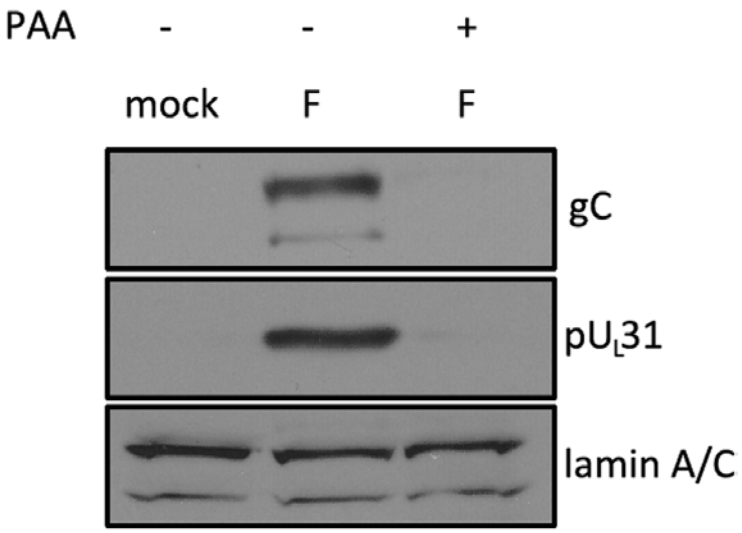

Figure 4.6 U_L31 expression is dependent on viral DNA replication. Hep2 cells were infected with wild type HSV-1(F) (MOI = 10 PFU per cell) or were mock infected in the presence or absence of 200 µg/mL phosphonoacetic acid (PAA) at the start of infection. At 12 hours post infection (hpi) total cell lysates were collected and proteins separated by SDS-PAGE. The immunoblot was reacted with antibody to gC, pU_L31 or lamin A/C. Bound antibodies were revealed by reaction with appropriately conjugated antibodies followed by chemiluminescence and exposure to X-ray film as described in materials and methods.

Discussion

Besides its well documented role in nuclear egress, the current data argue that pUL31 plays a role in optimizing viral protein production and activation of JNK and NFκB, especially in Hep2 and HeLa cells. These functions are separable kinetically. Specifically, U_L31 acts to increase early gene expression at times before the activation of JNK and NFκB, which normally occur at 6 hours post infection with HSV-1. It is therefore unclear whether pU_L31 itself, or another viral protein whose optimal expression depends on pU_L31, is responsible for activation of NFκB and JNK. After 6 hours, however, the failure to activate signaling molecules in cells infected with the U_L31 null virus can no longer be kinetically separated from defects in viral gene expression.

The degree to which pU_L31 mediates its effects on viral protein accumulation varies in different cell lines. For example, the block in NFκB and JNK activation is relieved with time in RSC and Vero cells, but less so in Hep2 and HeLa cells. The previously noted restriction of U_L31 deletion mutant replication in Vero cells, and relative permissivity of RSCs (80), is therefore experimentally separable from U_L31-mediated effects on NFκB and JNK activation. We have also shown that the defects of the U_L31 deletion virus cannot be rescued by expression of ICP27 *in trans*, suggesting that pU_L31 performs different functions than this potent viral regulator. Perhaps most importantly, the effect of pU_L31 on viral protein accumulation can be distinguished from its interaction with pU_L34, because protein expression defects were not observed in cells infected with a U_L34 deletion virus as noted previously (128). It follows that because the nuclear lamina is not perforated,

nor do particles bud from the nuclear membrane in cells infected with the U_L34 deletion virus (122,123,128), that the function of pU_L31 on protein expression is independent of its roles in nuclear egress or effects on the nuclear lamina. While we do not know the mechanism by which pU_L31 augments viral protein expression and cell signaling, its localization in the nucleoplasm must be sufficient to mediate these functions because pU_L31 is located solely in the nucleoplasm of cells with the U_L34 deletion virus (123). Such localization suggests possible roles in transcription, stability or export of mRNAs and studies are currently underway to distinguish between these possibilities. It is possible that the presence of pU_L31 early in infection is important for blocking nascent expression of the NFκB repressor, IκBα, during the second wave of NFκB activation (3). How and which of these putative activities are consequential to (or dependent on) U_L31-dependent JNK and NFκB activation will require further studies. It is logical that incomplete blocks in these processes could be relieved by prolonged incubation, just as we see in cells infected with the U_L31 deletion virus.

Acknowledgements

We thank Bill Ruyechan for the ICP8 antibody, Bernard Roizman for the ΔU_L31 and ΔU_L31-R viruses, Richard Roller for the ΔU_L34 virus and Stephen Rice for the V27 cell line and the d27-1 virus. These studies were supported by grants R01 AI52341 and T32 AI007618 from the National Institutes of Health.

CHAPTER V

U_L31 of herpes simplex virus 1 is necessary for optimal expression of viral gene products and host shut off

Kari L. Roberts and Joel D. Baines, Department of Microbiology and Immunology, Cornell University, Ithaca, NY 14853.

Abstract

Previous results suggested that the U_L31 gene of herpes simplex virus 1 (HSV-1) is required for envelopment of nucleocapsids at the inner nuclear membrane, and optimal viral DNA synthesis and DNA packaging. In the current study, viral gene expression of a herpes simplex virus mutant lacking the U_L31 gene, designated ΔU_L31, and its genetic repair, designated ΔU_L31-R, were studied in various cell lines. After propagation in pU_L31 complementing cell lines, expression of the immediate early protein ICP4, early protein ICP8, and late protein glycoprotein C (gC) were delayed significantly in all cell types in the next round of infection with ΔU_L31. In some cell types, expression of these proteins failed to eventually reach levels seen in cells infected with ΔU_L31-R or wild type HSV-1(F). These data suggest U_L31 facilitates initiation of infection and/or accelerates the onset of viral gene expression. The effects on very early events in expression suggest that it plays important (but perhaps indirect) roles later in the assembly pathway.

Introduction

Herpes simplex virus type 1 (HSV-1) is a large, enveloped DNA virus that expresses more than 70 genes during the course of an infection (88). Viral gene expression is organized into three distinct kinetic classes of genes designated immediate early (α), early (β) and late (γ) (67,68). The late genes can be further categorized as leaky late (γ_1) and true late (γ_2), where γ_1 gene expression is augmented by viral DNA replication and γ_2 gene expression completely depends upon it. The β and γ genes encode the proteins

necessary for viral replication, including the production of novel viral DNA and virion structural components (e.g. capsid proteins), respectively.

Upon entry, the tegument disperses into the cytoplasm and interacts with various host factors to help establish conditions conducive to HSV-1 protein expression. Functions known to contribute include (i) shut off of host protein synthesis by the U_L41 gene product vhs, which degrades mRNA to favor viral gene expression (78,119), and (ii) preferential transactivation of viral genes at the expense of host genes through the redirection of host transactivators to viral promoters by the U_L48 gene product VP16 (α-TIF) (76,117).

Several immediate early proteins also act to favor the viral transcription program over that of the host. For example, ICP4 is a major transactivator of some viral genes whereas the α gene product ICP27 augments HSV-1 gene expression at both pre- and post-transcriptional levels. ICP27 interacts with RNA polymerase II to help initiate transcription (176) and recruits the polymerase to viral replication sites within the nucleus (26). Once these viral transcripts are produced, ICP27 further assists expression by binding viral mRNA (23,135) and helping to mediate its export to the cytoplasm (75,135,145). Additionally, ICP27 has been shown to be necessary for the activation of NFκB during HSV-1 infection (57).

NFκB, a transcription regulator found in almost every cell type, is normally activated by cell stress such as that induced during inflammation and viral infection (59,60,72). In some viral infections the NFκB pathway is blocked by the invading viruses; however, HSV-1 is known to activate NFκB (48,113,129).

β gene expression is required for viral DNA replication. ICP8 is a long

established marker of this stage of infection and helps create the viral DNA replication compartment within the nucleus of the infected cell (26). While viral DNA synthesis augments protein expression of γ_1 genes, it is absolutely required for protein expression of γ_2 genes. During the γ phase of infection, a subset of structural proteins assemble into capsids and genomic viral DNA is inserted. The gene product for U_L31 [pU_L31, classified as γ_2 based on sensitivity of its mRNA to 1-β-D-arabinofuranosylthymine (13)] localizes to the nucleus where it interacts with pU_L34 (γ_2) at the nuclear rim. This interaction is critical for envelopment of nucleocapsids at the inner nuclear membrane (28) and there is also some evidence that pU_L31 is involved in viral DNA packaging (2).

In the current study, we observed a novel defect during infection with a U_L31-null virus (ΔU_L31) inasmuch as expression of the α protein ICP4, β protein ICP8, and γ gene glycoprotein C (gC) were delayed in several cell types infected with the U_L31 deletion mutant. These effects were not evident in infections with a mutant HSV-1 lacking the gene for pU_L34 (the binding partner of pU_L31) and correlated with poor activation of the transcription regulator NFκB as described in chapter IV. Despite the fact that pU_L31 is not a virion component, the data suggests that its well documented roles in viral assembly play important roles in subsequent initiation of viral infection.

Materials and Methods

Viruses and Cells

Wild type HSV-1 strain F [HSV-1(F)], ΔU_L31 and ΔU_L31-R were kindly

provided by Bernard Roizman and have been described previously (15,35). Virus stocks were propagated and titered on Vero cell monolayers [HSV-1(F)] or rabbit skin cells engineered to express pU_L31 (80). The cell lines were maintained in growth medium, consisting of Dulbecco's modified Eagle's medium (DMEM) supplemented with 125 units/mL penicillin, 0.125 mg/mL streptomycin and 10% newborn calf serum. Two different viral stocks of the U_L31 deletion virus were used in the reported studies. These stocks were titered on both Vero cells and the U_L31 expressing cell line (80), and produced at least 1000-fold more viral plaques per mL on monolayers of the complementing cell line than on Vero cells. For all experiments, cells were overlayed with 199V medium (DMEM supplemented with 1% newborn calf serum) after infection, and monitored for cytopathic effects until harvesting or fixation.

Immunoblot Analyses

Mock infected and HSV-1(F) infected cells were washed once in PBS then lysed in 100 µL of 2X sodium dodecyl sulfate-polyacrylamide gel electrophoresis (SDS-PAGE) sample buffer (100 mM TrisCl [pH 6.8], 200 mM dithiothreitol, 4% SDS, 20% glycerol, 0.2% bromophenol blue). Lysates were sonicated and boiled for 5 minutes prior to loading. Samples were separated on a 10% polyacrylamide gel and transferred to a nitrocellulose membrane (30 volts for 3.5 hours at 4°C). The membrane was blocked in 5% milk/TBST (1X tris-buffered saline plus 0.1% Tween) for 1 hour at room temperature. The following primary antibodies were diluted in 5% BSA in TBST as follows:

mouse anti-ICP4 (1:1000, Rumbaugh-Goodwin Institute for Cancer Research, Plantation, FL), rabbit anti-ICP8 (1:10000, a kind gift from Bill Ruyechan), mouse anti-gC (1:1000, Rumbaugh-Goodwin Institute for Cancer Research, Plantation, FL), mouse anti-Lamin A/C (1:1000, Santa Cruz Biotechnology sc7292). Diluted primary antibodies were reacted with blocked membrane for either 1 hour at room temperature or overnight at 4°C with gentile agitation. After extensive washing in PBS, bound primary antibody was detected by addition of anti-mouse (1:2000, Santa Cruz Biotechnology) or anti-rabbit (1:2000, Santa Cruz Biotechnology) horseradish peroxidase-conjugated secondary antibody diluted in 5% milk/TBST and visualized by enhanced chemiluminescence (Pierce) followed by exposure to X-ray film (Pierce).

^{35}S Met/Cys Metabolic Labeling

Hep2 cells were seeded into 6-well dishes and mock infected or infected with 20.0 PFU per cell of HSV-1(F), 20.0 PFU per cell of Δ31-R or 50.0 PFU per cell of Δ31 and held at 4°C with gentile agitation for 1 hour to allow for viral attachment. Next, cells were washed in PBS and incubated with DMEM lacking L-glutamine, methionine, and cysteine (starvation medium) for 30 minutes at 37°C. To label proteins, cells were overlayed with starvation medium supplemented with 20 μCi ^{35}S methionine per well for three hours at 0-3, 3-6, 6-9, 9-12 and 12-15 hours post infection. After the three hour labeling periods, cells were washed in PBS and collected in 150 μL 2X SDS sample buffer, sonicated and stored at -80°C. After all time points were collected, lysates were boiled for 5 minutes before loading. Radiolabeled lysates were

separated on a 12% polyacrylamide gel and transferred to a nitrocellulose membrane. Labeled proteins were visualized by autoradiography on X-ray film (Pierce).

Results

Viral protein accumulation and host shut-off are delayed in ΔUL31 infections.

To further document a role for pU_L31 in augmenting viral gene expression, Hep2 cells were infected with ΔU_L31, wild type HSV-1(F) or ΔU_L31-R (a virus derived from the U_L31 deletion virus but bearing a restored U_L31). The multiplicity of infection (MOI) for wild type (F) and ΔU_L31-R was 20 PFU/cell, while the MOI for ΔU_L31 was 50 PFU per cell to ensure each cell was infected. At various times after infection, proteins were radiolabeled for 3 hours with [^{35}S] methionine and cystine and cellular lysates were prepared after each labeling interval over 18 hours. Proteins were then denatured, electrophoretically separated on an SDS polyacrylamide gel, transferred to a nitrocellulose membrane and the membrane was exposed to X-ray film (Pierce) to visualize proteins. The results are presented in figure 5.1.

Expression of many prominent early viral proteins was delayed in cells infected with ΔU_L31. Some proteins in lysates of cells infected with HSV-1(F) and ΔU_L31-R (in bands denoted with •, † or ‡) likely represented immediate early or early gene products inasmuch as they were readily detectable by 0-3 hours with continued high expression up to 6 hours after infection (lanes 2-3 and 14-15, respectively). These same proteins were not expressed in ΔU_L31

until 3-6 hpi (lane 9) and the expression level was diminished compared to the wild type controls (lanes 2-3; 14-15). Bands denoted with • and ‡ did not peak in the ΔU_L31 infection until the 9-12 hpi time point (lane 11) and never reached corresponding levels obtained in the HSV-1(F) and ΔU_L31-R infected cell lysates (lanes 3 and 15, respectively). In addition to the delay and deficiency in viral protein synthesis by the ΔU_L31 virus, we also noted a delay in host shut off inasmuch as some bands present in mock infected cells (one is represented by *) were detected for longer amounts of time in cells infected with ΔU_L31 compared to levels seen in HSV-1(F) and ΔU_L31-R infections [compare lane 1 (mock) to lanes 2-3 and 14-15 (F and ΔU_L31-R, respectively) and lanes 8-11 (ΔU_L31)].

Effects of U_L31 on expression of viral proteins in different cell types

To determine if protein accumulation of viral gene products was delayed in other cell types, rabbit skin cells (RSC), Vero, HeLa and Hep2 cells, as well as the ΔU_L31 complementing cell line, clone #7 (an RSC derivative) were mock infected or were infected with the ΔU_L31, HSV-1(F) or ΔU_L31-R viruses. Equal amounts of proteins from each sample at each time point were separated by SDS-PAGE and transferred to nitrocellulose membranes, reacted with relevant antibodies as described in materials and methods. The results are shown in figure 5.2.

Sample loading was assessed by probing with an antibody directed against lamin A/C. Although the amounts loaded in each lane were consistent within samples from a given cell line, they varied somewhat between cell lines. The

Figure 5.1 ^{35}S metabolic labeling of total proteins produced during HSV-1 infection. Hep2 were mock infected or infected with 20.0 PFU per cell of HSV-1(F), 20.0 PFU per cell of Δ31-R or 50.0 PFU per cell of Δ31. Cells were overlayed with starvation medium supplemented with 20 μCi ^{35}S methionine per well for three hours at 0-3, 3-6, 6-9, 9-12 and 12-15 hours post infection. Radiolabeled lysates were separated on a 12% polyacrylamide gel, transferred to a nitrocellulose membrane and visualized by autoradiography.

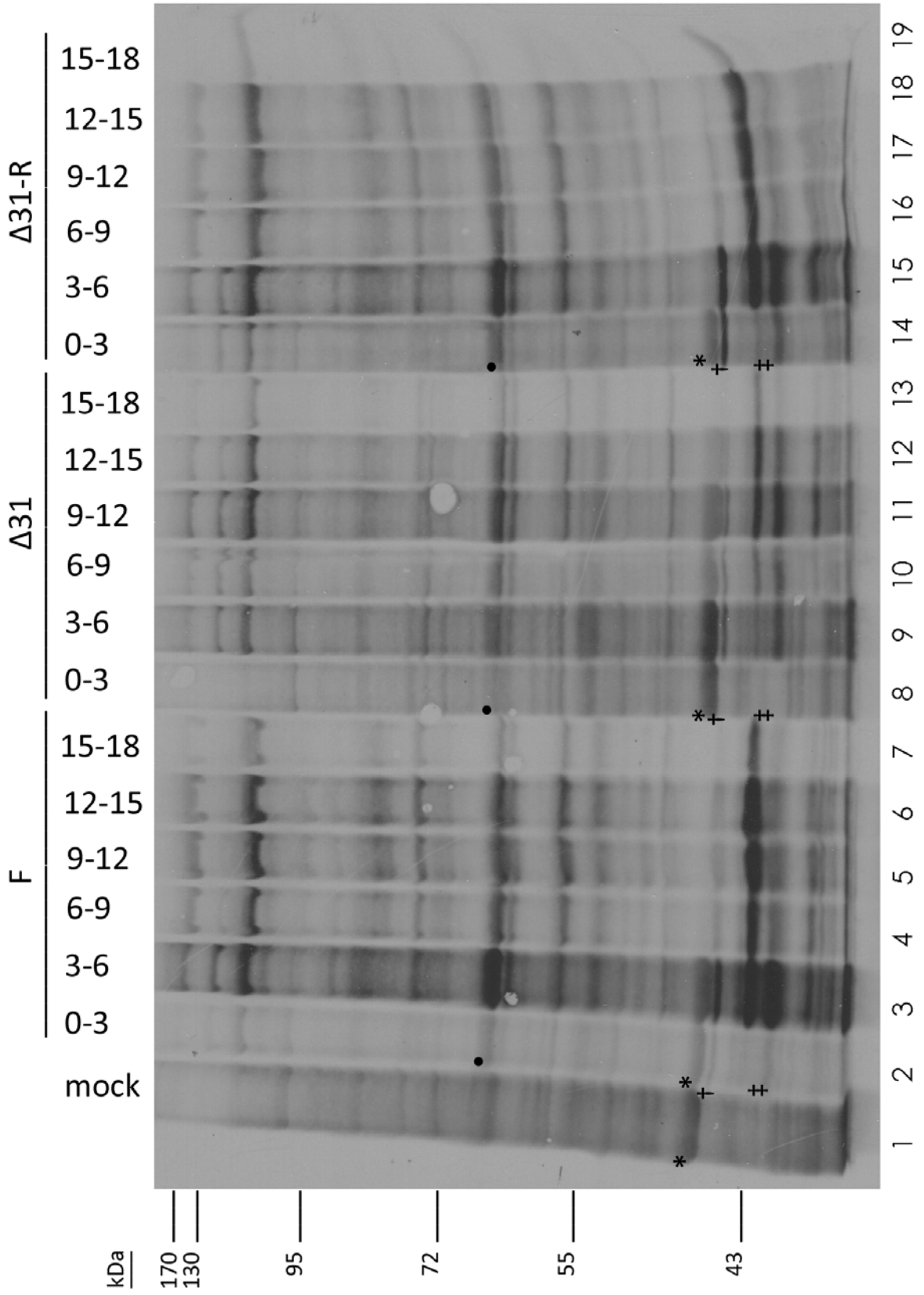
Δ31-R
15-18
12-15
9-12
6-9
3-6
0-3
Δ31
15-18
12-15
9-12
6-9
3-6
0-3
F
15-18
12-15
9-12
6-9
3-6
0-3
mock
1 2 3 4 5 6 7 8 9 10 11 12 13 14 15 16 17 18 19
kDa
170
130
95
72
55
43

Figure 5.2 Representative viral proteins from each kinetic class are down-regulated in ΔU_L31 infections of different cell types.

Cells were infected with HSV-1(F), ΔU_L31, ΔU_L31-R or mock infected at an MOI of 10 PFU per cell. Lamin A/C was used as a loading control. Bound antibodies were revealed by reaction with appropriately conjugated antibodies followed by chemiluminescence and exposure to X-ray film as described in materials and methods.

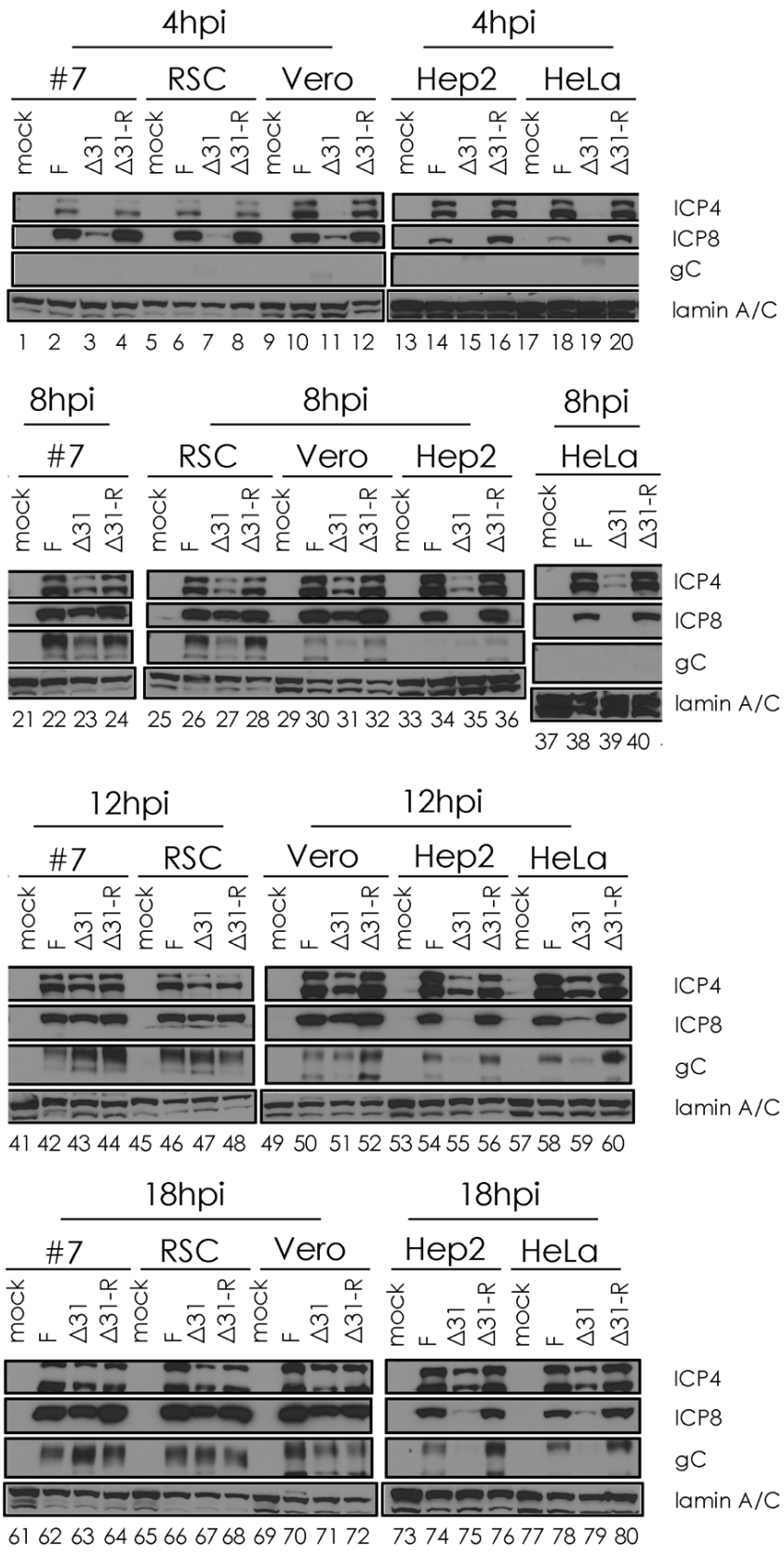
4hpi
4hpi
#7
RSC
Vero
Hep2
HeLa
mock
F
Δ31
Δ31-R
ICP4
ICP8
gC
lamin A/C
1 2 3 4 5 6 7 8 9 10 11 12 13 14 15 16 17 18 19 20
8hpi
8hpi
8hpi
21 22 23 24 25 26 27 28 29 30 31 32 33 34 35 36 37 38 39 40
12hpi
12hpi
41 42 43 44 45 46 47 48 49 50 51 52 53 54 55 56 57 58 59 60
18hpi
18hpi
61 62 63 64 65 66 67 68 69 70 71 72 73 74 75 76 77 78 79 80

consistency of loading between samples from each cell type enabled comparisons of protein expression by the different viruses in each cell type examined.

Expression of immediate early and early proteins was delayed in all cell types infected with ΔU_L31. Expression of the γ_2 gene product glycoprotein C (gC) was delayed slightly in clone #7, RSC and Vero cells at 8 hpi but reached wild type levels by 12 hpi.

Both Hep2 and HeLa cells were more restrictive to protein expression by ΔU_L31 since the delay of α and β gene expression was extended in these cell types. Specifically, wild type levels of ICP4 and ICP8 expression were not reached until 12 hpi in cells infected with ΔU_L31. Additionally, gC expression levels failed to reach wild type levels in Hep2 and HeLa cells by 18 hpi.

Infections of clone #7, RSC and Vero cells with ΔU_L31 all resulted in a delay of gC expression at 12 hpi compared to wild type levels. However, gC levels in these cell types infected with the ΔU_L31 mutant reached wild type levels by 18 hpi. Similar results were noted in cells infected with 50 PFU per cell of the U_L31 deletion mutant (data not shown), suggesting that the differences was not consequential to a failure to infect a subset of the cells.

Discussion

Besides its well documented role in nuclear egress, the data presented here argue that pU_L31 also plays a role in initiation of infection in some cell types. This is manifested by a delayed accumulation of early viral proteins in some cell types infected with a U_L31 deletion virus. The defect in viral protein

accumulation correlates well with inefficient activation of NFκB and the downstream signaling molecule JNK. For example, at 18 hours post infection (hpi) IκBα levels in the non-permissive HeLa cells were down regulated to 7% of mock levels in the wild type HSV-1(F) infection (figure 4.2). This indicates a strong actvation of NFκB in these cells, whereas the IκBα level in HeLa cells infected with the U_L31 deletion virus were at 78% of mock levels at 18 hpi (figure 4.2), indicating poor NFκB activation. Similarly, (activated) p-JNK levels in HeLa cells infected with the U_L31 deletion virus infection was only 15% of p-JNK levels in the repaired virus infection at 18 hpi (figure 4.2). Figure 5.2 shows that at 18 hpi in HeLa cells ICP4, ICP8 and gC are all expressed at dimished levels compared to the repaired virus. Taken together, this suggests that activation of NFκB and JNK is important to ensure optimal viral gene expression. Alternatively, the failure to activate these signaling molecules may occur secondarily to inefficient initiation of infection.

Acknowledgements

We thank Bill Ruyechan for the ICP8 antibody and Bernard Roizman for the ΔU_L31 and ΔU_L31-R viruses. These studies were supported by grants R01 AI52341 and T32 AI007618 from the National Institutes of Health.

CHAPTER VI

Conclusions and Future Work

This dissertation addresses several components of HSV-1 infection and the presented data supports new roles for the host protein myosin Va in HSV-1 secretion (chapter III) and the viral protein pU_L31 in cell signaling and gene expression (chapters IV and V). These data and potential future work is discussed below.

Myosin Va and HSV-1 Secretion

The goal of the work presented in chapter III was to determine the role of the actin motor myosin Va in HSV-1 secretion. While egress to the secondary envelopment site via microtubules has been described, little is known about how these vesicles transit the remaining distance to the plasma membrane for virion release. Based on the known roles for myosin Va in secretion of other vesicular cargo (130,173,174), it seemed possible that this motor may also be used for *trans*-Golgi network (TGN)-derived vesicles transporting HSV-1 virions to the extracellular space.

In order to determine whether or not HSV-1 utilized myosin Va during secretion, HeLa and Vero cells transfected to express a dominant negative myosin Va (DN-myoVa) construct were infected with HSV-1. Titration of total infectivity (intracellular and secreted virions) and secreted infectivity (virions in the supernatant only) revealed that cells expressing DN-myoVa secreted 50-75% less HSV-1 than control cells, while total infectivity produced by the DN-

myoVa expressing cells was not reduced compared to control cells (chapter III). This suggests that myosin Va activity is required for secretion of HSV-1, but not for intracellular production of virions.

The implication of this finding is that myosin Va's role appears to take place after secondary envelopment at the TGN and before these vesicles fuse with the plasma membrane to release the internalized virions. This fits with our proposed model (figure 6.1) that myosin Va is participating in a "hand-off" of virion-laden TGN vesicles from a kinesin motor in order to capture this cargo within the cortical actin and traffic the vesicle toward the plasma membrane. The observed decrease of viral glycoproteins B, M and D on the cell surface serves as an indication that the vesicles enriched with viral glycoproteins failed to fuse with the plasma membrane. Presumably, it is vesicles enriched with viral glycoproteins that are used by HSV-1 to egress from the cell (i.e. TGN-derived vesicles) (158). Finally, data presented in chapter III demonstrating colocalization of TGN markers with the cytoplasmic aggregations of DN-myoVa (tagged with red fluorescent protein) further support this model.

In order to further establish the model proposed above, future work includes directly correlating myosin Va activity with virion-laden vesicles in the cortical actin. HSV-1 labeled with two fluorescent tags, one on a capsid protein and another on an envelope protein, could be used to show whether or not myosin Va is necessary for virions to enter the cortical actin. Infecting cells expressing DN-myoVa with this dually-labeled virus and subsequently recording live cell dynamics by confocal or epifluorescence microscopy would reveal whether enveloped viruses (represented by pixels of the mixed

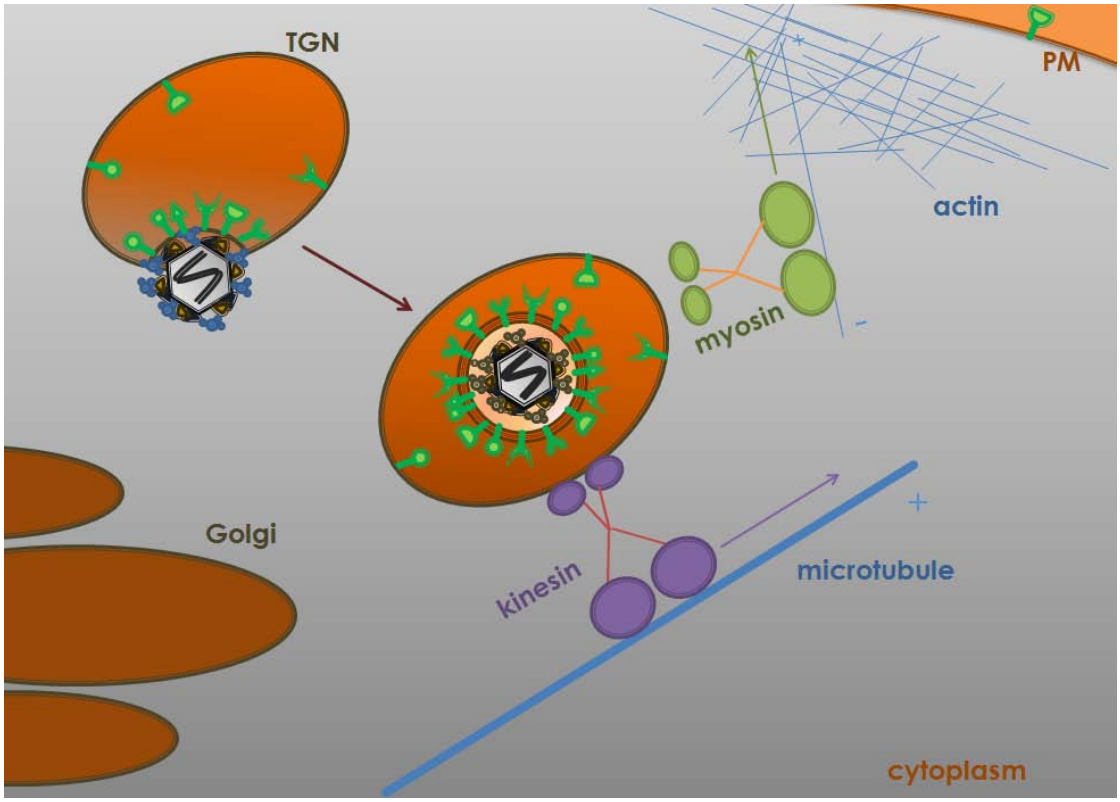

Figure 6.1 Model of HSV-1 Secretion via a Myosin Motor. Model depicting an HSV-1 capsid budding into a TGN-derived vesicle and subsequent transport along a microtubule filament via kinesin. Next, the vesicle is transferred to actin filaments and trafficked through cortical actin via myosin Va toward the plasma membrane for secretion.

fluorescent colors) reached the periphery of the cell. The required reagents are currently available to the laboratory.

It would also be of interest to determine what effector protein(s) are used by myosin Va to bind its vesicular cargo (i.e. TGN-derived vesicles) in HSV-1 infected cells. Effector proteins (including Rab GTPases) that interact with different exons of alternatively spliced myosin Va have already been described (24,64,127,165,173), and it would be of interest to know if myosin Va uses one or more of these proteins in epithelial cells, or if a different protein(s) is involved. Because both the brain and skin isoforms of DN-myoVa were effective at decreasing HSV-1 secretion, it is possible that in these (infected) cells the motor protein is associating with an unidentified effector that associates with a conserved region of myosin Va. Rab 11, which is known to associate with myosin Va in the brain, may also be a candidate since it is not know what region of the motor protein interacts with this GTPase. It is also formally possible that a viral protein is acting as a myosin Va effector. Data presented in chapter III indicated a robust activation of myosin Va at about 4 hours post infection (as indicated by an altered conformation) that was dependent upon viral protein synthesis. Thus, viral proteins are influencing myosin Va dynamics and may direct the motor to specific cargo.

One possible experiment to elucidate myosin Va effector protein(s) during HSV-1 infection is immunoprecipitation (IP) with a myosin Va antibody. Proteins complexing with the antibody would be separated on a polyacrylamide gel by electrophoresis and stained with Coomassie blue to visualize proteins. Comparing IPs from infected and mock infected cells would

reveal potential viral effector proteins by the presence of additional bands from proteins complexing in the infected cell IP but not with mock infected cells. The proteins harvested from the IP could be identified by mass spectrometry or alternatively by immunoblot if the molecular weight match to a known myosin Va effector protein. The results could be confirmed by siRNA knock down and/or dominant negative mutants expressed in cells that are subsequently infected with HSV-1. Infection would be followed by collection and titration of secreted and total infectivity at 20 hours post infection, as was done with the DN-myoVa constructs (chapter III).

pU_L31: Role in Cell Signaling and Gene Expression in HSV-1 Infections

pU_L31 has known roles in nucelocapsid egress as well as viral DNA (vDNA) replication and packaging (15,123,124,128). The data presented in chapters IV and V demonstrates additional roles for pU_L31 in cell signaling and viral gene expression. Specifically, NFκB activation was reduced and/or delayed in multiple cell types infected with the U_L31 deletion virus. This activation deficiency correlated with reduced/delayed activation of c-Jun-N-terminal kinase (JNK) as well as delayed expression of viral proteins. Metabolic labeling experiments (chapter V) also demonstrated a reduced ability for host shut off compared to infections with wild type (F) or the repair virus. These defects were not due to inability to infect cells as ICP4 expression was noted in cell monolayers infected with the U_L31 deletion virus at levels comparable to infections with the repair virus, albeit delayed.

The mechanism by which pU_L31 mediates its effects on NFκB activation

and viral protein accumulation is unclear. pU_L31 is not a component of extracellular virions (83). Proper virion assembly at later stages may be dependent on proper vDNA packaging and primary envelopment at the nuclear membrane (15,123). For example, defects in vDNA packaging might later compromise vDNA uncoating upon infection of new cells. It should be noted that these hypotheses assume complementation of the U_L31 null mutant is incomplete in the pU_L31 expressing cell line used to propagate the U_L31 virus, an assumption that is supported by the incomplete rescue of NFκB activation in the U_L31 complementing cell line infected with the U_L31 deletion virus (80).

Whatever the role of pU_L31 to help initiate viral infection, eventually this block is relieved with time in RSC and Vero cells, though infection in some cell types such as Hep2 and HeLa are considerably more dependent on U_L31. Previously presented data demonstrated that detectable levels of U_L31 protein exist as early as 2 hpi (chapter IV). This presents the possibility that the nascent pUL31 accumulating at early times post infection is necessary for transcription and/or translation of viral genes.

Data presented in chapter IV showed that the defects of ΔU_L31 cannot be rescued by expression of ICP27 *in trans*, suggesting that pU_L31 performs different functions than this potent viral regulator. Importantly, the effect of pU_L31 on viral protein accumulation can be distinguished from its interaction partner pU_L34, because protein expression defects were not noted in cells infected with a U_L34 deletion virus, consistent with previous reports (128).This, along with the fact that pU_L31 exists solely in the nucleus in the absence of its

binding partner, argues against pU_L31 acting on gene expression at the translational level. It follows logically that because pU_L31 is located almost exclusively in the nucleoplasm in cells infected with the U_L34 null virus (123), that the role pU_L31 plays in augmenting viral infection is mediated not by viral budding from the inner nuclear membrane, but by other functions of pU_L31 performed in the nucleoplasm. Such roles might include transcriptional activation as well as an ancillary but important role in capsid assembly, DNA packaging as previously reported (15).

Incorrect DNA packaging or capsid assembly could conceivably confer early defects in subsequent infection by inefficiencies in entry or DNA uncoating at the nuclear pore (109). It is logical that incomplete blocks in these processes could be relieved by prolonged incubation, just as we see in cells infected with the U_L31 deletion virus.

The most pressing future work for this project is the elucidation of a mechanism for pU_L31's role in gene activation. Because of pU_L31's strictly nuceloplasmic localization, its most likely role early in infection is related to transcription. In order to determine if transcription is down regulated during infection with the U_L31-null virus, RNA isolation and subsequent analysis on DNA microarray chips would reveal which HSV-1 genes are actively transcribed. Comparing the U_L31-null virus to RNA collected from the repaired would answer this question. Selected genes could be verified by real time PCR. Such a microarray is available to our laboratory through a collaborator.

BIBLIOGRAPHY

1. **Aebi, U., J. Cohn, L. Buhle, and L. Gerace**. 1986. The nuclear lamina is a meshwork of intermediate-type filaments. Nature **323**:560-564.

2. **Amici, C., G. Belardo, A. Rossi, and M. G. Santoro**. 2001. Activation of I kappa B kinase by herpes simplex virus type 1 - A novel target for anti-herpetic therapy. J Biol Chem **276**:28759-28766.

3. **Amici, C., A. Rossi, A. Costanzo, S. Ciafre, B. Marinari, M. Balsamo, M. Levrero, and M. G. Santoro**. 2006. Herpes simplex virus disrupts NF-kappa B regulation by blocking its recruitment on the I kappa B alpha promoter and directing the factor on viral genes. J Biol Chem **281**:7110-7117.

4. **Arii, J., H. Goto, T. Suenaga, M. Oyama, H. Kozuka-Hata, T. Imai, A. Minowa, H. Akashi, H. Arase, Y. Kawaoka, and Y. Kawaguchi**. 2010. Non-muscle myosin IIA is a functional entry receptor for herpes simplex virus-1. Nature **467**:859-862.

5. **Baines, J. D., C. E. Hsieh, E. Wills, C. Mannella, and M. Marko**. 2007. Electron Tomography of Nascent Herpes Simplex Virus Virions. J Virol. **81**:2726-2735.

6. **Batterson, W., D. Furlong, and B. Roizman**. 1983. Molecular genetics of herpes simplex virus. VIII. further characterization of a temperature-sensitive mutant defective in release of viral DNA and in other stages of the viral reproductive cycle. J Virol. **45**:397-407.

7. **Roizman, B. and A.E. Sears**. 1996. Herpes Simplex Viruses and Their Replication, p. 2231-2296. *In* Bernard N.Fields, David M.Knipe, Peter M.Howley, Robert M.Chanock, Joseph L.Melnick, Thomas P.Monath, Bernard Roizman, and Stephen E.Straus (eds.), Fields Virology. Lippincott-Raven, Philadelphia.

8. **Bjerke, S. L. and R. J. Roller**. 2006. Roles for herpes simplex virus type 1 UL34 and US3 proteins in disrupting the nuclear lamina during herpes simplex virus type 1 egress. Virology **347**:261-276.

9. **Bossard, C., D. Bresson, R. S. Polishchuk, and V. Malhotra**. 2007. Dimeric PKD regulates membrane fission to form transport carriers at the TGN. J Cell Biol **179**:1123-1131.

10. **Calistri, A., P. Sette, C. Salata, E. Cancellotti, C. Forghieri, A. Comin, H. Gottlinger, G. Campadelli-Fiume, G. Palu, and C. Parolin**. 2007. Intracellular Trafficking and Maturation of Herpes Simplex Virus

Type 1 gB and Virus Egress Require Functional Biogenesis of Multivesicular Bodies. J Virol. **81**:11468-11478.

11. **Campellone, K. G. and M. D. Welch**. 2010. A nucleator arms race: cellular control of actin assembly. Nat Rev Mol Cell Biol **11**:237-251.

12. **Carpenter, J. E., E. P. Henderson, and C. Grose**. 2009. Enumeration of an Extremely High Particle-to-PFU Ratio for Varicella-Zoster Virus. J.Virol. **83**:6917-6921.

13. **Carrozza, M. J. and N. A. DeLuca**. 1996. Interaction of the viral activator protein ICP4 with TFIID through TAF250. Mol Cell Biol **16**:3085-3093.

14. **Ch'ng, T. H. and L. W. Enquist**. 2005. Neuron-to-Cell Spread of Pseudorabies Virus in a Compartmented Neuronal Culture System. J Virol. **79**:10875-10889.

15. **Chang, Y. E., C. Van Sant, P. W. Krug, A. E. Sears, and B. Roizman**. 1997. The null mutant of the U(L)31 gene of herpes simplex virus 1: construction and phenotype in infected cells. J Virol. **71**:8307-8315.

16. **Chen, D. H., H. Jiang, M. Lee, F. Liu, and Z. H. Zhou**. 1999. Three-Dimensional Visualization of Tegument/Capsid Interactions in the Intact Human Cytomegalovirus. Virology **260**:10-16.

17. **Chi, J. H., C. A. Harley, A. Mukhopadhyay, and D. W. Wilson**. 2005. The cytoplasmic tail of herpes simplex virus envelope glycoprotein D binds to the tegument protein VP22 and to capsids. J Gen Virol **86**:253-261.

18. **Chimini, G. and P. Chavrier**. 2000. Function of Rho family proteins in actin dynamics during phagocytosis and engulfment. Nat Cell Biol **2**:E191-E196.

19. **Clement, C., V. Tiwari, P. M. Scanlan, T. Valyi-Nagy, B. Y. J. T. Yue, and D. Shukla**. 2006. A novel role for phagocytosis-like uptake in herpes simplex virus entry. J Cell Biol **174**:1009-1021.

20. **Cockrell, S. K., M. E. Sanchez, A. Erazo, and F. L. Homa**. 2009. Role of the UL25 Protein in Herpes Simplex Virus DNA Encapsidation. J Virol. **83**:47-57.

21. **Coen, D. M., S. P. Weinheimer, and S. L. McKnight**. 1986. A genetic approach to promoter recognition during trans induction of viral gene expression. Science **234**:53-59.

22. **Conti, M. A. and R. S. Adelstein**. 2008. Nonmuscle myosin II moves in

new directions. J Cell Sci **121**:11-18.

23. **Corbin-Lickfett, K. A., I. H. B. Chen, M. J. Cocco, and R. M. Sandri-Goldin**. 2009. The HSV-1 ICP27 RGG box specifically binds flexible, GC-rich sequences but not G-quartet structures. Nucl Acids Res **37**:7290-7301.

24. **Correia, S. S., S. Bassani, T. C. Brown, M. F. Lise, D. S. Backos, A. El-Husseini, M. Passafaro, and J. A. Esteban**. 2008. Motor protein-dependent transport of AMPA receptors into spines during long-term potentiation. Nat Neurosci **11**:457-466.

25. **Crump, C. M., C. Yates, and T. Minson**. 2007. Herpes Simplex Virus Type 1 Cytoplasmic Envelopment Requires Functional Vps4. J Virol. **81**:7380-7387.

26. **Dai-Ju, J. Q., L. Li, L. A. Johnson, and R. M. Sandri-Goldin**. 2006. ICP27 Interacts with the C-Terminal Domain of RNA Polymerase II and Facilitates Its Recruitment to Herpes Simplex Virus 1 Transcription Sites, Where It Undergoes Proteasomal Degradation during Infection. J Virol. **80**:3567-3581.

27. **De Regge, N., H. J. Nauwynck, K. Geenen, C. Krummenacher, G. H. Cohen, R. J. Eisenberg, T. C. Mettenleiter, and H. W. Favoreel**. 2006. Alpha-Herpesvirus glycoprotein D interaction with sensory neurons triggers formation of varicosities that serve as virus exit sites. J Cell Biol **174**:267-275.

28. **del Rio, T., C. J. DeCoste, and L. W. Enquist**. 2005. Actin Is a Component of the Compensation Mechanism in Pseudorabies Virus Virions Lacking the Major Tegument Protein VP22. J Virol. **79**:8614-8619.

29. **Desai, P. and S. Person**. 1998. Incorporation of the Green Fluorescent Protein into the Herpes Simplex Virus Type 1 Capsid. J Virol. **72**:7563-7568.

30. **Desai, P., G. L. Sexton, J. M. McCaffery, and S. Person**. 2001. A Null Mutation in the Gene Encoding the Herpes Simplex Virus Type 1 UL37 Polypeptide Abrogates Virus Maturation. J Virol. **75**:10259-10271.

31. **Desai, P. J.** 2000. A Null Mutation in the UL36 Gene of Herpes Simplex Virus Type 1 Results in Accumulation of Unenveloped DNA-Filled Capsids in the Cytoplasm of Infected Cells. J Virol. **74**:11608-11618.

32. **Dohner, K., A. Wolfstein, U. Prank, C. Echeverri, D. Dujardin, R. Vallee, and B. Sodeik**. 2002. Function of Dynein and Dynactin in Herpes Simplex Virus Capsid Transport. Mol Biol Cell **13**:2795-2809.

33. **Eichler, T. W., T. Kogel, N. V. Bukoreshtliev, and H. H. Gerdes**. 2006. The role of myosin Va in secretory granule trafficking and exocytosis. Biochem Soc Trans. **34**:671-674.

34. **Eisenberg, S. P., D. M. Coen, and S. L. McKnight**. 1985. Promoter domains required for expression of plasmid-borne copies of the herpes simplex virus thymidine kinase gene in virus-infected mouse fibroblasts and microinjected frog oocytes. Mol Cell Biol. **5**:1940-1947.

35. **Ejercito, P. M., E. D. Kieff, and B. Roizman**. 1968. Characterization of Herpes Simplex Virus Strains Differing in their Effects on Social Behaviour of Infected Cells. J Gen Virol **2**:357-364.

36. **Etienne-Manneville, S. and A. Hall**. 2002. Rho GTPases in cell biology. Nature **420**:629-635.

37. **Faith, S. A., T. J. Sweet, E. Bailey, T. Booth, and J. J. Docherty**. 2006. Resveratrol suppresses nuclear factor-kappa B in herpes simplex virus infected cells. Antiviral Research **72**:242-251.

38. **Farnsworth, A., K. Goldsmith, and D. C. Johnson**. 2003. Herpes Simplex Virus Glycoproteins gD and gE/gI Serve Essential but Redundant Functions during Acquisition of the Virion Envelope in the Cytoplasm. J Virol. **77**:8481-8494.

39. **Farnsworth, A., T. W. Wisner, M. Webb, R. Roller, G. Cohen, R. Eisenberg, and D. C. Johnson**. 2007. Herpes simplex virus glycoproteins gB and gH function in fusion between the virion envelope and the outer nuclear membrane. PNAS **104**:10187-10192.

40. **Favoreel, H. W., G. Van Minnebruggen, D. Adriaensen, and H. J. Nauwynck**. 2005. Cytoskeletal rearrangements and cell extensions induced by the US3 kinase of an alphaherpesvirus are associated with enhanced spread. PNAS **102**:8990-8995.

41. **Feierbach, B., S. Piccinotti, M. Bisher, W. Denk, and L. W. Enquist**. 2006. Alpha-herpesvirus infection induces the formation of nuclear actin filaments. PLoS Pathog. **2**:e85.

42. **Fenwick, M. L. and M. M. McMenamin**. 1984. Early Virion-associated Suppression of Cellular Protein Synthesis by Herpes Simplex Virus is Accompanied by Inactivation of mRNA. J Gen Virol **65**:1225-1228.

43. **Forest, T., S. Barnard, and J. D. Baines**. 2005. Active intranuclear movement of herpesvirus capsids. Nat Cell Biol. **7**:429-431.

44. **Fuchs, W., B. G. Klupp, H. Granzow, N. Osterrieder, and T. C. Mettenleiter**. 2002. The interacting UL31 and UL34 gene products of

pseudorabies virus are involved in egress from the host-cell nucleus and represent components of primary enveloped but not mature virions. J Virol. **76**:364-378.

45. **Fuchs, W., H. Granzow, B. G. Klupp, M. Kopp, and T. C. Mettenleiter**. 2002. The UL48 Tegument Protein of Pseudorabies Virus Is Critical for Intracytoplasmic Assembly of Infectious Virions. J Virol. **76**:6729-6742.

46. **Fuchs, W., B. G. Klupp, H. Granzow, and T. C. Mettenleiter**. 2004. Essential Function of the Pseudorabies Virus UL36 Gene Product Is Independent of Its Interaction with the UL37 Protein. J Virol. **78**:11879-11889.

47. **Gerster, T. and R. G. Roeder**. 1988. A herpesvirus trans-activating protein interacts with transcription factor OTF-1 and other cellular proteins. PNAS **85**:6347-6351.

48. **Gimble, J. M., E. Duh, J. M. Ostrove, H. E. Gendelman, E. E. Max, and A. B. Rabson**. 1988. Activation of the human immunodeficiency virus long terminal repeat by herpes simplex virus type 1 is associated with induction of a nuclear factor that binds to the NF-kappa B/core enhancer sequence. J Virol. **62**:4104-4112.

49. **Goldman, R. D., Y. Gruenbaum, R. D. Moir, D. K. Shumaker, and T. P. Spann**. 2002. Nuclear lamins: building blocks of nuclear architecture. Genes Dev. **16**:533-547.

50. **Gregory, D., D. Hargett, D. Holmes, E. Money, and S. L. Bachenheimer**. 2004. Efficient replication by herpes simplex virus type 1 involves activation of the I kappa B kinase-I kappa B-p65 pathway. J Virol. **78**:13582-13590.

51. **Grunewald, K., P. Desai, D. C. Winkler, J. B. Heymann, D. M. Belnap, W. Baumeister, and A. C. Steven**. 2003. Three-Dimensional Structure of Herpes Simplex Virus from Cryo-Electron Tomography. Science **302**:1396-1398.

52. **Gu, B. and N. DeLuca**. 1994. Requirements for activation of the herpes simplex virus glycoprotein C promoter in vitro by the viral regulatory protein ICP4. J.Virol. **68**:7953-7965.

53. **Gu, B., R. Kuddus, and N. A. DeLuca**. 1995. Repression of activator-mediated transcription by herpes simplex virus ICP4 via a mechanism involving interactions with the basal transcription factors TATA-binding protein and TFIIB. Mol Cell Biol. **15**:3618-3626.

54. **Guzowski, J. F. and E. K. Wagner**. 1993. Mutational analysis of the

herpes simplex virus type 1 strict late UL38 promoter/leader reveals two regions critical in transcriptional regulation. J Virol. **67**:5098-5108.

55. **Hall, A.** 1998. Rho GTPases and the Actin Cytoskeleton. Science **279**:509-514.

56. **Hammer, J. A. and X. Wu**. 2007. Slip sliding away with myosin V. PNAS **104**:5255-5256.

57. **Hargett, D., S. Rice, and S. L. Bachenheimer**. 2006. Herpes simplex virus type I ICP27-Dependent activation of NF-kappa B. J Virol **80**:10565-10578.

58. **Hargett, D., T. McLean, and S. L. Bachenheimer**. 2005. Herpes Simplex Virus ICP27 Activation of Stress Kinases JNK and p38. J Virol. **79**:8348-8360.

59. **Hayden, M. S. and S. Ghosh**. 2008. Shared principles in NF-kappa B signaling. Cell **132**:344-362.

60. **Hayden, M. S., A. P. West, and S. Ghosh**. 2006. NF-[kappa]B and the immune response. Oncogene **25**:6758-6780.

61. **Hayden, M. S. and S. Ghosh**. 2004. Signaling to NF-{kappa}B. Genes Dev. **18**:2195-2224.

62. **Heldwein, E. and C. Krummenacher**. 2008. Entry of herpesviruses into mammalian cells. Cell Mol Life Sci **65**:1653-1668.

63. **Hiscott, J., H. Kwon, and P. Genin**. 2001. Hostile takeovers: viral appropriation of the NF-kappaB pathway. J Clin Invest **107**:143-151.

64. **Hodi, Z., A. L. Nemeth, L. Radnai, C. Hetenyi, K. Schlett, A. Bodor, A. Perczel, and L. Nyitray**. 2006. Alternatively Spliced Exon B of Myosin Va Is Essential for Binding the Tail-Associated Light Chain Shared by Dynein. Biochem **45**:12582-12595.

65. **Holland, L. E., R. M. Sandri-Goldin, A. L. Goldin, J. C. Glorioso, and M. Levine**. 1984. Transcriptional and genetic analyses of the herpes simplex virus type 1 genome: coordinates 0.29 to 0.45. J Virol. **49**:947-959.

66. **Homa, F. L., T. M. Otal, J. C. Glorioso, and M. Levine**. 1986. Transcriptional control signals of a herpes simplex virus type 1 late (gamma 2) gene lie within bases -34 to +124 relative to the 5' terminus of the mRNA. Mol Cell Biol **6**:3652-3666.

67. **Honess, R. W. and B. Roizman**. 1975. Regulation of herpesvirus

macromolecular synthesis: sequential transition of polypeptide synthesis requires functional viral polypeptides. PNAS **72**:1276-1280.

68. **Honess, R. W. and B. Roizman**. 1974. Regulation of Herpesvirus Macromolecular Synthesis I. Cascade Regulation of the Synthesis of Three Groups of Viral Proteins. J Virol. **14**:8-19.

69. **Hoppe, S., M. Schelhaas, V. Jaeger, T. Liebig, P. Petermann, and D. Knebel-Morsdorf**. 2006. Early herpes simplex virus type 1 infection is dependent on regulated Rac1/Cdc42 signalling in epithelial MDCKII cells. J Gen Virol **87**:3483-3494.

70. **Baines, J.D. and K.L. Roberts**. 2011. Nuclear Egress and Envelopment of HSV, p. 195-206. Sandra K.Weller (ed.), Alphaherpesviruses Molecular Virology. Caister Academic Press, Norfolk, UK.

71. **Johnson, D. C. and P. G. Spear**. 1982. Monensin inhibits the processing of herpes simplex virus glycoproteins, their transport to the cell surface, and the egress of virions from infected cells. J Virol. **43**:1102-1112.

72. **Karin, M. and Y. Ben-Neriah**. 2000. Phosphorylation Meets Ubiquitination: The Control of NF-kappaB Activity. Ann Rev Immunol **18**:621-663.

73. **Kibler, P. K., J. Duncan, B. D. Keith, T. Hupel, and J. R. Smiley**. 1991. Regulation of herpes simplex virus true late gene expression: sequences downstream from the US11 TATA box inhibit expression from an unreplicated template. J Virol. **65**:6749-6760.

74. **Klupp, B. G., W. Fuchs, H. Granzow, R. Nixdorf, and T. C. Mettenleiter**. 2002. Pseudorabies Virus UL36 Tegument Protein Physically Interacts with the UL37 Protein. J Virol. **76**:3065-3071.

75. **Koffa, M. D., J. B. Clements, E. Izaurralde, S. Wadd, S. A. Wilson, I. W. Mattaj, and S. Kuersten**. 2001. Herpes simplex virus ICP27 protein provides viral mRNAs with access to the cellular mRNA export pathway. EMBO J **20**:5769-5778.

76. **Kristie, T. M. and B. Roizman**. 1987. Host cell proteins bind to the cis-acting site required for virion-mediated induction of herpes simplex virus 1 alpha genes. PNAS **84**:71-75.

77. **Kuddus, R., B. Gu, and N. A. DeLuca**. 1995. Relationship between TATA-binding protein and herpes simplex virus type 1 ICP4 DNA-binding sites in complex formation and repression of transcription. J Virol. **69**:5568-5575.

78. **Kwong, A. D. and N. Frenkel**. 1987. Herpes simplex virus-infected cells contain a function(s) that destabilizes both host and viral mRNAs. PNAS **84**:1926-1930.

79. **Leach, N., S. L. Bjerke, D. K. Christensen, J. M. Bouchard, F. Mou, R. Park, J. Baines, T. Haraguchi, and R. J. Roller**. 2007. Emerin Is Hyperphosphorylated and Redistributed in Herpes Simplex Virus Type 1-Infected Cells in a Manner Dependent on both UL34 and US3. J Virol. **81**:10792-10803.

80. **Liang, L., M. Tanaka, Y. Kawaguchi, and J. D. Baines**. 2004. Cell lines that support replication of a novel herpes simplex virus 1 UL31 deletion mutant can properly target UL34 protein to the nuclear rim in the absence of UL31. Virol **329**:68-76.

81. **Ligas, M. W. and D. C. Johnson**. 1988. A herpes simplex virus mutant in which glycoprotein D sequences are replaced by beta-galactosidase sequences binds to but is unable to penetrate into cells. J Virol. **62**:1486-1494.

82. **Liu, X., K. Fitzgerald, E. Kurt-Jones, R. Finberg, and D. M. Knipe**. 2008. Herpesvirus tegument protein activates NF-kappaB signaling through the TRAF6 adaptor protein. PNAS **105**:11335-11339.

83. **Loret, S., G. Guay, and R. Lippe**. 2008. Comprehensive characterization of extracellular herpes simplex virus type 1 virions. J Virol. **82**:8605-8618.

84. **Luxton, G. W. G., J. I. H. Lee, S. Haverlock-Moyns, J. M. Schober, and G. A. Smith**. 2006. The Pseudorabies Virus VP1/2 Tegument Protein Is Required for Intracellular Capsid Transport. J Virol. **80**:201-209.

85. **Lyman, M. G. and L. W. Enquist**. 2009. Herpesvirus Interactions with the Host Cytoskeleton. J Virol. **83**:2058-2066.

86. **Massol, P., P. Montcourrier, J. C. Guillemot, and P. Chavrier**. 1998. Fc receptor-mediated phagocytosis requires CDC42 and Rac1. EMBO J **17**:6219-6229.

87. **Mavromara-Nazos, P. and B. Roizman**. 1989. Delineation of regulatory domains of early (beta) and late (gamma 2) genes by construction of chimeric genes expressed in herpes simplex virus 1 genomes. PNAS **86**:4071-4075.

88. **McGeoch, D. J., M. A. Dalrymple, A. J. Davison, A. Dolan, M. C. Frame, D. McNab, L. J. Perry, J. E. Scott, and P. Taylor**. 1988. The complete DNA sequence of the long unique region in the genome of

herpes simplex virus type 1. J Gen Virol. **69 (Pt 7)**:1531-1574.

89. **McKnight, S. L.** 1983. Constitutive Transcriptional Control Signals of the Herpes Simplex Virus tk Gene. CSHSQB **47**:945-958.

90. **McKnight, S. L. and R. Kingsbury**. 1982. Transcriptional control signals of a eukaryotic protein-coding gene. Science **217**:316-324.

91. **McKnight, S. L.** 1980. The nucleotide sequence and transcript map of the herpes simplex virus thymidine kinase gene. Nucl Acids Res **8**:5949-5964.

92. **McKnight, Steven L.** 1982. Functional relationships between transcriptional control signals of the thymidine kinase gene of herpes simplex virus. Cell **31**:355-365. 12-1-1982.

93. **McNab, A. R., P. Desai, S. Person, L. L. Roof, D. R. Thomsen, W. W. Newcomb, J. C. Brown, and F. L. Homa**. 1998. The Product of the Herpes Simplex Virus Type 1 UL25 Gene Is Required for Encapsidation but Not for Cleavage of Replicated Viral DNA. J Virol. **72**:1060-1070.

94. **Menasche, G., C. H. Ho, O. Sanal, J. Feldmann, I. Tezcan, F. Ersoy, A. Houdusse, A. Fischer, and B. G. de Saint**. 2003. Griscelli syndrome restricted to hypopigmentation results from a melanophilin defect (GS3) or a MYO5A F-exon deletion (GS1). J Clin Invest **112**:450-456.

95. **Mercer, J., M. Schelhaas, and A. Helenius**. 2010. Virus Entry by Endocytosis. Annu Rev Biochem. **79**:803-833.

96. **Mettenleiter, T. C.** 2002. Herpesvirus Assembly and Egress. J Virol. **76**:1537-1547.

97. **Mettenleiter, T. C., B. G. Klupp, and H. Granzow**. 2006. Herpesvirus assembly: a tale of two membranes. Curr Opin Microbiol **9**:423-429.

98. **Mettenleiter, T. C., B. G. Klupp, and H. Granzow**. 2009. Herpesvirus assembly: An update. Virus Research **143**:222-234.

99. **Michael, K., B. G. Klupp, T. C. Mettenleiter, and A. Karger**. 2006. Composition of Pseudorabies Virus Particles Lacking Tegument Protein US3, UL47, or UL49 or Envelope Glycoprotein E. J Virol. **80**:1332-1339.

100. **Milne, R. S. B., A. V. Nicola, J. C. Whitbeck, R. J. Eisenberg, and G. H. Cohen**. 2005. Glycoprotein D Receptor-Dependent, Low-pH-Independent Endocytic Entry of Herpes Simplex Virus Type 1. J Virol. **79**:6655-6663.

101. **Miserey-Lenkei, S., G. Chalancon, S. Bardin, E. Formstecher, B. Goud, and A. Echard**. 2010. Rab and actomyosin-dependent fission of transport vesicles at the Golgi complex. Nat Cell Biol **12**:645-654.

102. **Monier, K., J. C. G. Armas, S. Etteldorf, P. Ghazal, and K. F. Sullivan**. 2000. Annexation of the interchromosomal space during viral infection. Nat Cell Biol **2**:661-665.

103. **Mou, F., E. G. Wills, R. Park, and J. D. Baines**. 2008. Effects of Lamin A/C, Lamin B1, and Viral US3 Kinase Activity on Viral Infectivity, Virion Egress, and the Targeting of Herpes Simplex Virus UL34-Encoded Protein to the Inner Nuclear Membrane. J Virol. **82**:8094-8104.

104. **Naranatt, P. P., S. M. Akula, C. A. Zien, H. H. Krishnan, and B. Chandran**. 2003. Kaposi's Sarcoma-Associated Herpesvirus Induces the Phosphatidylinositol 3-Kinase-PKC-{zeta}-MEK-ERK Signaling Pathway in Target Cells Early during Infection: Implications for Infectivity. J Virol. **77**:1524-1539.

105. **Neco, P., C. Fernandez-Peruchena, S. Navas, L. M. Gutierrez, G. A. de Toledo, and E. Ales**. 2008. Myosin II Contributes to Fusion Pore Expansion during Exocytosis. J Biol Chem. **283**:10949-10957.

106. **Nicola, A. V., J. Hou, E. O. Major, and S. E. Straus**. 2005. Herpes Simplex Virus Type 1 Enters Human Epidermal Keratinocytes, but Not Neurons, via a pH-Dependent Endocytic Pathway. J Virol. **79**:7609-7616.

107. **Nicola, A. V., A. M. McEvoy, and S. E. Straus**. 2003. Roles for Endocytosis and Low pH in Herpes Simplex Virus Entry into HeLa and Chinese Hamster Ovary Cells. J Virol. **77**:5324-5332.

108. **O'Hare, P. and C. R. Goding.** 1998. Herpes simplex virus regulatory elements and the immunoglobulin octamer domain bind a common factor and are both targets for virion transactivation. Cell **52:**435-445.

109. **Ojala, P. M., B. Sodeik, M. W. Ebersold, U. Kutay, and A. Helenius**. 2000. Herpes Simplex Virus Type 1 Entry into Host Cells: Reconstitution of Capsid Binding and Uncoating at the Nuclear Pore Complex In Vitro. Mol Cell Biol. **20**:4922-4931.

110. **Ostap, E. M.** 2002. 2,3-Butanedione monoxime (BDM) as a myosin inhibitor. J Muscle Res Cell Motil. **23**:305-308.

111. **Park, R. and J. D. Baines**. 2006. Herpes Simplex Virus Type 1 Infection Induces Activation and Recruitment of Protein Kinase C to the Nuclear Membrane and Increased Phosphorylation of Lamin B. J Virol. **80**:494-504.

112. **Pastural, E., F. J. Barrat, R. Dufourcq-Lagelouse, S. Certain, O. Sanal, N. Jabado, R. Seger, C. Griscelli, A. Fischer, and B. G. de Saint**. 1997. Griscelli disease maps to chromosome 15q21 and is associated with mutations in the myosin-Va gene. Nat Genet. **16**:289-292.

113. **Patel, A., J. Hanson, T. I. McLean, J. Olgiate, M. Hilton, W. E. Miller, and S. L. Bachenheimer**. 1998. Herpes Simplex Virus Type 1 Induction of Persistent NF-[kappa]B Nuclear Translocation Increases the Efficiency of Virus Replication. Virology **247**:212-222.

114. **Petermann, P., I. Haase, and D. Knebel-Morsdorf**. 2009. Impact of Rac1 and Cdc42 Signaling during Early Herpes Simplex Virus Type 1 Infection of Keratinocytes. J Virol. **83**:9759-9772.

115. **Preston, C. M., M. G. Cordingley, and N. D. Stow**. 1984. Analysis of DNA sequences which regulate the transcription of a herpes simplex virus immediate early gene. J Virol. **50**:708-716.

116. **Preston, C.M., Frame, M.C., and M.E.M. Campbell.** 1988. A complex formed between cell components and an HSV structural polypeptide binds to a viral immediate early gene regulatory DNA sequence. Cell **52**:425-434.

117. **Preston, C. M., M. C. Frame, and M. E. M. Campbell**. 1988. A complex formed between cell components and an HSV structural polypeptide binds to a viral immediate early gene regulatory DNA sequence. Cell **52**:425-434.

118. **Purves, F. C. and B. Roizman**. 1992. The UL13 gene of herpes simplex virus 1 encodes the functions for posttranslational processing associated with phosphorylation of the regulatory protein alpha 22. PNAS **89**:7310-7314.

119. **Read, G. S. and N. Frenkel**. 1983. Herpes simplex virus mutants defective in the virion-associated shutoff of host polypeptide synthesis and exhibiting abnormal synthesis of alpha (immediate early) viral polypeptides. J Virol. **46**:498-512.

120. **Remillard-Labrosse, G., C. Mihai, J. Duron, G. Guay, and R. Lippe**. 2009. Protein Kinase D-Dependent Trafficking of the Large Herpes simplex Virus Type 1 Capsids from the TGN to Plasma Membrane. Traffic **10**:1074-1083.

121. **Reske, A., G. Pollara, C. Krummenacher, B. M. Chain, and D. R. Katz**. 2007. Understanding HSV-1 entry glycoproteins. Rev Med Virol. **17**:205-215.

122. **Reynolds, A. E., L. Liang, and J. D. Baines**. 2004. Conformational changes in the nuclear lamina induced by herpes simplex virus type 1 require genes U(L)31 and U(L)34. J Virol. **78**:5564-5575.

123. **Reynolds, A. E., B. J. Ryckman, J. D. Baines, Y. Zhou, L. Liang, and R. J. Roller**. 2001. U(L)31 and U(L)34 proteins of herpes simplex virus type 1 form a complex that accumulates at the nuclear rim and is required for envelopment of nucleocapsids. J Virol. **75**:8803-8817.

124. **Reynolds, A. E., E. G. Wills, R. J. Roller, B. J. Ryckman, and J. D. Baines**. 2002. Ultrastructural localization of the herpes simplex virus type 1 UL31, UL34, and US3 proteins suggests specific roles in primary envelopment and egress of nucleocapsids. J Virol. **76**:8939-8952.

125. **Rice, S. A. and D. M. Knipe**. 1990. Genetic evidence for two distinct transactivation functions of the herpes simplex virus alpha protein ICP27. J Virol. **64**:1704-1715.

126. **Roberts, K. L. and J. D. Baines**. 2010. Myosin Va Enhances Secretion of Herpes Simplex Virus 1 Virions and Cell Surface Expression of Viral Glycoproteins. J Virol. **84**:9889-9896.

127. **Roland, J. T., L. A. Lapierre, and J. R. Goldenring**. 2009. Alternative Splicing in Class V Myosins Determines Association with Rab10. J Biol Chem. **284**:1213-1223.

128. **Roller, R. J., Y. Zhou, R. Schnetzer, J. Ferguson, and D. DeSalvo**. 2000. Herpes Simplex Virus Type 1 UL34 Gene Product Is Required for Viral Envelopment. J Virol. **74**:117-129.

129. **Rong, B. L., T. A. Libermann, K. Kogawa, S. Ghosh, L. X. Cao, D. Pavan-Langston, and E. C. Dunkel**. 1992. HSV-1-inducible proteins bind to NF-[kappa]B-like Sites in the HSV-1 genome. Virology **189**:750-756.

130. **Rudolf, R., T. Kogel, S. A. Kuznetsov, T. Salm, O. Schlicker, A. Hellwig, J. A. Hammer, III, and H. H. Gerdes**. 2003. Myosin Va facilitates the distribution of secretory granules in the F-actin rich cortex of PC12 cells. J Cell Sci **116**:1339-1348.

131. **Ryckman, B. J. and R. J. Roller**. 2004. Herpes Simplex Virus Type 1 Primary Envelopment: UL34 Protein Modification and the US3-UL34 Catalytic Relationship. J Virol. **78**:399-412.

132. **Flint, S.J., Enquist, L.W., Racaniello, V.R., and A.M. Skalka**. 2004. Principles of Virology: Molecular Biology, Pathogenesis, and Control of Animal Viruses, p. 1-918. ASM Press, Washington DC.

133. **Saksena, M. M., H. Wakisaka, B. Tijono, R. A. Boadle, F. Rixon, H. Takahashi, and A. L. Cunningham**. 2006. Herpes Simplex Virus Type 1 Accumulation, Envelopment, and Exit in Growth Cones and Varicosities in Mid-Distal Regions of Axons. J Virol. **80**:3592-3606.

134. **Salmon, B., C. Cunningham, A. J. Davison, W. J. Harris, and J. D. Baines**. 1998. The Herpes Simplex Virus Type 1 UL17 Gene Encodes Virion Tegument Proteins That Are Required for Cleavage and Packaging of Viral DNA. J Virol. **72**:3779-3788.

135. **Sandri-Goldin, R. M.** 1998. ICP27 mediates HSV RNA export by shuttling through a leucine-rich nuclear export signal and binding viral intronless RNAs through an RGG motif. Genes Dev. **12**:868-879.

136. **Satoh, T., J. Arii, T. Suenaga, J. Wang, A. Kogure, J. Uehori, N. Arase, I. Shiratori, S. Tanaka, Y. Kawaguchi, P. G. Spear, L. L. Lanier, and H. Arase**. 2008. PILRalpha Is a Herpes Simplex Virus-1 Entry Coreceptor That Associates with Glycoprotein B. Cell **132**:935-944.

137. **Schek, N. and S. L. Bachenheimer**. 1985. Degradation of cellular mRNAs induced by a virion-associated factor during herpes simplex virus infection of Vero cells. J Virol. **55**:601-610.

138. **Scholtes, L. and J. D. Baines**. 2009. Effects of Major Capsid Proteins, Capsid Assembly, and DNA Cleavage/Packaging on the pUL17/pUL25 Complex of Herpes Simplex Virus 1. J Virol. **83**:12725-12737.

139. **Schumacher, D., B. K. Tischer, S. Trapp, and N. Osterrieder**. 2005. The Protein Encoded by the US3 Orthologue of Marek's Disease Virus Is Required for Efficient De-Envelopment of Perinuclear Virions and Involved in Actin Stress Fiber Breakdown. J Virol. **79**:3987-3997.

140. **Sciortino, M. T., M. A. Medici, F. Marino-Merlo, D. Zaccaria, M. Giuffre, A. Venuti, S. Grelli, and A. Mastino**. 2007. Signaling pathway used by HSV-1 to induce NF-kappa B activation - Possible role of herpes virus entry receptor A. Sig Trans Path, Pt D **1096**:89-96.

141. **Seperack, P. K., J. A. Mercer, M. C. Strobel, N. G. Copeland, and N. A. Jenkins**. 1995. Retroviral sequences located within an intron of the dilute gene alter dilute expression in a tissue-specific manner. EMBO J. **14**:2326-2332.

142. **Simpson-Holley, M., J. Baines, R. Roller, and D. M. Knipe**. 2004. Herpes Simplex Virus 1 UL31 and UL34 Gene Products Promote the Late Maturation of Viral Replication Compartments to the Nuclear Periphery. J Virol. **78**:5591-5600.

143. **Simpson-Holley, M., R. C. Colgrove, G. Nalepa, J. W. Harper, and D. M. Knipe**. 2005. Identification and Functional Evaluation of Cellular and Viral Factors Involved in the Alteration of Nuclear Architecture during Herpes Simplex Virus 1 Infection. J Virol. **79**:12840-12851.

144. **Sodeik, B., M. W. Ebersold, and A. Helenius**. 1997. Microtubule-mediated Transport of Incoming Herpes Simplex Virus 1 Capsids to the Nucleus. J Cell Biol **136**:1007-1021.

145. **Soliman, T. M., R. M. Sandri-Goldin, and S. J. Silverstein**. 1997. Shuttling of the herpes simplex virus type 1 regulatory protein ICP27 between the nucleus and cytoplasm mediates the expression of late proteins. J Virol. **71**:9188-9197.

146. **Spear, P. G. and R. Longnecker**. 2003. Herpesvirus Entry: an Update. J Virol. **77**:10179-10185.

147. **Stackpole, C. W.** 1969. Herpes-Type Virus of the Frog Renal Adenocarcinoma: I. Virus Development in Tumor Transplants Maintained at Low Temperature. J Virol. **4**:75-93.

148. **Stern, S., M. Tanaka, and W. Herr**. 1989. The Oct-1 homoeodomain directs formation of a multiprotein-DNA complex with the HSV transactivator VP16. Nature **341**:624-630.

149. **Stow, N. D.** 2001. Packaging of Genomic and Amplicon DNA by the Herpes Simplex Virus Type 1 UL25-Null Mutant KUL25NS. J Virol. **75**:10755-10765.

150. **Strobel, M. C., P. K. Seperack, N. G. Copeland, and N. A. Jenkins**. 1990. Molecular analysis of two mouse dilute locus deletion mutations: spontaneous dilute lethal20J and radiation-induced dilute prenatal lethal Aa2 alleles. Mol Cell Biol. **10**:501-509.

151. **Strom, T. and N. Frenkel**. 1987. Effects of herpes simplex virus on mRNA stability. J Virol. **61**:2198-2207.

152. **Taus, N. S., B. Salmon, and J. D. Baines**. 1998. The Herpes Simplex Virus 1 UL17 Gene Is Required for Localization of Capsids and Major and Minor Capsid Proteins to Intranuclear Sites Where Viral DNA Is Cleaved and Packaged. Virology **252**:115-125.

153. **Thirumurugan, K., T. Sakamoto, J. A. Hammer, J. R. Sellers, and P. J. Knight**. 2006. The cargo-binding domain regulates structure and activity of myosin 5. Nature **442**:212-215.

154. **Tognon, M., D. Furlong, A. J. Conley, and B. Roizman**. 1981. Molecular genetics of herpes simplex virus. V. Characterization of a

mutant defective in ability to form plaques at low temperatures and in a viral fraction which prevents accumulation of coreless capsids at nuclear pores late in infection. J Virol. **40**:870-880.

155. **Trus, B. L., W. W. Newcomb, F. P. Booy, J. C. Brown, and A. C. Steven**. 1992. Distinct monoclonal antibodies separately label the hexons or the pentons of herpes simplex virus capsid. PNAS **89**:11508-11512.

156. **Trus, B. L., W. W. Newcomb, N. Cheng, G. Cardone, L. Marekov, F. L. Homa, J. C. Brown, and A. C. Steven**. 2007. Allosteric Signaling and a Nuclear Exit Strategy: Binding of UL25/UL17 Heterodimers to DNA-Filled HSV-1 Capsids. Mol Cell **26**:479-489.

157. **Trybus, K. M.** 2008. Myosin V from head to tail. Cell Mol Life Sci. **65**:1378-1389.

158. **Turcotte, S., J. Letellier, and R. Lippe**. 2005. Herpes Simplex Virus Type 1 Capsids Transit by the trans-Golgi Network, Where Viral Glycoproteins Accumulate Independently of Capsid Egress. J Virol. **79**:8847-8860.

159. **Vale, R. D.** 2003. Myosin V motor proteins: marching stepwise towards a mechanism. J Cell Biol. **163**:445-450.

160. **Van den Broeke, C., M. Radu, M. Deruelle, H. Nauwynck, C. Hofmann, Z. M. Jaffer, J. Chernoff, and H. W. Favoreel**. 2009. Alphaherpesvirus US3-mediated reorganization of the actin cytoskeleton is mediated by group A p21-activated kinases. PNAS **106**:8707-8712.

161. **van, L. H., G. Elliott, and P. O'Hare**. 2002. Evidence of a role for nonmuscle myosin II in herpes simplex virus type 1 egress. J Virol. **76**:3471-3481.

162. **Vicente-Manzanares, M., X. Ma, R. S. Adelstein, and A. R. Horwitz**. 2009. Non-muscle myosin II takes centre stage in cell adhesion and migration. Nat Rev Mol Cell Biol **10**:778-790.

163. **Wagenaar, F., J. M. A. Pol, B. Peeters, A. L. J. Gielkens, N. de Wind, and T. G. Kimman**. 1995. The US3-encoded protein kinase from pseudorabies virus affects egress of virions from the nucleus. J Gen Virol **76**:1851-1859.

164. **Wagner, E. K., J. F. Guzowski, and J. Singh**. 1995. Transcription of the Herpes Simplex Virus Genome during Productive and Latent Infection, p. 123-165. *In* Waldo E.Cohn and Kivie Moldave (ed.), Prog Nuc Acid Res Mol Biol. Academic Press.

165. **Wagner, W., E. Fodor, A. Ginsburg, and J. A. Hammer**. 2006. The Binding of DYNLL2 to Myosin Va Requires Alternatively Spliced Exon B and Stabilizes a Portion of the Myosin's Coiled-Coil Domain. Biochem **45**:11564-11577.

166. **Wang, F., K. Thirumurugan, W. F. Stafford, J. A. Hammer, P. J. Knight, and J. R. Sellers**. 2004. Regulated conformation of myosin V. J Biol Chem. **279**:2333-2336.

167. **Wild, P., M. Engels, C. Senn, K. Tobler, U. Ziegler, E. M. Schraner, E. Loepfe, M. Ackermann, M. Mueller, and P. Walther**. 2005. Impairment of Nuclear Pores in Bovine Herpesvirus 1-Infected MDBK Cells. J Virol. **79**:1071-1083.

168. **Wild, P., C. Senn, C. L. Manera, E. Sutter, E. M. Schraner, K. Tobler, M. Ackermann, U. Ziegler, M. S. Lucas, and A. Kaech**. 2009. Exploring the Nuclear Envelope of Herpes Simplex Virus 1-Infected Cells by High-Resolution Microscopy. J Virol. **83**:408-419.

169. **Wittels, M. and P. G. Spear**. 1991. Penetration of cells by herpes simplex virus does not require a low pH-dependent endocytic pathway. Virus Research **18**:271-290.

170. **Wolfstein, A., C. H. Nagel, K. Radtke, K. Dohner, V. J. Allan, and B. Sodeik**. 2006. The Inner Tegument Promotes Herpes Simplex Virus Capsid Motility Along Microtubules in vitro. Traffic **7**:227-237.

171. **Wong, M. L. and C. H. Chen**. 1998. Evidence for the internal location of actin in the pseudorabies virion. Virus Research **56**:191-197.

172. **Worman, H. J., J. Yuan, G. Blobel, and S. D. Georgatos**. 1988. A lamin B receptor in the nuclear envelope. PNAS **85**:8531-8534.

173. **Wu, X. S., K. Rao, H. Zhang, F. Wang, J. R. Sellers, L. E. Matesic, N. G. Copeland, N. A. Jenkins, and J. A. Hammer, III**. 2002. Identification of an organelle receptor for myosin-Va. Nat Cell Biol. **4**:271-278.

174. **Wu, X., B. Bowers, K. Rao, Q. Wei, and J. A. Hammer, III**. 1998. Visualization of Melanosome Dynamics within Wild-Type and Dilute Melanocytes Suggests a Paradigm for Myosin V Function In Vivo. J Cell Biol. **143**:1899-1918.

175. **Wysocka, J. and W. Herr**. 2003. The herpes simplex virus VP16-induced complex: the makings of a regulatory switch. Trends Biochem Sci **28**:294-304.

176. **Zhou, C. and D. M. Knipe**. 2002. Association of Herpes Simplex Virus

Type 1 ICP8 and ICP27 Proteins with Cellular RNA Polymerase II Holoenzyme. J Virol. **76**:5893-5904.

177. **Zhou, Z. H., D. H. Chen, J. Jakana, F. J. Rixon, and W. Chiu**. 1999. Visualization of Tegument-Capsid Interactions and DNA in Intact Herpes Simplex Virus Type 1 Virions. J Virol. **73**:3210-3218.